SC-RR-71 0714
Unlimited Release

Improvements in the Chart D Radiation-Hydrodynamic CODE III: Revised Analytic Equations of State

S. L. Thompson, H. S. Lauson

Prepared by Sandia Laboratories, Albuquerque, New Mexico 87115 and Livermore, California 94550 for the United States Atomic Energy Commission under Contract AT (29-1)-789

Reprinted August 1975

Sandia Laboratories

UNLIMITED RELEASE

SC-RR-71 0714

IMPROVEMENTS IN THE CHART D RADIATION-HYDRODYNAMIC CODE III: REVISED ANALYTIC EQUATIONS OF STATE

S. L. Thompson
H. S. Lauson
Code Development Division, 5162
Sandia Laboratories
Albuquerque, New Mexico
87115

March 1972

(Reprinted August 1975)

ABSTRACT

A revised set of in-line equation-of-state subroutines for the CHART D hydrodynamic code is described. The information generated is thermodynamically complete and self-consistent. The temperature and density range of validity is large. Solids, liquids, vapors, plasmas, and all types of phase mixtures are treated. Energy transport properties are calculated.

The set of subroutines form a package which can easily be included in other hydrodynamic codes.

CONTENTS

CONTENTS (Cont)

ACKNOWLEDGMENTS

This work has been greatly aided by the suggestions and criticisms of D. A. Dahlgren, D. J. McCloskey, R. K. Cole, Jr., A. J. Chabai, J. H. Renken, and L. D. Bertholf.

IMPROVEMENTS IN THE CHART D RADIATION-HYDRODYNAMIC CODE III: REVISED ANALYTIC EQUATIONS OF STATE

I. INTRODUCTION

Through 1970, three reports were issued concerning the CHART D radiation diffusion-hydrodynamic code.[1-3] This report is the second of three currently being published to update the program. The main body of CHART D is described in the first report.[4] The third report details several user aid programs.[5] In the following these reports will be referred to as R1, R2, R3, R4, and R5.

The present subject is the analytic or in-line equation-of-state (EOS) subroutines originally considered in R2. Some of the calculations in the current version are identical to those in the earlier work. In others, the physical models are the same, but modifications have been made to the numerical methods to improve accuracy and speed. Finally, several new features have been added. Among others, these include a melt transition, hot electron conduction properties, and a system of changing interatomic potentials to match gas phase and critical point data.

As detailed in R4, CHART D has two types of EOS. Either or both can be employed in a given problem. The tabular form is capable of handling nearly any data but requires extensive data processing and tape and machine storage. In general, this form is quite inflexible in that the user has no control over the thermodynamic properties in the table and normally must rely on someone else to generate the data.

The analytic forms, on the other hand, are quite flexible and easy to use. Programs are described in R5 with which the input parameters can be adjusted to yield an EOS of nearly anything. However, this form is slower in code operation than the tabular data and sometimes yields results of less accuracy. For example, the radiation opacities are normally better in the tables.

As with the calculation in R2, several ground rules were established:

1. The input parameters are to be kept at a minimum and as simple as possible.

2. The package of subroutines, when called with temperature and density defined, should unfalteringly return complete and self-consistent thermodynamic data and an effective Rosseland opacity, including conduction effects.

3. The speed of evaluation and storage requirements should be compatible with hydrodynamic code conditions.

4. The range of validity should cover all possible equilibrium conditions.

5. Models should be as physically realistic as possible, considering the other conditions.

6. Linkage to the rest of the hydrodynamic code should be minimized to allow easy inclusion of the entire package into other codes with no modifications.

It is felt that the current computation satisfies the requirements as well as is possible.

One major limitation is that no provisions are included to treat molecules. An accurate method of handling molecules was ruled out by the third of the above conditions. If they are necessary in the problem at hand, a tabular EOS must be used.[6] The magnitude of this problem becomes more apparent by observing that, for many-element materials, the number of molecular combinations becomes extremely large. The storage and time required for such a calculation would be out of range of that possible.

As before, only equilibrium properties are treated. No effort has been made to describe deviatory, rate-dependent, or nonequilibrium effects. These computations can be handled as perturbations to the equilibrium conditions as, for example, is the elastic-plastic calculation given in R4.

The notation and units employed are as follows:

ρ = density (gm/cc)

T = temperature (eV $\approx$ 11605°K)

F = Helmholtz free energy (ergs/gm)

P = pressure (dynes/cm^2)

E = specific energy (ergs/gm)

S = specific entropy (ergs/gm eV)

C_V = heat capacity (ergs/gm eV)

C_s = sound speed (cm/sec)

K = Rosseland opacity (cm^2/gm)

In the description of a material, a set of constants (C_j, j = 1, 54) will be generated. The elements of this array are defined throughout the report. A summary is given in Appendix B.

II. GENERAL FORMULATION

The generation of thermodynamically complete and consistent equation-of-state (EOS) information is most easily accomplished by formulation in terms of one of the thermodynamic potentials in its natural variables. For the present work, the logical choice is the Helmholtz free energy F, with density ρ and temperature T as the independent variables. All other thermodynamic functions may be computed from various derivatives of the free energy. The required relations are

$$P = \rho^2 \frac{\partial F}{\partial \rho} , \tag{2.1}$$

$$S = - \frac{\partial F}{\partial T} , \tag{2.2}$$

$$E = F + TS = - T^2 \frac{\partial}{\partial T} \left(\frac{F}{T}\right) , \tag{2.3}$$

$$C_V = \frac{\partial E}{\partial T} = - T \frac{\partial^2 F}{\partial T^2} , \tag{2.4}$$

$$\frac{\partial P}{\partial T} = \rho^2 \frac{\partial^2 F}{\partial \rho \partial T} , \tag{2.5}$$

and

$$\frac{\partial P}{\partial \rho} = 2\rho \frac{\partial F}{\partial \rho} + \rho^2 \frac{\partial^2 F}{\partial \rho^2} . \tag{2.6}$$

The procedure for treating these variables in hydrodynamic calculations has been discussed in R4.

For stability of the numerical integration of the hydrodynamic equations, the time step is limited by a function containing the sound speed C_s. From the definition

$$C_s = \sqrt{\left(\frac{\partial P}{\partial \rho}\right)_S} \tag{2.7}$$

and various thermodynamic relations, it can be shown that

$$C_s = \left\{ \left(\frac{\partial P}{\partial \rho}\right)_T + \frac{T\left(\frac{\partial P}{\partial T}\right)^2_\rho}{\rho^2 C_v} \right\}^{1/2} . \tag{2.8}$$

Other interesting relations are the expressions for the constant pressure heat capacity C_P,

$$C_P = C_v + \frac{T\left(\frac{\partial P}{\partial T}\right)^2_\rho}{\rho^2\left(\frac{\partial P}{\partial \rho}\right)_T} , \tag{2.9}$$

the linear expansion coefficient α ,

$$\alpha = -\frac{1}{3\rho}\left(\frac{\partial \rho}{\partial T}\right)_P = \frac{1}{3\rho}\frac{\left(\frac{\partial P}{\partial T}\right)_\rho}{\left(\frac{\partial P}{\partial \rho}\right)_T} , \tag{2.10}$$

and the isothermal bulk modulus B,

$$B = \rho\left(\frac{\partial P}{\partial \rho}\right)_T . \tag{2.11}$$

A fundamental assumption in the formulation presented here is that the EOS may be written as a superposition of terms appropriate to various physical phenomena. Three major divisions are made for atomic and electronic interactions at absolute zero temperature, thermal motion of atoms and ions, and thermal motion, excitation, and ionization of electrons. The free energy expressing this division is written as

$$F(\rho, T) = E_c(\rho) + F_n(\rho, T) + F_e(\rho, T) , \tag{2.12}$$

where the subscript c refers to the zero-temperature isotherm or cold component, n refers to the nuclear or atomic component, and e refers to the electronic component. This does not imply that the effects are independent; the opposite is true. However, in the models, the coupling will be minimized.

According to the third law of thermodynamics, the entropy must vanish at zero temperature so that the energy and free energy are identical. This result is built into the notation of Eq. (2.12). Both F_n and F_e are defined to vanish at zero temperature. Each of the thermo-

dynamic functions may be written in a form similar to (2.12). For example, it follows from (2.1) that the pressure is given by

$$P = \rho^2 \frac{dE_c}{d\rho} + \rho^2 \frac{\partial F_n}{\partial \rho} + \rho^2 \frac{\partial F_e}{\partial \rho} \tag{2.13}$$

$$= P_c(\rho) + P_n(\rho, T) + P_e(\rho, T) .$$

In the following sections, models are constructed for the various terms. Using the above method insures thermodynamic consistency.

III. ZERO-TEMPERATURE ISOTHERM

First consider the equation of state at zero absolute temperature. The energy and pressure are related by the expression

$$P_c = \rho^2 \frac{dE_c}{d\rho} . \tag{3.1}$$

Define ρ_{oo} as the density of the solid at zero pressure and temperature and

$$\eta = \rho/\rho_{oo} \tag{3.2}$$

as the compression. It should be noted that ρ_{oo} is slightly greater than the normal room temperature density ρ_o because of thermal expansion. The relation of ρ_o and ρ_{oo} is considered in Section III-3. Equation (3.1) can be written as

$$E_c = \frac{1}{\rho_{oo}} \int_1^{\eta} P_c \eta^{-2} \, d\eta , \tag{3.3}$$

where the zero point of energy has been defined to be at ρ_{oo}.

Expressions for these terms are developed in the following sections. Different forms of description will be used for different compression regions. The relations are special cases of those employed with the tabular EOS as related in Section VI-2 in R4.

III-1. Compressed States

For compressed states ($\eta > 1$), there are only two regions where the equation of state is well known. For sufficiently large compressions ($\eta \gtrsim 20$), it is generally assumed that zero-temperature Thomas-Fermi statistical calculations are realistic. The pressures at these densities are sufficient to crumple any electronic energy levels or bands near the edge of the atom into a continuum. Possibly the most realistic of these types of calculations are those of Kirshnits[7] and Kalitkin[8] (TFC), since both quantum and exchange corrections are applied. Theoretically, the region near η=1 is not well understood. Very large attractive and repulsive forces tend to cancel, and the accuracy required in the computation of each would be out of the question. Normal methods cannot consistently predict the density ρ_{oo} to better than about 10 percent. Progress is being made in the area but the cancellation problem is so severe that it is unlikely that sufficient improvement will be available in the near future.

Fortunately, experimental data are available near $\eta = 1$. This information is, however, limited to pressures far below the high compression region. There is a wide range of compressions of interest where there are no experimental or theoretical data.

To the upper reaches of experimental data, many substances show phase transitions which result in a more closely packed structure and decreased compressibility. This, of course, leads to kinks, or discontinuities, in the slope of P_c. In simple materials, most of the phase changes observed in Hugoniot data appear to be of the second order, although a few first-order changes are clearly seen. A summary by Al'tshuler and Bakanova[9] illustrates much of the available data. For composite materials, it should be expected that much more complex structure should be found. Such transitions generally occur at pressures of less than a megabar. At higher pressures, transitions accompanied by changes in band populations are possible. However, these should not affect the compressibility to any great extent, since the crystal symmetry is unchanged. Hence, it is expected that P_c should be a smooth function at sufficiently large compressions. Insofar as Hugoniot states are concerned, the last transition encountered is the melting transition. In aluminum this occurs at about 2 megabars.

A discussion of phase changes is given in Section V. For the present, only materials where P_c is a smooth function of η are considered. A simple interpolation from the experimental data at $\eta = 1$ to the high-density limits is employed. For simple materials, this procedure has been studied[10] and is probably as accurate as any available method, since extrapolations of low- and high-density data tend to merge. For more complex materials, little else can be done because of the almost total lack of data.

An interpolation function for the pressure which is both convenient and well-behaved is

$$P_c = C_{32}\eta^{5/3} \exp(-C_{33}\eta^{-1/3}) - (C_{34} + C_{35}\eta^{1/3} + C_{36}\eta^{2/3}), \quad \eta > 1 , \tag{3.4}$$

where the subscripts are identical to those used in the computer coding. For large compressions, Eq. (3.4) is identical to the TFC result, provided the first two coefficients are given by[10]

$$C_{32} = \frac{3h^2}{20\pi M_e}\left(\frac{\pi}{3}\right)^{1/3}\left\{\frac{\rho_{oo}Z}{M_a}\right\}^{5/3} \tag{3.5}$$

and

$$C_{33} = \frac{10\pi M_e e^2}{9h^2}\left\{\frac{18}{5}Z^{1/3} + \frac{11}{(12\pi^2 Z)^{1/3}}\right\}\left\{\frac{M_a}{2\rho_{oo}}\right\}^{1/3}, \tag{3.6}$$

where Z is the atomic number, M_a is atomic mass, h is Planck's constant, M_e is electronic mass, and e is the electronic charge.

In the limiting form for large compressions, C_{32} and C_{33} yield the coefficients of the two leading powers, $\eta^{5/3}$ and $\eta^{4/3}$. The first term is that of a free electron gas. The advantages of writing the two leading powers of η is the form given by the first term in (3.4) was pointed out by Barnes.[11] However, the exponential coefficient is determined by a slightly different rule in the present calculation. This term accurately describes the entire Thomas-Fermi calculation for compressions down to about 5 or 10. For smaller values of η it gives a smaller and more realistic pressure than the exact Thomas-Fermi result.

The three remaining coefficients in (3.4) are determined by experimental data at $\eta = 1$. By definition, the pressure is required to vanish, and the bulk modulus and Grüneisen coefficient are related to its first and second derivatives. The bulk modulus at $\eta = 1$ is given by

$$B_{oo} = \left.\frac{dP_c}{d\eta}\right|_{\eta=1}. \tag{3.7}$$

The Grüneisen coefficient

$$\Gamma = \frac{1}{\rho}\left(\frac{\partial P}{\partial E}\right)_{\rho} \tag{3.8}$$

can be related to the cold compression curve by use of any of several theoretical models. The three most widely accepted models are of Slater,[12] Dugdale and MacDonald,[13] and free-volume theory.[14] It has been shown that the results of all three calculations can be written in the single expression[15]

$$\Gamma = -\frac{1}{3}(2-t) + \frac{1}{2}\,\frac{\eta^2\dfrac{d^2P_c}{d\eta^2} + 2\eta\left(1-\dfrac{2t}{3}\right)\dfrac{dP_c}{d\eta} - \dfrac{2t}{3}\left(1-\dfrac{2t}{3}\right)P_c}{\eta\dfrac{dP_c}{d\eta} - \dfrac{2t}{3}P_c}, \tag{3.9}$$

where t = 0, 1, or 2 for Slater, Dugdale and MacDonald, and free-volume relations, respectively. If we define

$$T_\Gamma = t - 1 , \tag{3.10}$$

the expression of current interest is

$$\Gamma_{oo} = \frac{1}{2B_{oo}} \frac{d^2 P_c}{d\eta^2}\Big|_{\eta=1} - \frac{1}{3} T_\Gamma . \tag{3.11}$$

It is often observed that the Dugdale and MacDonald form ($T_\Gamma = 0$) is superior for metals, and ionic crystals are best described by the free-volume relations ($T_\Gamma = 1$). However, there are exceptions to both rules; for example, aluminum seems to require the Slater relations ($T_\Gamma = -1$). In Section VIII-1 a method of determining a proper value of T_Γ from Hugoniot and zero pressure isobar data is given. Here it is assumed that T_Γ is known. All constants in (3.4) are now determined. The results are

$$C_{34} = \left\{ 6 + 3 C_{33} + 1/2 C_{33}^2 \right\} C_{32} e^{-C_{33}} - 9 B_{oo} \hat{\Gamma} , \tag{3.12}$$

$$C_{35} = - \left\{ 15 + 7 C_{33} + C_{33}^2 \right\} C_{32} e^{-C_{33}} + 3 B_{oo} \left\{ 6\hat{\Gamma} + 1 \right\} , \tag{3.13}$$

$$C_{36} = \left\{ 10 + 4 C_{33} + 1/2 C_{33}^2 \right\} C_{32} e^{-C_{33}} - 3B_{oo} \left\{ 3\hat{\Gamma} + 1 \right\} , \tag{3.14}$$

where

$$\hat{\Gamma} = \Gamma_{oo} + \frac{1}{3} T_\Gamma . \tag{3.15}$$

Rather wide ranges of the input quantities B_{oo}, Γ_{oo}, and T_Γ are acceptable; however, there are some physical limitations to be considered. It is not difficult to show that the second derivative in (3.11) must be positive if shock waves are to propagate as shocks and not dispersing pressure pulses. This means that the stiffness must increase with compression. Otherwise, compressive shock waves cannot exist. It then follows that

$$\Gamma_{oo} + \frac{1}{3} T_\Gamma > 0 . \tag{3.16}$$

In most situations this causes no problem.

The internal energy is determined by substitution of (3.4) into (3.3). The resulting expression can be integrated with the result that

$$E_c = \frac{1}{\rho_{oo}}\left\{3C_{32}\eta^{2/3} \quad \mathscr{E}_3(C_{33}\eta^{-1/3}) + \frac{C_{34}}{\eta} + \frac{3C_{35}}{2\eta^{2/3}} + \frac{3C_{36}}{\eta^{1/3}} - C_{37}\right\}, \quad \eta > 1, \tag{3.17}$$

where

$$C_{37} = 3C_{32}\mathscr{E}_3(C_{33}) - C_{34} - \frac{3C_{35}}{2} - 3C_{36}, \tag{3.18}$$

and

$$\mathscr{E}_3(x) \equiv \int_1^\infty t^{-3} e^{-xt}\, dt \tag{3.19}$$

is the third exponential integral.

III-2. Expanded States

There are several features to be considered in relation to the form for expanded states $\eta \leq 1$. For slightly expanded states, $0.8 \lesssim \eta \lesssim 1$, and temperatures below melt, a tension region will be built into the state surface. At low densities the material should be gas-like. In the intermediate region, the mixed-phase properties are very much dependent on P_c and E_c which, in effect, determine the form of the interatomic potential. The full extent of these functions is given later.

Two forms for P_c are available when $\eta \leq 1$. Except for slight modifications, the first form is identical to that given in R2. The second treatment is a system whereby corrections to the first method can be inserted by hindsight if the results seem unsatisfactory.

A modified form of the Morse interatomic potential yields a pressure of the form

$$P_c = C_4\eta^{2/3}\left\{e^{C_5\nu} - e^{C_6\nu}\right\}, \quad \eta \leq 1, \tag{3.20}$$

$$\nu = 1 - \eta^{-1/3}. \tag{3.21}$$

This form was selected over other theoretically justifiable expressions, for example, a Lennard-Jones (6-12), 6-9, or Morse-Coulomb potential, since Eq. 3.20 seems to yield the most reasonable results under the widest circumstances.

The corresponding energy is easily shown to be

$$E_c = \frac{3C_4}{\rho_{oo}} \left\{ \frac{1}{C_5} \left(e^{C_5 \nu} - 1 \right) - \frac{1}{C_6} \left(e^{C_6 \nu} - 1 \right) \right\} , \quad \eta \leq 1 . \tag{3.22}$$

The lattice separation or zero-temperature sublimation energy is then

$$E_S = \frac{3C_4}{\rho_{oo}} \left\{ \frac{1}{C_6} - \frac{1}{C_5} \right\} . \tag{3.23}$$

As P_c given by (3.20) clearly vanishes at $\eta = 1$, the two additional conditions required to determine the coefficients in (3.20) are taken from (3.7) and (3.11). The procedure insures that E_c, P_c and $\frac{dP_c}{d\eta}$ are continuous at $\eta=1$. Eq. (3.11) is rewritten as

$$\frac{1}{2B_{oo}} \frac{d^2 P_c}{d\eta^2} \Big|_{\eta=1} = \Gamma_{oo} + \frac{1}{3} \tilde{T}_\Gamma = \tilde{\Gamma} . \tag{3.24}$$

It is normally assumed that

$$\tilde{T}_\Gamma = T_\Gamma \tag{3.25}$$

and

$$\tilde{\Gamma} = \hat{\Gamma} , \tag{3.26}$$

so that $\frac{d^2 P_c}{d\eta^2}$ is also continuous at $\eta=1$. If difficulty is encountered, these relations are modified. The discontinuity in the second derivative creates no major problems in such cases.

From these relations it follows that

$$C_5 = 3\tilde{\Gamma} \left\{ 1 + \sqrt{1 - \frac{B_{oo}}{\rho_{oo} E_s \tilde{\Gamma}^2}} \right\} , \tag{3.27}$$

$$C_6 = 3\tilde{\Gamma} \left\{ 1 - \sqrt{1 - \frac{B_{oo}}{\rho_{oo} E_s \tilde{\Gamma}^2}} \right\} , \tag{3.28}$$

and

$$C_4 = 3B_{oo} / (C_5 - C_6) . \tag{3.29}$$

While, on theoretical grounds, imaginary coefficients might be justifiable, it is clear from (3.27) and (3.29) that we must require

$$\frac{B_{oo}}{\rho_{oo} E_s \tilde{\Gamma}^2} < 1 \tag{3.30}$$

for numerical reasons. If condition (3.30) is not satisfied by the given values, $\tilde{\Gamma}$ is increased until it is.

Problems can also be encountered with (3.20) at low densities. As $\eta \to 0$, P_c also vanishes. The question is, however, whether it vanishes with sufficient rapidity to be physically realistic. Since $C_5 > C_6$ follows from (3.27) and (3.28), the dominant term in (3.20) at low densities is

$$P_a = C_4 \eta^{2/3} e^{C_6 \nu} . \tag{3.31}$$

Quite arbitrarily, we impose the condition that P_a should not exceed a value P_{max} at $\eta = 10^{-3}$. P_{max} is taken currently as 1 atm. This insures that regions of large tensions will not exist in the vapor phase. Substitution of expressions for C_4 and C_6 into (3.31) yield the result that

$$\frac{B_{oo}}{200 \tilde{\Gamma} S_q} \exp \left\{27 \tilde{\Gamma} (1 - S_q)\right\} \leq P_{max} , \tag{3.32}$$

where S_q is the square root term in (3.27) and (3.28). If (3.32) is not satisfied by the given values, $\tilde{\Gamma}$ is decreased until it is, if possible. The exact form of (3.32) is not critically important. The main purpose is to insure that C_6 is sufficiently large so that the gas phase acts as a gas.

Note that, of the two reasons for not using (3.25), the first yields $\tilde{T}_\Gamma > T_\Gamma$, while the second results in $\tilde{T}_\Gamma < T_\Gamma$. In either case a message will be generated by the code, explaining that the change has been made. It is unlikely that any other observable effects will be found.

In some situations it has been found that the above expression for P_c, when coupled to the thermal components discussed in Section IV, can produce some features objectionable to the problem at hand. For example, the critical point could occur at too high a temperature and pressure, or the sound velocity in the liquid state could be in error. Provisions have been made to permit corrections to be made by hindsight to obtain the desired property. For compressions less than $C_{54} \leq 0.95$, the function

$$P = C_{53} \eta^2 \left\{1 - \frac{\eta}{C_{54}}\right\}^3 \left\{\frac{\eta}{C_{54}} - 0.2\right\} , \quad \eta \leq C_{54} \tag{3.33}$$

can be added to the right-hand side of (3.20). The values of C_{53} and C_{54} are input parameters. The corresponding energy term is

$$\mathcal{E} = -\frac{C_{53}\,\eta}{5\rho_{oo}}\left\{1-\frac{\eta}{C_{54}}\right\}^4, \quad \eta \le C_{54} \tag{3.34}$$

which is added to the right-hand side of (3.22). These forms join smoothly and do not alter the separation energy, so that (3.23) is still valid. The computed constants in (3.20) are unchanged. In effect, the addition of (3.33) changes the shape of the interatomic potential while not modifying its basic properties. At lower densities, (3.33) has the form of a Van der Waal's interaction. Thoughts on the selection of C_{53} and C_{54} are given in Appendix E.

III-3. Relation to Reference Point Conditions

The three parameters ρ_{oo}, B_{oo}, and Γ_{oo} are required as inputs for the following calculation. Unfortunately, exact values are not normally known for materials of interest. The more usual situation is that the properties of a material are known at some reference point ρ_o, T_o (usually room temperature), and it is important that the EOS correctly predict these properties.

It should be noted that ρ_{oo} and B_{oo} are the most critical insofar as the solid material is concerned. Because of the way Γ_{oo} and T_Γ enter the relations, they are of lesser importance. Hence only slight error results from the approximation

$$\Gamma_{oo} = \Gamma_o \tag{3.35}$$

in the present calculation. With the solid thermal components given in the next section and a power series expansion of P_c about ρ_{oo}, approximate values are obtained for ρ_{oo} and B_{oo}. In the calculation given in R2 these values were considered as final and most of the time they were sufficient. However, for materials with a relatively small bulk modulus, the truncated power series is in error. A final iteration has been added to complete the calculation. It is a two-variable Newton iteration for the values of B_{oo} and ρ_{oo} to yield the correct values of the reference point pressure P_o (usually zero or one atmosphere) and the bulk modulus B_o. The required expressions are

$$B_o = B_o + \frac{\partial B_o}{\partial B_{oo}}\Delta B_{oo} + \frac{\partial B_o}{\partial \rho_{oo}}\Delta\rho_{oo} \tag{3.36}$$

and

$$P_o = P_o + \frac{\partial P_o}{\partial B_{oo}}\Delta B_{oo} + \frac{\partial P_o}{\partial \rho_{oo}}\Delta\rho_{oo}, \tag{3.37}$$

where the quantities on the right-hand side are evaluated from the current values and those on the left are the desired results. The procedure is repeated until ΔB_{oo} and $\Delta \rho_{oo}$ vanish.

The input parameters for this computation are ρ_o, T_o, P_o, E_s, B_o, and T_Γ. In Section VIII-1 an input option is discussed in which Hugoniot data can be substituted for the latter two of these. A simple calculation is provided to relate the Hugoniot parameters to B_o and T_Γ. Details are given later; however, it should be remembered that the above calculation is always employed, regardless of the input option.

IV. NUCLEAR CONTRIBUTION TO THE EQUATION OF STATE

In this section the nuclear contribution is considered. These terms are intended to describe the kinetic motion of atoms and ions in both solid and gaseous states.

IV-1. Debye-Grüneisen Solid

The thermodynamics of simple solids are usually well described by the Debye-Grüneisen equation of state, with appropriate density variations of the Debye temperature and Grüneisen coefficient. The thermal contribution to the free energy is

$$F_D = N_o kT \left\{ 3 \ell n(1 - e^{-\theta/T}) - D(\theta/T) \right\} , \tag{4.1}$$

where θ is the density-dependent Debye temperature, N_o is the number of atoms per unit mass, and

$$D(X) = \frac{3}{X^3} \int_o^X \frac{Y^3 dY}{e^Y - 1} . \tag{4.2}$$

The corresponding expressions for pressure, energy, and entropy are

$$P_D = 3\Gamma \rho N_o kTD(\theta/T) , \tag{4.3}$$

$$E_D = 3N_o kTD(\theta/T) , \tag{4.4}$$

and

$$S_D = - N_o k \left\{ 3 \ell n(1 - e^{-\theta/T}) - 4D(\theta/T) \right\} , \tag{4.5}$$

where Γ is the Grüneisen coefficient and related to θ by

$$\Gamma = \frac{\rho}{\theta} \frac{d\theta}{d\rho} \quad . \tag{4.6}$$

In the case where $T >> \theta$, the above expressions may be written

$$F_D = N_o kT \left\{ 3 \ell n(\theta/T) - 1 \right\} , \tag{4.7}$$

$$P_D = 3\Gamma \rho N_o kT \quad , \tag{4.8}$$

$$E_D = 3N_o kT \quad , \tag{4.9}$$

and

$$S_D = - N_o k \left\{ 3 \ell n(\theta/T) - 4 \right\} . \tag{4.10}$$

The density variation of Γ and θ could be calculated from either the Slater, Dugdale and MacDonald, or free-volume relations, Eq. (3.9), with the cold compression curve discussed in the last section. However, it is often observed experimentally that, for small compressions, Γ is nearly inversely proportional to the density. This also seems to be a fair approximation to the results of the theoretical models over small ranges. For large compressions the limiting value of Γ for all materials is that of a free electron gas of 2/3. A relation that approaches both limits, is properly behaved in the intermediate region, and leads to much faster evaluation than the above theoretical models is

$$\Gamma = \frac{\Gamma_o \rho_o}{\rho} + C_{24} \left(1 - \frac{\rho_o}{\rho} \right)^2 , \quad \rho > \rho_o \, . \tag{4.11}$$

The coefficient C_{24} should be 2/3 to reach the correct limit as $\rho \to \infty$. However, in problems where only slight compressions are encountered ($\eta \lesssim 1.3$), C_{24} may be set to zero to improve speed. The Debye temperature is found from integration of (4.6). If θ_o is the reference Debye temperature, then it is easily shown that

$$\theta = \theta_o \left(\frac{\rho}{\rho_o} \right)^{C_{24}} \exp \left\{ \Gamma_o (1 - \rho_o/\rho) - \frac{1}{2} C_{24} \left(3 - 4 \frac{\rho_o}{\rho} + \frac{\rho_o^2}{\rho^2} \right) \right\} . \tag{4.12}$$

IV-2. Ideal Gas

At sufficiently high temperatures or low densities, the nuclear term should describe an ideal gas. Let us define N_ℓ as the number of atoms per unit mass with atomic number Z_ℓ and m_ℓ as its atomic mass. Clearly, the relation

$$N_o = \sum_\ell N_\ell \tag{4.13}$$

follows from the definitions. The thermodynamic expressions appropriate to this situation are

$$F_G = - kT \sum_\ell N_\ell \left\{ \ell n \left[\frac{U_\ell (2\pi m_\ell kT)^{3/2}}{N_\ell \rho h^3} \right] + 1 \right\} , \tag{4.14}$$

$$P_G = N_o \rho kT \ , \tag{4.15}$$

$$E_G = \frac{3}{2} N_o kT \ , \tag{4.16}$$

and

$$S_G = k \sum_\ell N_\ell \left\{ \ell n \left[\frac{U_\ell (2\pi m_\ell kT)^{3/2}}{N\ell \rho h^3} \right] + 5/2 \right\} , \tag{4.17}$$

where U_ℓ are the internal partition functions. In the present calculation all U_ℓ are taken as unity. For ionized gases, the above expressions should be modified so that the sums include all states of ionization. However, since the treatment of ionization discussed in the later sections is of the average atom type, only one term is required for each atomic number. Note that these relations assume a monatomic gas phase. No provisions are made for molecules.

IV-3. Interpolation Method

The principal difficulty in joining these two limiting theories together is the region of melting. This transition is considered in Section V-1. Here an interpolation method suggested by the Russians,[16] but in a somewhat different form, is developed. The nuclear free energy is boldly written as

$$F_n = N_o kT \left[3 \ \ell n \ (\theta/T) - 1 + \frac{3}{2} \ \ell n \ (1 + \psi) \right] \ , \tag{4.18}$$

where

$$\psi = \frac{C_{13} \rho^{2/3} \ T}{\theta^2} \tag{4.19}$$

and

$$C_{13} = \frac{N_o^{5/3} h^2}{2\pi k} \exp\left\{\frac{2}{3} \sum_{\ell} \frac{N_\ell}{N_o} \ell n \left(\frac{N_\ell}{N_o^{5/2} M_\ell^{3/2}}\right)\right\} . \tag{4.20}$$

At low temperatures ($\psi \ll 1$), Eq. (4.18) reduces to (4.7) and the thermodynamics to that of a solid. For sufficiently high temperatures ($\psi \gg 1$), gaseous thermodynamics are the result as the limiting form of (4.14) is obtained. Communal free energy and entropy terms are properly included. The corresponding interpolation equations for pressure, energy, and entropy are

$$P_n = \rho N_o k T \left\{\frac{3\Gamma + \psi}{1 + \psi}\right\} , \tag{4.21}$$

$$E_n = \frac{3}{2} N_o k T \left\{\frac{2 + \psi}{1 + \psi}\right\} , \tag{4.22}$$

and

$$S_n = - N_o k \left\{3 \ell n(\theta/T) - 4 + \frac{3}{2} \ell n(1 + \psi) + \frac{3}{2} \frac{\psi}{1 + \psi}\right\} . \tag{4.23}$$

Clearly, these expressions do not yield a true melting transition, but in many cases they are acceptable for hydrodynamic code use in this form.

There is still one major problem in the development of these relations. Both (4.11) and (3.9) are unacceptable for Γ at low densities. It has been found that a simple extrapolation of the form

$$\Gamma = C_{16} \rho^2 + C_{17} \rho + 1, \quad \rho < \rho_o \tag{4.24}$$

is sufficient, where C_{16} and C_{17} are determined so that Γ and $\frac{d\Gamma}{d\rho}$ are continuous at $\rho = \rho_o$. This form has no physical basis and is used only because it works well. To illustrate fully the nature of this expression, further relations are required. When Eq. (4.6) is integrated, the result is

$$\theta = C_{14} \rho \exp\left\{\frac{1}{2} C_{16} \rho^2 + C_{17} \rho\right\} , \tag{4.25}$$

where

$$C_{14} = \frac{\theta_o}{\rho_o} \exp(-2\Gamma_o + 3/2) . \tag{4.26}$$

The Debye temperature given by (4.25) clearly has no relation to Debye theory and is purely an extrapolation. However, the value of θ given by (4.25) decreases rapidly as the density decreases from ρ_o. Hence ψ, given by (4.19), increases rapidly with decreasing density, thereby yielding gaseous thermodynamic relations in which Γ is not used. An important point is that the rapid change from solid to vapor equation-of-state relations occurs in a region where the one-phase calculation is not used. It will be eliminated from the final thermodynamic functions by a Maxwellian construction between the solid or liquid and vapor phases as discussed in Section V. The overall effect of (4.24) is to provide a reasonable extrapolation of the high-density properties to the mixed-phase boundary, a gas at low densities, and a single form convenient for numerical computation.

With increasing temperature the interpolation problem diminishes. Near the critical point, ψ is generally in the range of 10 to 100. The exact critical point parameters depend only slightly on the form given by (4.24). Because of the relation given by (4.6), a change in Γ is reflected by a change in θ and ψ which have opposite effects on the equation of state and tend to cancel. Under the present formulation, the critical parameters are principally determined by the expressions used for the zero-temperature isotherm and melt transition.

The approximation leading from (4.1) to (4.7) has some undesirable effects on the equation of state. The entropy calculated from (4.23) does not vanish at zero temperature. It would be a simple matter to correct this by including the proper terms in (4.18) and its derivatives. However, this would require the evaluation of the Debye function in the hydrodynamic code. While this presents no difficulty, it is not believed that the accuracy gained is worth the increased computational time required. The only noticeable effect in a hydrodynamic calculation is seen in materials with unusually high Debye temperatures. The calculated entropy at low temperatures can be negative. This has no real effect on the hydrodynamic calculation.

The derivatives of the thermodynamic functions which are required can be shown to be

$$C_{vn} = \frac{\partial E_n}{\partial T} = \frac{E_n}{T}\left\{1 - \frac{\psi}{(1+\psi)(2+\psi)}\right\}, \tag{4.27}$$

$$\frac{\partial P_n}{\partial T} = \frac{P_n}{T}\left\{1 - \left(\frac{\psi}{1+\psi}\right)\frac{(3\Gamma - 1)}{(3\Gamma + \psi)}\right\}, \tag{4.28}$$

and

$$\frac{\partial P_n}{\partial \rho} = \frac{P_n}{\rho}\left\{1 + \left(\frac{\psi}{1+\psi}\right)\frac{2(3\Gamma - 1)^2}{3(3\Gamma + \psi)}\right\} + \frac{3\rho N_o k T}{1+\psi}\frac{d\Gamma}{d\rho}, \tag{4.29}$$

where

$$\frac{d\Gamma}{d\rho} = -\frac{\rho_o}{\rho^2}\left\{\Gamma_o - 2C_{24}(1 - \rho_o/\rho)\right\}, \quad \rho \geq \rho_o , \tag{4.30}$$

and

$$\frac{d\Gamma}{d\rho} = 2C_{16}\rho + C_{17}, \quad \rho < \rho_o . \tag{4.31}$$

IV-4. Relation of the Grüneisen Coefficient and Other Material Properties

Extensive tables of reference for Grüneisen coefficients (Γ_o) are available. Unfortunately, many of these have been adjusted for special purposes or do not represent what they are supposed to represent. A serious error is made by using an "effective" Grüneisen coefficient determined from a porous material by the relation

$$\Gamma_{eff} = \frac{1}{\rho}\frac{\Delta P}{\Delta E}, \tag{4.32}$$

where the pressures are in excess of the yield point. Γ_o in this paper applies only to the full density material. An effective value for a porous state calculated by (4.32) can be, and normally is, considerably different.

Γ_o may be expressed in terms of quantities easily measured at low temperatures. When the relation

$$\left(\frac{\partial P}{\partial T}\right)_\rho = -\left(\frac{\partial \rho}{\partial T}\right)_P \left(\frac{\partial P}{\partial \rho}\right)_T \tag{4.33}$$

is examined, it is clear that (3.8) may be written as

$$\Gamma = \frac{-1}{\rho C_v}\left(\frac{\partial \rho}{\partial T}\right)_P \left(\frac{\partial P}{\partial \rho}\right)_T . \tag{4.34}$$

The difference in the heat capacity at constant volume C_v and that at constant pressure C_p is given by

$$C_P - C_v = \frac{T}{\rho^2}\left(\frac{\partial \rho}{\partial T}\right)_P^2 \left(\frac{\partial P}{\partial \rho}\right)_T . \tag{4.35}$$

At the point of reference the above quantities are

$$\left(\frac{\partial P}{\partial \rho}\right)_T = \frac{B_o}{\rho_o} \tag{4.36}$$

and

$$\left(\frac{\partial \rho}{\partial T}\right)_P = -3\alpha_o \rho_o \ , \tag{4.37}$$

where α_o is the coefficient of linear expansion. The reference value of the Grüneisen coefficient is then

$$\Gamma_o = \frac{3\alpha_o B_o}{\rho_o C_v} = \frac{3\alpha_o B_o}{\rho_o C_P - 9\alpha_o^2 T_o B_o} \ . \tag{4.38}$$

In the present situation,

$$C_v = 3N_o k \ . \tag{4.39}$$

It is clear from (4.38) that a small value of Γ_o will yield a small expansion coefficient. This can sometimes cause unrealistic behavior when the porous material computation of R4 is used. Using a small effective value of Γ determined by (4.32) and experimental data, as Γ_o, in effect includes the distention properties twice.

V. PHASE TRANSITIONS AND RELATED PROPERTIES

There exist certain areas on the thermodynamic surface where several phases of the material are simultaneously present. An example of such a coexistence region is the melt transition, where both the liquid and solid states are found. It is generally not possible to describe material in such a condition by a single function such as given by (2.12). Each phase must be considered separately and mixture rules applied to find the effective properties. Consider a mixture of Phase 1 and Phase 2. One expression of the Gibbs phase rule says that in equilibrium the temperatures, pressures, and chemical or Gibbs potentials of the phases must be the same:

$$T_1 = T_2 = T \ , \tag{5.1}$$

$$P_1(\rho_1, T) = P_2(\rho_2, T) \tag{5.2}$$

and

$$G_1(\rho_1, T) = G_2(\rho_2, T) \quad , \tag{5.3}$$

where ρ_1 and ρ_2 are the respective phase densities and

$$G = E - TS + P/\rho = F + P/\rho \tag{5.4}$$

is the Gibbs potential. Assume that

$$\rho_2 \geq \rho_1 \quad . \tag{5.5}$$

One of the main problems in employing this type of formulation is determination of these phase densities. The numerical difficulties involved are covered below. For the present it is assumed that ρ_1 and ρ_2 are known as functions of temperature.

To evaluate the thermodynamic properties of a state

$$\rho_1 < \rho < \rho_2 \tag{5.6}$$

and of the proper temperature, the following relations apply. The mass fractions of 1 and 2 are

$$M_1 = \frac{\rho_1}{\rho}\left(\frac{\rho_2 - \rho}{\rho_2 - \rho_1}\right) \tag{5.7}$$

and

$$M_2 = 1 - M_1 = \frac{\rho_2}{\rho}\left(\frac{\rho - \rho_1}{\rho_2 - \rho_1}\right) \quad . \tag{5.8}$$

The thermodynamic functions are then

$$E = M_1 E_1 + M_2 E_2 \quad , \tag{5.9}$$

$$S = M_1 S_1 + M_2 S_2 \quad , \tag{5.10}$$

$$P = P_1 = P_2 \quad , \tag{5.11}$$

$$\frac{\partial P}{\partial T} = \left(\frac{\rho_1 \rho_2}{\rho_2 - \rho_1}\right)\left(S_1 - S_2\right) \quad , \tag{5.12}$$

$$\frac{\partial P}{\partial \rho} = 0 \quad , \tag{5.13}$$

and

$$C_v = (E_2 - E_1)\frac{dM_2}{dT} + M_1\frac{dE_1}{dT} + M_2\frac{dE_2}{dT}, \tag{5.14}$$

where (5.12) is the Clapeyron-Clausius relation and the total derivatives in (5.14) must be determined from the component phase data. With some effort it can be shown that

$$\frac{dM_2}{dT} = \frac{1}{\rho(\rho_1 - \rho_2)}\left\{\rho_2\left[\frac{\rho_2 - \rho}{\rho_2 - \rho_1}\right]\frac{d\rho_1}{dT} + \rho_1\left[\frac{\rho - \rho_1}{\rho_2 - \rho_1}\right]\frac{d\rho_2}{dT}\right\}, \tag{5.15}$$

and for each phase,

$$\frac{dE_i}{dT} = C_{vi} + \frac{1}{\rho_i^2}\left\{P_i - T\frac{\partial P_i}{\partial T}\right\}\frac{d\rho_i}{dT}. \tag{5.16}$$

The phase density derivatives are determined along the boundaries of the mixed-phase region. When the chain rule

$$\frac{\partial P}{\partial T} = \frac{\partial P_i}{\partial T} + \frac{\partial P_i}{\partial \rho_i}\frac{\partial \rho_i}{\partial T} \tag{5.17}$$

and (5.12) are employed, it follows that

$$\frac{\partial \rho_i}{\partial T} = \left[\left\{\frac{\rho_2\,\rho_2}{\rho_2 - \rho_1}\right\}\{S_1 - S_2\} - \frac{\partial P_i}{\partial T}\right]\Big/\frac{\partial P_i}{\partial \rho_i}. \tag{5.18}$$

Mixed-phase states possess several interesting properties. Note from (2.9) and (2.10) that both the constant pressure heat capacity C_p and the linear expansion coefficient α are undefined. This result reflects the fact that, at constant pressure, the temperature of a phase mixture cannot be increased. Also note that the isothermal bulk modulus vanishes. The adiabatic bulk modulus and the sound speed do not vanish but can become very small in some regions. This causes some strange and interesting effects in hydrodynamic calculations.

Methods have been included to treat four types of phase transitions. Liquid-solid (melting), liquid-vapor (boiling), solid-vapor (sublimation), and some simple solid-solid transitions which are optional. The first of these was not available in the computation in R2. Since all these phase changes occur at relatively low temperatures, the thermal electronic terms are not included in the mixture relations, since they would have little effect other than to slow the computation.

V-1. Melt Transition and the Liquid Equation of State

The method of treating the melt transition in the current version is a recent addition. An earlier unreported method was found to be inadequate in several cases. Some calculations in which the previous form is used have been reported.[17] The changes in the present form will not modify the results and conclusions of these calculations to any great extent.

The present calculation is still experimental and might be modified. The physical relations employed seem to be realistic and reliable. However, the numerical procedure can be quite slow in relation to other thermodynamic regions. Work is under way to try to improve the situation.

The normal approach to this problem would be to generate independent state surfaces for the liquid and solid with the methods used in Sections III and IV or an equivalent. Denote the liquid functions by ℓ and the solid by s. The difference is

$$F_m(\rho, T) = F_\ell(\rho, T) - F_s(\rho, T) \quad , \tag{5.19}$$

where m denotes the "melt contribution." In terms of the notation of (2.12),

$$F_s(\rho, T) = E_c(\rho) + F_n(\rho, T) \quad . \tag{5.20}$$

The approach employed here is to rewrite (5.19) as

$$F_\ell(\rho, T) = F_s(\rho, T) + F_m(\rho, T) \tag{5.21}$$

and try to generate expressions for the melt contribution. The liquid functions are then computed by adding these terms to the solid expressions. This procedure has several advantages, the principal one being that there is a much greater chance of producing usable relations. On the other hand, it is suggested that the results be checked by one of the test programs in R5 before a hydrodynamic code run is attempted.

Clearly, the main problem is to find the proper function for $F_m(\rho, T)$. It is not hard to find a form that gives proper behavior in the region of zero pressure melt. The difficulty is to determine functions which fit this requirement and which do not destroy the description in other regions. This is more severe than it might seem, since $F_m(\rho, T)$ and all of its derivatives must asymptotically become negligible with respect to the corresponding term in $F_s(\rho, T)$ at high temperatures and both high and low densities. If it fits these requirements, the exact form does not seem to be of great importance. Such a function is

$$F_m(\rho, T) = C_{43} \sqrt{T}\, \rho^{\alpha} + C_{44} \rho^{\beta} + C_{45} \rho^{\gamma} \quad , \tag{5.22}$$

where

$$\gamma > \beta \tag{5.23}$$

and α, β, γ, C_{43}, C_{44}, and C_{45} are constants. It is not difficult to show from the expressions for P_s that α, β, and γ must all lie between 0 and 1/2. The values in current use are

$$\begin{aligned} \alpha &= 0.3 \ , \\ \beta &= 0.1 \ , \\ \gamma &= 0.2 \ , \end{aligned} \tag{5.24}$$

but they can easily be changed if the need arises. The C parameters are treated as material constants determined by input parameters and properties of F_s. The temperature dependence of (5.22) is constrained by the corresponding terms in F_s. The required thermodynamic functions are:

$$P_m = \alpha C_{43} \sqrt{T}\, \rho^{\alpha+1} + \beta C_{44} \rho^{\beta+1} + \gamma C_{45} \rho^{\gamma+1} \ , \tag{5.25}$$

$$E_m = 1/2\, C_{43} \sqrt{T}\, \rho^{\alpha} + C_{44} \rho^{\beta} + C_{45} \rho^{\gamma} \ , \tag{5.26}$$

$$S_m = - \frac{C_{43} \rho^{\alpha}}{2 \sqrt{T}} \ , \tag{5.27}$$

$$C_{vm} = \frac{C_{43} \rho^{\alpha}}{4 \sqrt{T}} \ , \tag{5.28}$$

$$\frac{\partial P_m}{\partial T} = \frac{\alpha C_{43} \rho^{\alpha+1}}{2 \sqrt{T}} \ , \tag{5.29}$$

and

$$\frac{\partial P_m}{\partial \rho} = \alpha(\alpha+1)\, C_{43} \sqrt{T}\, \rho^{\alpha} + \beta(\beta+1)\, C_{44} \rho^{\beta} + \gamma(\gamma+1)\, C_{45} \rho^{\gamma} \ . \tag{5.30}$$

It can be shown that each term becomes small compared to the corresponding solid expression at extremes of temperature and density.

Two input material quantities must be given: the heat of fusion H_f and a parameter which defines the density of the liquid at the triple temperature $\rho_{\ell m}$. The C constants are determined as follows: From the solid and vapor EOS, the end points of the triple line are calculated. Define

ρ_{sm} as the solid density and T_m as the triple line or reference melt temperature. This computation is part of the procedure detailed in Section V-2.

It is assumed that

$$\rho_{sm} > \rho_{\ell m} . \tag{5.31}$$

The three relations required to compute the C values are:

$$P_\ell(\rho_{\ell m}, T_m) = P_s(\rho_{sm}, T_m) = P_s(\rho_{\ell m}, T_m) + P_m(\rho_{\ell m}, T_m) , \tag{5.32}$$

$$E_\ell(\rho_{\ell m}, T_m) = E_s(\rho_{sm}, T_m) + H_f = E_s(\rho_{\ell m}, T_m) + E_m(\rho_{\ell m}, T_m) , \tag{5.33}$$

and

$$G_\ell(\rho_{\ell m}, T_m) = G_s(\rho_{sm}, T_m) , \tag{5.34}$$

where G is the Gibbs potential. A more useful form of (5.34) is

$$\begin{aligned} S_\ell(\rho_{\ell m}, T_m) &= S_s(\rho_{sm}, T_m) + \frac{H_f}{T_m} + \frac{P_s(\rho_{sm}, T_m)}{T_m}\left|\frac{\rho_{sm}-\rho_{\ell m}}{\rho_{sm}\rho_{\ell m}}\right| \\ &= S_s(\rho_{\ell m}, T_m) + S_m(\rho_{\ell m}, T_m). \end{aligned} \tag{5.35}$$

The liquid state surface is now completely defined.

The entire extent of the equilibrium phase boundaries can now be calculated as a function of temperature. As an example, the results for aluminum are shown in Fig. 1. In this case, $H_f = 3.98 \times 10^9$ ergs/gm and $\rho_{\ell m}/\rho_{sm} = 0.924$. More details are given in Appendix D. Note that the melt curve extends into regions of tensions ($P < 0$) for $T < T_m$.

The phase densities may be computed by a two-variable Newton's iteration. The quantities

$$\mathscr{P} = P_s - P_\ell \tag{5.36}$$

and

$$\mathscr{G} = G_s - G_\ell \tag{5.37}$$

are defined. Given the proper densities, both $\mathscr{P}$ and $\mathscr{G}$ vanish. After noting the relation

$$\frac{\partial G}{\partial \rho} = \frac{1}{\rho}\frac{\partial P}{\partial \rho} , \tag{5.38}$$

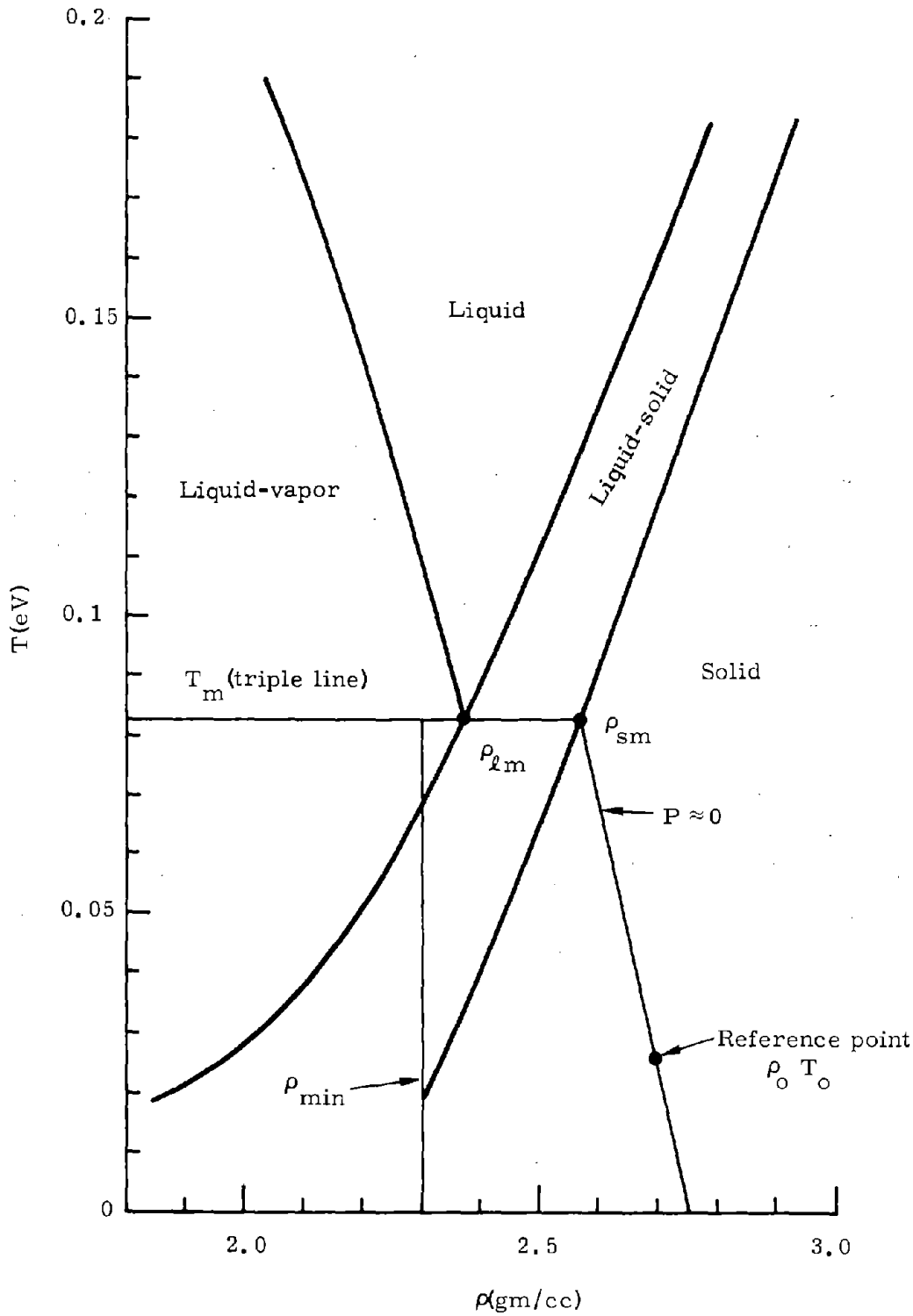

Fig. 1 Phase diagram for aluminum.

it is easily shown that the corrections are

$$\Delta\rho_s = \frac{\rho_s}{\frac{\partial P_s}{\partial \rho}} \left\{ \frac{\mathscr{P} - \rho_\ell \mathscr{E}}{\rho_\ell - \rho_s} \right\} \tag{5.39}$$

and

$$\Delta\rho_\ell = \frac{\rho_\ell}{\frac{\partial P_\ell}{\partial \rho}} \left\{ \frac{\mathscr{P} - \rho_s \mathscr{E}}{\rho_\ell - \rho_s} \right\} . \tag{5.40}$$

The problem of how to employ this in the code must now be resolved. One approach would be to compute the phase densities at a mesh of temperatures during the initialization calculation and interpolate for intermediate values during the running mode. This type of procedure is used for those transitions involving the vapor as related in Section V-2. However, in the present situation, a rather large number of points would be required for accuracy because of the steepness of the surfaces and the nearness of the two densities. As a result, in the current version the Newton iteration is used in the running mode of operation. A number of checks have been included to make this computation as fast as possible, but future modifications are probably required in this area if all else proves satisfactory.

When the EOS package is called, with temperature and density defined, a set of tests is applied to determine whether the point in question clearly lies in either the one-phase liquid or solid regions. This is the condition if the point does not lie in the shaded area in Fig. 2. Temperatures C_{48}, C_{49}, and C_{52} are determined to help bound the melt region. Lines A and B serve the same purpose and, respectively, have the forms

$$T = T_m + C_{50}(\rho - \rho_{\ell m}) \tag{5.41}$$

and

$$T = T_m + C_{51}(\rho - \rho_o) . \tag{5.42}$$

For a point in the shaded area the iteration is started to determine ρ_ℓ and ρ_s. This computation is performed in the subroutine ANLS.

Under certain conditions this iteration may be terminated before final convergence. The exact values of ρ_ℓ and ρ_s are important only if

$$\rho_\ell < \rho < \rho_s . \tag{5.43}$$

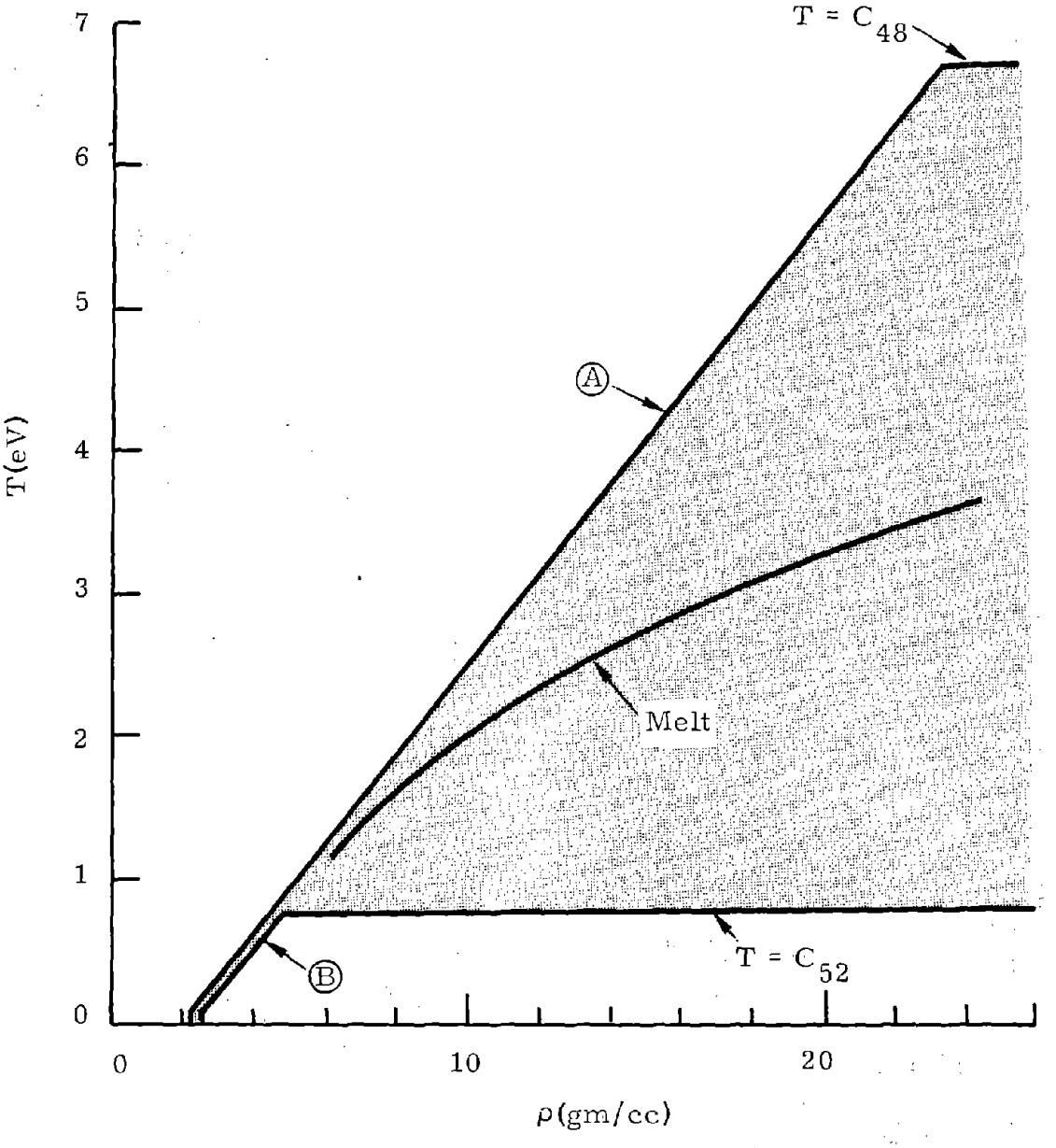

Fig. 2a Iteration regions in the melt transition computation.

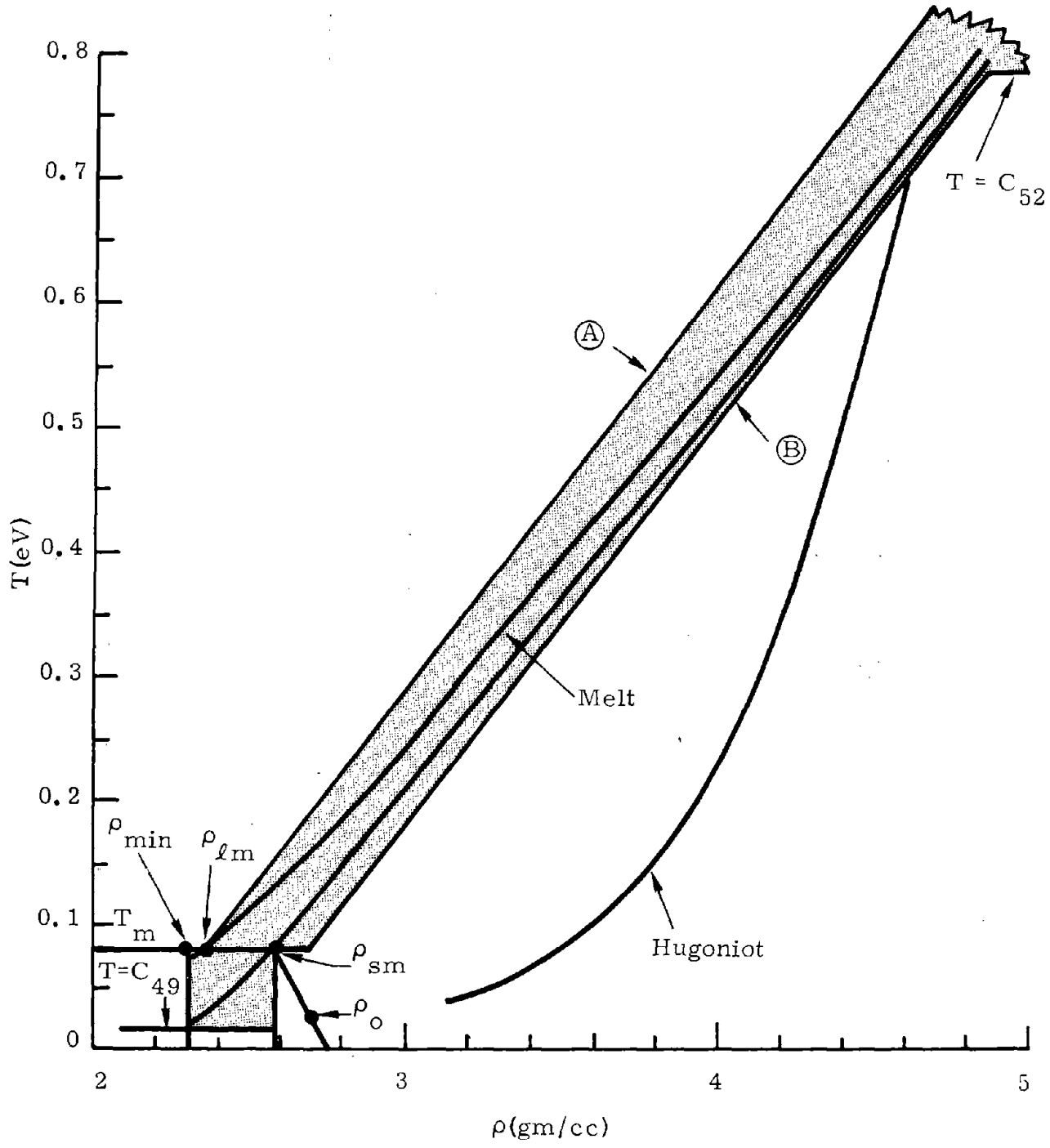

Fig. 2b Iteration regions in the melt transition computation.

If, during the iteration, it becomes clear that (5.43) is not satisfied, no more computations are performed. In the case where a step in the iteration yields

$$1.04\,\rho < \rho_\ell \ ,$$

$$\Delta\rho_\ell > 0 \ , \tag{5.44}$$

and

$$\Delta\rho_s > 0 \ ,$$

it is assumed that ρ, T represents a liquid state. On the other extreme,

$$\rho > 1.04\,\rho_s \ ,$$

$$\Delta\rho_\ell < 0 \ , \tag{5.45}$$

and

$$\Delta\rho_s < 0$$

indicate a solid state. Both conditions state that the iteration is moving away from the given density. There is no assurance that this procedure (called the fast iteration) will always give the correct answer. Hence, during the initialization, an extensive series of test calculations is made to test the method. If the computation at any point fails, the slower method of forcing complete convergence is imposed.

When the iteration is completed, it should be clear which phase or phases and thermodynamic relations are appropriate. If (5.43) is satisfied, Eqs. (5.7) through (5.18) are used with 1 = liquid and 2 = solid.

As stated before, a study is under way to try to improve the numerical methods employed in this computation. Clearly, storage limitations and reliability requirements pose some major problems.

V-2. Liquid-Vapor and Solid-Vapor Transitions

In nearly all problems involving materials which are heated above melt, mixed-phase regions involving the vapor are encountered in the relief process. This area is also of great importance in the rapid heating of porous materials.[4] The treatment given here is much like that detailed in R2. Little trouble has been found with the previous method. One addition is a backup computation in the determination of the critical point. The temperature mesh was also modified slightly for equations of state with a melt transition as defined in the last section. However, much of the coding had to be redone because of the order in which information was required.

Generally, the method is as follows. First, for those materials where the melt transition is to be included, the triple line properties are determined. This must be done so that the liquid EOS or, more correctly, the melt contribution can be defined. Then, with use of the liquid EOS, the critical point is located. At a set of temperatures determined by the critical and melting temperatures, the phase densities are located. On the high-density side, either the liquid or solid EOS is used, depending on the relation to the melting point. In the running mode, the properties of mixed-phase states are determined by interpolation in this stored mesh.

The critical point is located by determining the density, ρ_c, and temperature, T_c, where

$$\frac{\partial P}{\partial \rho} = \frac{\partial^2 P}{\partial \rho^2} = 0 . \tag{5.46}$$

As in R2, a two-variable Newton's method is employed. Temperature and density corrections are computed by

$$\Delta\rho = \frac{\frac{\partial P}{\partial \rho}\frac{\partial^3 P}{\partial T \partial \rho^2} - \frac{\partial^2 P}{\partial \rho^2}\frac{\partial^2 P}{\partial \rho \partial T}}{\frac{\partial^2 P}{\partial T \partial \rho}\frac{\partial^3 P}{\partial \rho^3} - \frac{\partial^2 P}{\partial \rho^2}\frac{\partial^3 P}{\partial T \partial \rho^2}} \tag{5.47}$$

and

$$\Delta T = \frac{\left(\frac{\partial^2 P}{\partial \rho^2}\right)^2 - \frac{\partial P}{\partial \rho}\frac{\partial^3 P}{\partial \rho^3}}{\frac{\partial^2 P}{\partial T \partial \rho}\frac{\partial^3 P}{\partial \rho^3} - \frac{\partial^2 P}{\partial \rho^2}\frac{\partial^3 P}{\partial T \partial \rho^2}} \tag{5.48}$$

until the corrections are negligible. Only the quantities $\frac{\partial P}{\partial \rho}$ and $\frac{\partial P}{\partial T}$ are calculated from analytic expressions. The higher order derivatives required in (5.47) and (5.48) are computed numerically by using a grid of nine points.

In some cases, problems can arise when the third derivatives in the above expressions happen to be near zero. A backup calculation is provided if this procedure fails. The code attempts to follow the curve defined by

$$\frac{\partial P}{\partial \rho} = 0 . \tag{5.49}$$

The critical point is taken to be the first maximum temperature computed on this curve.

Below the critical point, the phase densities are computed in a method similar to that in Section V-1. The relations are

$$\mathscr{P} = P_x - P_v \tag{5.50}$$

and

$$\mathscr{G} = G_x - G_v \ , \tag{5.51}$$

where the subscript v represents vapor and x either liquid or solid, depending on whether the temperature is above or below melt. The corrections to the phase densities are

$$\Delta \rho_x = \frac{\rho_x}{\dfrac{\partial P_x}{\partial \rho}} \left\{ \frac{\mathscr{P} - \rho_v \mathscr{G}}{\rho_v - \rho_x} \right\} \tag{5.52}$$

and

$$\Delta \rho_v = \frac{\rho_v}{\dfrac{\partial P_v}{\partial \rho}} \left\{ \frac{\mathscr{P} - \rho_x \mathscr{G}}{\rho_v - \rho_x} \right\} . \tag{5.53}$$

Special care must be taken to treat very small vapor-phase densities which may occur at low temperatures.

The results for aluminum are typical and are shown in Fig. 3. The section of the melt curve is the same as that in Fig. 1. The position of the critical point has been adjusted by using the function given by (3.33). Details are given in Appendix E. This is not yet the final form of the EOS to be used in the hydrodynamic code. Below the triple line, a modification is made to treat tensions in solid materials. This feature is detailed in the next section.

The two curves resulting from (5.46) on the single-phase surface for a normal EOS are shown in Fig. 4. This surface must be used in all the mixed-phase construction. The critical point is at the intersection. Under some conditions these curves may not have the proper form. A clearly unacceptable result is shown in Fig. 5. Three points satisfy the mathematical conditions defining the critical point. The difficulty is reflected in the code output as a lack of convergence in the mixed-phase calculation. Because of a rather complex interaction of the input parameters, no single input can be blamed for this problem. Generally, some unrealistic input number is the cause. In any case, something must be changed slightly to produce a usable form. The test programs in R5 can be used to study and correct the problem.

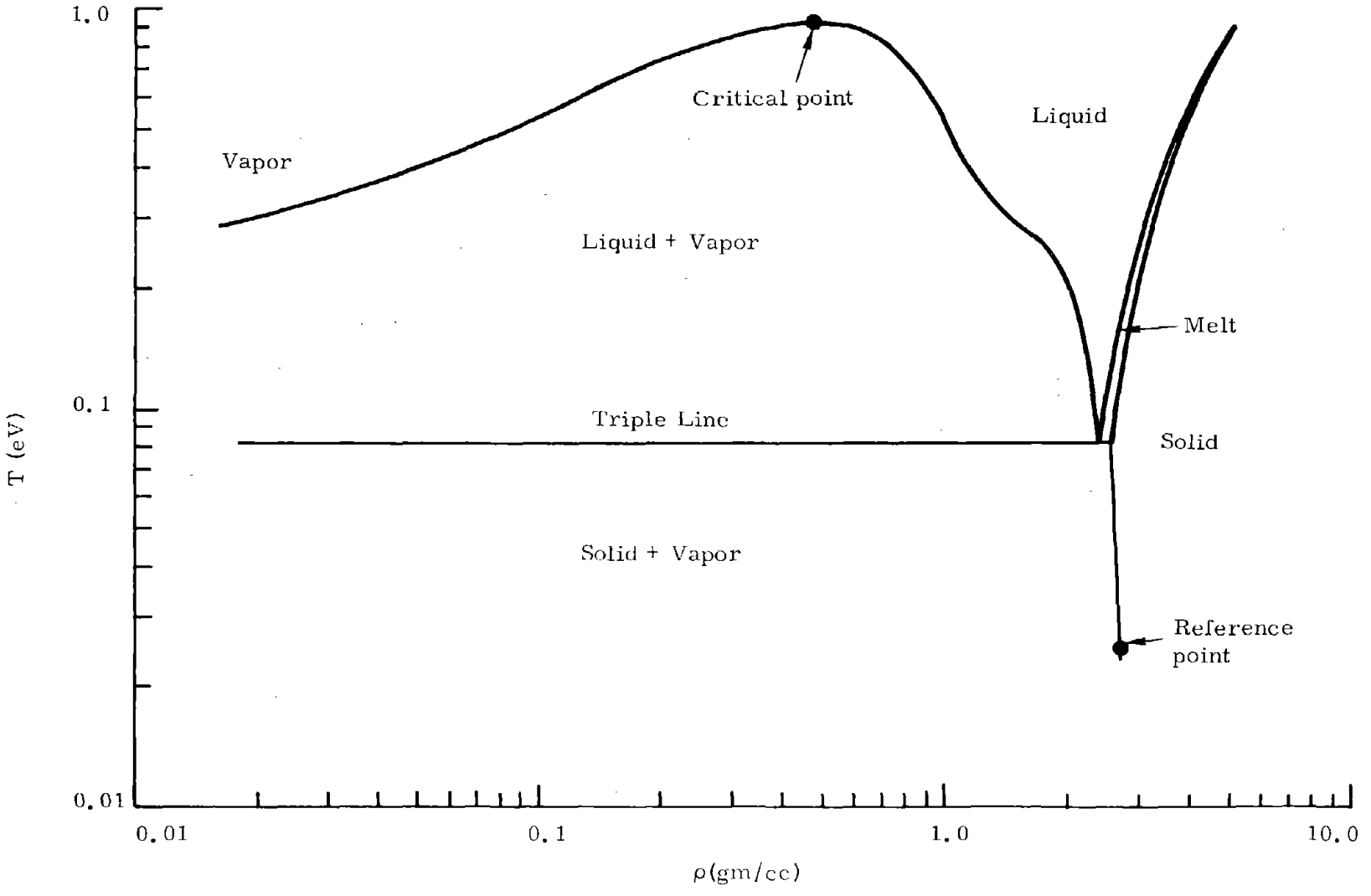

Fig. 3 Extended phase diagram for aluminum.

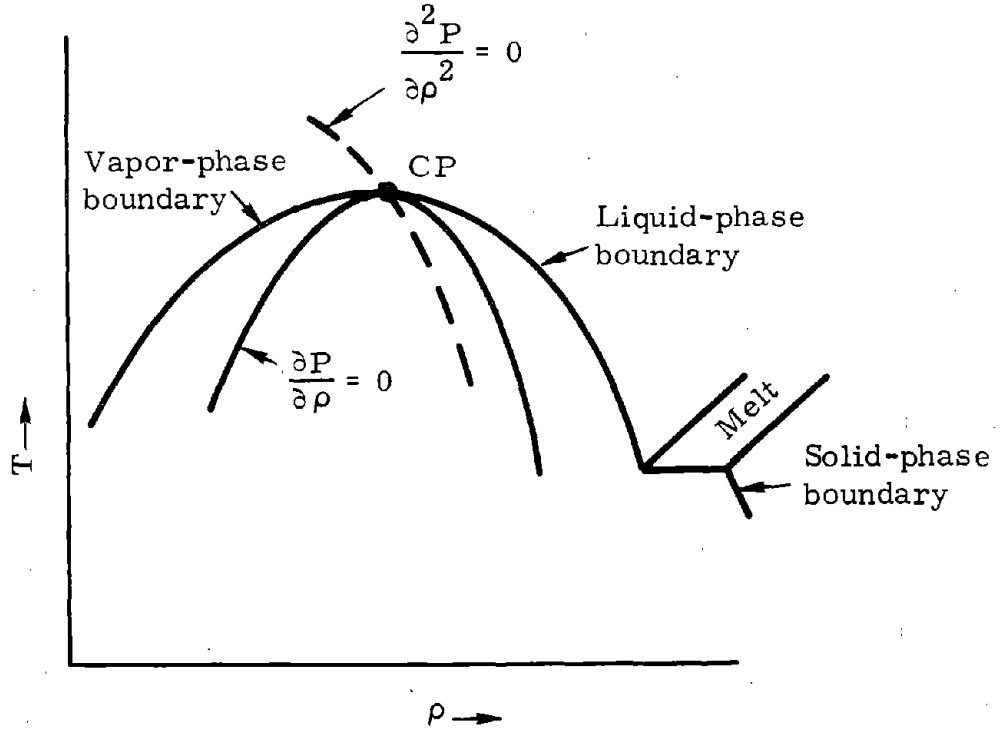

Fig. 4 Normal properties of a state surface.

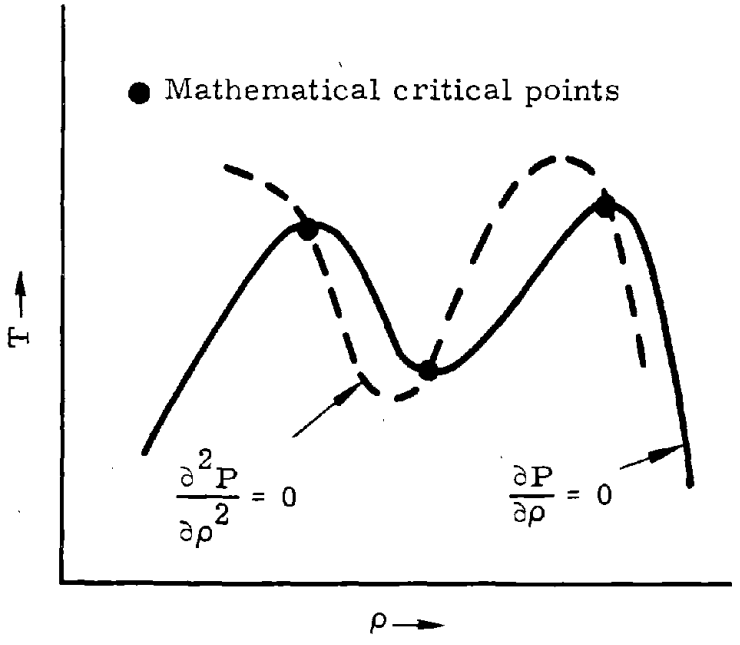

Fig. 5 Abnormal properties of a state surface with multiple critical points.

In the running mode, the EOS package must be called, with temperature and density defined. The routines first check to determine whether the point in question lies in a region where a liquid-vapor or solid-vapor state might exist. When the results of this test are positive, phase densities are interpolated from the stored arrays. The check given by (5.6) is then applied. In the current situation, 1 = vapor and 2 = x, as defined above. For a mixed-phase state the thermodynamic functions are determined by using Eqs. (5.7) through (5.16), except that (5.11) is modified slightly in some cases when $M_x \approx 1$ to insure continuity. The phase density derivatives are determined directly from the interpolation expressions so that (5.18) is not used.

V-3. Tensions in Solid Materials

To properly treat the response of solid materials, allowance must be made for regions of tensions ($P < 0$) in the state functions. In CHART D this is accomplished by using a part of the one-phase surface in a region that, by equilibrium thermodynamic logic, should be a mixed-phase solid-vapor state. Figure 6-4 in R4 illustrates the procedure used for both the tabular and analytic EOS forms. For any state where

$$\rho \geq \rho_{min}, \quad T \leq T_{min}, \tag{5.54}$$

the one-phase result is used. The term ρ_{min} is an input parameter with a default value of $0.8\,\rho_o$. The above condition includes solid, solid-liquid, and a small pure liquid region on the one-phase state surface.

There are two checks which should be applied to ρ_{min}. First of all, the tensions allowed should be more than sufficient to satisfy the fracture models; i.e., $P(\rho_{min}, T)$, $T \leq T_m$ must be larger in magnitude than any stress calculated in the code before fracture. Clearly, this means that at least

$$\rho_{min} < \rho_{\ell m}, \tag{5.55}$$

where $\rho_{\ell m}$ is the density of the liquid at the triple line as discussed in Section V-1. A nonfatal message will be generated if (5.55) is not satisfied.

The other condition is numerical and related to the melt transition. The results for aluminum are shown in Fig. 6. Note that the melt transition extends into the tension region and intersects the line at ρ_{min} (= 2.305 gm/cc). For numerical reasons it is required that the solid-phase line and ρ_{min} intersect. In some cases the code will increase the value of ρ_{min} to satisfy this requirement. However no automatic adjustment in conflict with (5.55) is allowed. In this case the code will generate a message concerning a low-temperature melt error, and an alternate treatment of the melt transition described in the next section will be used.

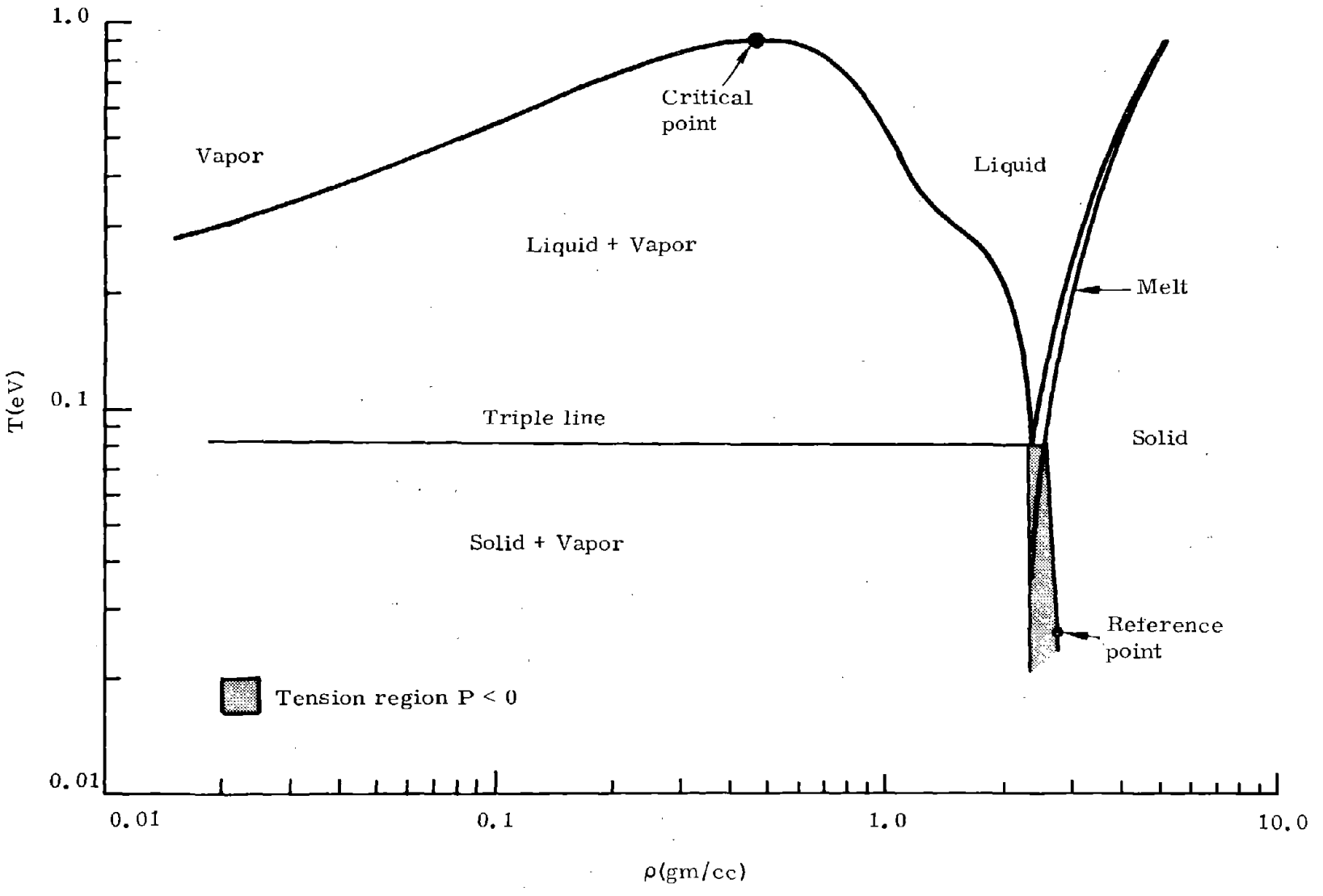

Fig. 6 Tension region for solids.

V-4. Alternate Treatment of Melting

In many problems the full treatment of the melt transition given in Section V-1 is not required. Some of the more obvious are calculations where the material is either well above or below melt. For these cases an alternate method is provided.

This calculation was the only option provided in R2 and is, in reality, no special calculation at all. The melt corrections are not included and the liquid and solid equations of state are identical. In this case

$$\rho_{\ell m} = \rho_{sm} \tag{5.56}$$

and

$$H_f = 0 \ , \tag{5.57}$$

as related to Section V-1. On the other hand, the tension region of Section V-3 is retained.

It is suggested that this option be used whenever possible after the relation of the melt temperature and energy below are studied.

V-5. Relation of Melt Temperature and Energy

Input options are provided so that either the melt temperature T_m or the melt point energy E_m may be defined. These quantities are related so that only one can be specified. In either case T_m is the variable stored. When E_m is given, the code follows the zero pressure isobar to find a temperature corresponding to E_m.

The variable E_m can represent two different quantities, depending on which treatment of the melt transition is employed. For the full calculation of Section V-1, E_m is the energy of incipient melt with respect to the reference point. This is expressed as

$$E_m = E_s(\rho_{sm}, T_m) - E_s(\rho_o, T_o) \tag{5.58}$$

in the notation of (5.33).

For the simplified treatment of melting in Section V-4, E_m should be the energy of completed melt. The two values differ by the heat of fusion H_f. Obviously, the latter method will yield a higher melting temperature than the former.

The heats of fusion for most simple materials are all well known. For those substances where H_f is not available, a simple scaling relation has been developed by Grover.[18] Expressed in the units of current interest, the result is

$$H_f = 1.117 \times 10^{12} \frac{T_m}{A} \left(\frac{ergs}{gm}\right) , \tag{5.59}$$

where A is the atomic weight.

V-6. Alternate Treatment of Liquid-Vapor and Solid-Vapor Transitions

The detailed computation explained in Section V-2 is not required for some problems. One of the more obvious cases is where the temperatures remain below melt and the mixed-phase regions are never entered. An alternate method of treatment, similar in concept to that in Section V-4 is provided.

This calculation simply ignores the existence of phase mixtures and evaluates from the single-phase surface, except that tensions are suppressed above the melt temperature. This violates a multitude of thermodynamic inequalities and destroys the carefully constructed self-consistence of the EOS information. For this reason it is suggested that this option only be used for materials that remain in the solid state. Under this condition, the results of the present calculation are identical to those of the more complex form and there is a saving of computer time.

This computation is employed as a backup to the more detailed method. In case of a catastrophic failure of the iterations in Section V-2 during the generate mode, this form is tried in order to save the calculation. Error messages are generated when this occurs. The test programs in R5 should be used to locate and correct the difficulty.

V-7. Simple Solid-Solid Transitions*

As discussed in Section III, many substances undergo phase transitions upon compression which result in a more closely packed structure and decreased compressibility. In this section, a method is given whereby some such transitions may be treated in an approximate manner. Both first- and second-order transitions are considered. However, the discussion is restricted to cases that do not depend on the temperature. In many instances, especially those that occur at high pressures, this seems sufficient. This restriction allows all changes to be made in the cold components. The thermal components will not be altered. While this procedure is surely not completely correct, it does allow at least a partial treatment.

---

*This section is identical to Section IX in R2.

In Fig. 7, three types of cold compression curves and the associated Hugoniots are shown. Curve (a) is for a simple material showing no apparent phase changes. This type of data is treated by the method given in Section III. Curves (b) and (c) represent second- and first-order changes, respectively. The second-order transition is clearly a special case of the first-order transition. Thus all relations developed below will be for the more complex case.

The notation is as shown in Fig. 7. The term P_{tr} is the pressure at which the first odd behavior is noted in the Hugoniot. The term P_{ctr} is the cold pressure and ρ_1 is the density at this point. The lower density Phase 1 exists at this density and below. The higher density Phase 2 exists for $\rho \geq \rho_2$, where $\rho_2 \geq \rho_1$. If $\rho_2 = \rho_1$, the transition is of the second order; if $\rho_2 > \rho_1$, it is of the first.

Denote

$$\eta_1 = \rho_1/\rho_{oo} \tag{5.60}$$

and

$$\eta_2 = \rho_2/\rho_{oo} \ . \tag{5.61}$$

A three-part description of P_c is required. In the region $\eta \leq \eta_1$, Eq. (3.4) is employed with a slight modification. At $\eta = \eta_1$, we require that $P_c = P_{ctr}$. As (3.4) has no free parameters, this is accomplished by ignoring condition (3.11). An effective value of T_Γ is calculated so that the above requirement is satisfied. New values of C_{34}, C_{35}, C_{36}, and C_{37} are computed.

In the region $\eta_1 < \eta \leq \eta_2$, the value of $P_c = P_{ctr}$ is constant. The energy is given by

$$\begin{aligned} E_c(\eta) &= E_c(\eta_1) + \frac{P_{ctr}}{\rho_{oo}} \int_{\eta_1}^{\eta} \frac{d\eta}{\eta^2} \\ &= E_c(\eta_1) + \frac{P_{ctr}}{\rho_{oo}} \left\{ \frac{\eta - \eta_1}{\eta \eta_1} \right\} \ , \ \eta_1 < \eta \leq \eta_2 \ , \end{aligned} \tag{5.62}$$

where $E_c(\eta_1)$ is computed by (3.17). In this region a unique Hugoniot curve may not be defined. If the thermal components of pressure do not increase with sufficient rapidity, a two-wave shock structure will result. Discussions of this phenomenon are found in Al'tshuler's work.[15]

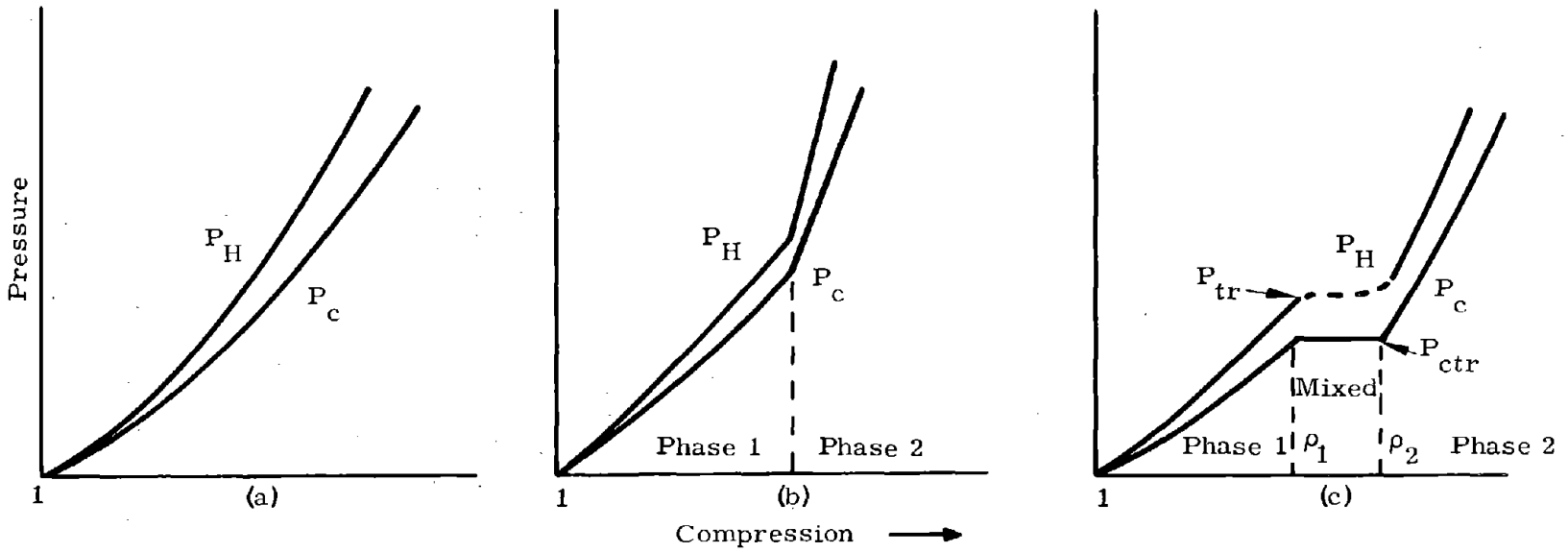

Fig. 7 Three types of Hugoniots. Curve (a) indicates no phase transition, curve (b), second-order phase transition, and curve (c), first-order phase transition.

For $\eta > \eta_2$, the form given by (3.4) is again employed but with new coefficients in the interpolation terms,

$$P_c(\eta) = C_{32}\eta^{5/3}\exp(-C_{33}\eta^{-1/3}) - \{C_{38}+C_{39}\eta^{1/3}+C_{40}\eta^{2/3}\} ,$$

$$\eta > \eta_2 , \tag{5.63}$$

where C_{32} and C_{33} are as previously defined. The remaining coefficients are determined by the value of P_c and its first two derivatives at η_2. The energy is given by

$$E_c(\eta) = C_9 + \frac{1}{\rho_{oo}} \left\{ 3C_{32}\eta^{2/3}\mathscr{E}_3(C_{33}\eta^{-1/3}) + \frac{C_{38}}{\eta} + \frac{3}{2}\frac{C_{39}}{\eta^{2/3}} + \frac{3C_{40}}{\eta^{1/3}} \right\} , \tag{5.64}$$

where

$$C_9 = E_c(\eta_1) - \frac{1}{\rho_{oo}} \left\{ 3C_{32}\eta_2^{2/3}\mathscr{E}_3(C_{33}\eta_2^{-1/3}) + \frac{C_{38}}{\eta_2} + \frac{3}{2}\frac{C_{39}}{\eta_2^{2/3}} + \frac{3C_{40}}{\eta_2^{1/3}} \right\} , \tag{5.65}$$

$\mathscr{E}_3$ is given by (3.19), and $E_c(\eta_2)$ is computed from (5.62). For pressures sufficiently high, a well-defined Hugoniot is again formed in this region for compressions somewhat greater than η_2.

Some approximate relations can be given for the form of the Hugoniot for the above relations. However, this calculation has not as yet been fully tested in hydrodynamic code use. The interaction with nonthermodynamic quantities, e.g., artificial viscosity, is not completely known. For this reason only the input quantities will be given here, and it is suggested that this calculation be used only with the greatest care.

Five input quantities are required. Let these be denoted by D_1, D_2, D_3, D_4, and D_5. D_1 is the density ρ_1. If $D_1 < \rho_{oo}$, this calculation is not used. D_2 is the density ρ_2. If $D_2 < D_1$, the value of D_2 is set equal to D_1. This defines a second-order transition. D_3 is the pressure P_{ctr}. If $D_3 \leq 0$, the value of T_Γ used in Section III is employed to calculate D_3. D_4 is related to $\left.\frac{dP_c}{d\eta}\right|_{\eta_2}$.

If

$$\begin{aligned} &D_4 > 0 , \quad \left.\frac{dP_c}{d\eta}\right|_{\eta_2} = D_4 ; \\ &D_4 = 0 , \quad \left.\frac{dP_c}{d\eta}\right|_{\eta_2} = \left(\frac{\eta_2}{\eta_1}\right)\left.\frac{dP_c}{d\eta}\right|_{\eta_1} ; \\ &D_4 < 0 , \quad \left.\frac{dP_c}{d\eta}\right|_{\eta_2} = -D_4 \left.\frac{dP_c}{d\eta}\right|_{\eta_1} . \end{aligned} \tag{5.66}$$

D_5 is related to $\left.\frac{d^2P_c}{d\eta^2}\right|_{\eta_2}$.

If

$$
\begin{aligned}
&D_5 > 0 \ , \quad \left.\frac{d^2P_c}{d\eta^2}\right|_{\eta_2} = D_5 \ ; \\
&D_5 = 0 \ , \quad \left.\frac{d^2P_c}{d\eta^2}\right|_{\eta_2} = \left(\frac{\eta_2}{\eta_1}\right)^2 \left.\frac{d^2P_c}{d\eta^2}\right|_{\eta_1} \ ; \qquad (5.67) \\
&D_5 < 0 \ , \quad \left.\frac{d^2P_c}{d\eta^2}\right|_{\eta_2} = - D_5 \left.\frac{d^2P_c}{d\eta^2}\right|_{\eta_1} .
\end{aligned}
$$

Note that if D_1 is properly defined but $D_2 = D_3 = D_4 = D_5 = 0$, no transition occurs, since all functions are continuous.

VI. ELECTRONIC CONTRIBUTION TO THE EQUATION OF STATE*

In nearly all calculations of the equation of state, the electronic contribution is the most complex and costly. There are two methods of determining these terms in common use. At low densities, ionization equilibrium calculations are appropriate and, with valid expressions for electrostatic interactions, can be used at relatively high densities. For high compressions, temperature-dependent Thomas-Fermi calculations are available.

One of the fundamental differences in these two calculations is that, in the former, the average thermodynamics is computed with regard for all possible systems, whereas in the latter the thermodynamics of a single average system is calculated. In spite of this and numerous other differences, it has been found that the two methods, properly employed, are not in serious disagreement. It should be remembered that the electronic term is defined to vanish at zero temperature. Hence the zero-temperature Thomas-Fermi values must be subtracted from the normal calculation of the same density. This eliminates many of the effects of degeneracy. Surprisingly, the largest differences in the two calculations, in regions where electronic terms are important, occur at relatively high temperatures where the ionization calculation yields an atomic shell structure effect that the Thomas-Fermi calculation does not.

---

*This section is identical to Section V in R2.

The method used here is the simplest available. The average atom ionization model developed by the Russians, with modifications for low and high degrees of ionization, is of both sufficient accuracy and speed to be used in a calculation of this type. Any number of elements can be treated with a very dependable method. The reader is referred to the excellent text of Zel'dovich and Raizer[19] for a complete discussion. Here, only the information required for numerical evaluation is given.

In the original development of the routines given here, it was planned that the ionization calculation should be used only at low densities and high temperatures. An exact and consistent table of scaled temperature-dependent Thomas-Fermi values was available.[20] However, once it was discovered that the two calculations were quite similar, the method was changed to the present form. There is a considerable saving in storage requirements, and the problem of switching calculations in a consistent manner is eliminated.

The following notations are used:

Z_ℓ = atomic number of element ℓ

A_ℓ = atomic weight of element ℓ

m_ℓ = atomic mass of element ℓ

C_ℓ = number fraction of element ℓ

N_o = total number of atoms per unit mass

N_ℓ = number of ℓ atoms per unit mass

N_e = number of free electrons per unit mass

N_ℓ^i = number of ℓ atoms per unit mass of net ionic charge i

I_ℓ^i = $i^{\underline{th}}$ ionization potential of element ℓ

$\overline{m}$ = average atomic mass

$\overline{Z}_\ell$ = average ionization number of element ℓ

$\overline{Z}$ = average ionization number

$\overline{A}$ = average atomic weight

Z_m = average atomic number

Self-obvious relations involving these quantities that will later be required are:

$$\sum_{\ell} C_{\ell} = 1 \ , \tag{6.1}$$

$$\overline{A} = \sum_{\ell} C_{\ell} A_{\ell} \ , \tag{6.2}$$

$$m_{\ell} = A_{\ell}/N_{av} \ , \tag{6.3}$$

$$\overline{m} = \overline{A}/N_{av} = \sum_{\ell} C_{\ell} m_{\ell} \ , \tag{6.4}$$

$$Z_m = \sum_{\ell} C_{\ell} Z_{\ell} \ , \tag{6.5}$$

$$\overline{Z}_{\ell} = \sum_{i} i N_{\ell}^{i} \ , \tag{6.6}$$

$$\overline{Z} = \sum_{\ell} C_{\ell} \overline{Z}_{\ell} \ , \tag{6.7}$$

$$N_e = \overline{Z} N_o \ , \tag{6.8}$$

$$N_{\ell} = C_{\ell} / \overline{m} = \sum_{i} N_{\ell}^{i} \ , \tag{6.9}$$

and

$$N_o = \sum_{\ell} N_{\ell} \ , \tag{6.10}$$

where N_{av} is the Avogadro number.

The principle problem in this calculation is determination of the average degree of ionization of the various atoms. Ideal gas relations are used in computing the thermodynamics. No pressure ionization or related effects are considered. The electronic free energy is

$$F_e = - \overline{Z} N_o kT \left\{ \ell n \left(\frac{A T^{3/2}}{\rho N_o \overline{Z}} \right) + 1 \right\} + \sum_{\ell} N_{\ell} Q(\overline{Z}_{\ell}) \ , \tag{6.11}$$

where

$$A = \frac{2(2\pi M_e k)^{3/2}}{h^3} \simeq 6 \times 10^{21} (\text{ev})^{-3/2} \text{ cm}^{-3} , \tag{6.12}$$

$$Q(\overline{Z}_\ell) = \sum_{i=1}^{k} I_\ell^i + (\overline{Z}_\ell - k) I_\ell^{k+1} , \tag{6.13}$$

and $k = k(\ell)$ is the next integer smaller than $\overline{Z}_\ell$. The relations of interest are

$$P_e = \overline{Z} N_o \rho k T , \tag{6.14}$$

$$E_e = \frac{3}{2} \overline{Z} N_o k T + \sum_\ell N_\ell Q(\overline{Z}_\ell) , \tag{6.15}$$

$$S_e = \overline{Z} N_o k \left\{ \ell n \left(\frac{A T^{3/2}}{\rho N_o \overline{Z}} \right) + 5/2 \right\} , \tag{6.16}$$

$$C_{ve} = 3/2 \, N_o k \left\{ \overline{Z} + T \frac{\partial \overline{Z}}{\partial T} \right\} + \sum_\ell N_\ell I_\ell^{k+1} \frac{\partial \overline{Z}_\ell}{\partial T} , \tag{6.17}$$

$$\frac{\partial P_e}{\partial T} = N_o \rho k \left\{ \overline{Z} + T \frac{\partial \overline{Z}}{\partial T} \right\} , \tag{6.18}$$

and

$$\frac{\partial P_e}{\partial \rho} = N_o k T \left\{ \overline{Z} + \rho \frac{\partial \overline{Z}}{\partial \rho} \right\} . \tag{6.19}$$

In an ionization equilibrium calculation, the ionic populations are determined by a set of equations of the form

$$\frac{N_\ell^i}{N_\ell^{i-1}} = K(\rho, T) , \tag{6.20}$$

subject to the constraints on the total number of particles given by (6.9). The function $K(\rho, T)$ can be extremely complex in detailed calculations. In the simplest case, the normal Saha equations, it can be shown that[21]

$$K(\rho, T) = \frac{U_\ell^i}{U_\ell^{i-1}} \exp\left\{-\frac{\mu_e + I_\ell^i}{kT}\right\}$$

$$= \frac{U_\ell^i}{U_\ell^{i-1}} \frac{2(2\pi M_e kT)^{3/2}}{\rho N_e h^3} \exp\left(-\frac{I_\ell^i}{kT}\right) \tag{6.21}$$

by matching chemical potentials through appropriate relations, where U_ℓ^i is the internal partition function, μ_e is the electronic chemical potential, and nondegenerate statistics are assumed. All U_ℓ^i are assumed to be equal. By combining (6.12), (6.20), and (6.21), it is easily shown that

$$\frac{N_\ell^i}{N_\ell^{i-1}} = \frac{AT^{3/2}}{\rho N_e} \exp\left(-\frac{I_\ell^i}{T}\right) , \tag{6.22}$$

where both the temperature and ionization potential are in units of electron volts.

The above set of equations may be solved by iteration. However, the Russian method is considerably faster, requires less storage, and usually yields nearly the same result. For reasons that will become clear shortly, there are separate calculations for single- and multi-element materials.

VI-1. Single-Element Ionization

First consider low and high degrees of ionization. These two cases will be solved exactly, with the assumption that only two ionic species are present. The subscript ℓ, denoting the element number, will be retained for continuity.

For $\overline{Z} \leq 1/2$, it is assumed that only neutral and singly ionized atoms are present. It then follows that

$$N_e = N_\ell^1 = \overline{Z} N_o , \tag{6.23}$$

$$N_\ell^o = N_o(1 - \overline{Z}) , \tag{6.24}$$

and

$$\frac{N_\ell^1}{N_\ell^o} = \frac{\overline{Z}}{1 - \overline{Z}} = \frac{K_1}{\overline{Z}} , \tag{6.25}$$

where

$$K_1 = \frac{AT^{3/2}}{\rho N_o} \exp(-I_\ell^1/T) \tag{6.26}$$

and T and I_ℓ^1 are both assumed to be in units of electron volts. Clearly, the desired quantities are

$$\overline{Z} = \frac{1}{2} \left\{ \sqrt{K_1^2 + 4K_1} - K_1 \right\} , \tag{6.27}$$

$$\frac{\partial \overline{Z}}{\partial T} = \frac{K_1}{T} \left(\frac{1 - \overline{Z}}{K_1 + 2\overline{Z}} \right) \left(\frac{3}{2} + \frac{I_\ell^1}{T} \right) , \tag{6.28}$$

and

$$\frac{\partial \overline{Z}}{\partial \rho} = - \frac{K_1}{\rho} \left(\frac{1 - \overline{Z}}{K_1 + 2\overline{Z}} \right) . \tag{6.29}$$

When $\overline{Z} \geq Z_\ell - 1/2$, only the ions of net charge Z_ℓ and $Z_\ell - 1$ are present. In this case

$$N_e = \overline{Z} N_o = Z_\ell N_\ell^{Z_\ell} + (Z_\ell - 1) N_\ell^{Z_\ell - 1} \tag{6.30}$$

and

$$N_o = N_\ell = N_\ell^{Z_\ell} + N_\ell^{Z_\ell - 1} . \tag{6.31}$$

With the definition

$$K_2 = \frac{AT^{3/2}}{\rho N_o} \exp(-I_\ell^{Z_\ell}/T) , \tag{6.32}$$

the result is easily shown to be

$$\overline{Z} = \frac{1}{2}\left\{Z_\ell - 1 - K_2 + \sqrt{(Z_\ell - 1 - K_2)^2 + 4K_2 Z_\ell}\right\} , \tag{6.33}$$

$$\frac{\partial \overline{Z}}{\partial T} = \frac{K_2}{T}\left\{\frac{Z_\ell - \overline{Z}}{2\overline{Z} - K_2 + Z_\ell - 1}\right\}\left\{\frac{3}{2} + \frac{I_\ell^{Z_\ell}}{T}\right\} , \tag{6.34}$$

and

$$\frac{\partial \overline{Z}}{\partial \rho} = -\frac{K_2}{\rho}\left\{\frac{Z_\ell - \overline{Z}}{2\overline{Z} - K_2 + Z_\ell - 1}\right\} . \tag{6.35}$$

If neither of the above calculations apply, the Russian method is used in the range $1/2 < \overline{Z} < Z_\ell - 1/2$. Equation (6.22) is replaced by an expression of the form

$$\overline{Z} = \frac{AT^{3/2}}{\rho N_o} \exp\left(-\overline{I}_\ell / T\right) , \tag{6.36}$$

where $\overline{I}_\ell$ is an interpolated ionization potential function. If n is an integer and

$$n - 1/2 \le \overline{Z} < n + 1/2 , \tag{6.37}$$

then

$$\overline{I}_\ell = I_\ell^n(n + 1/2 - \overline{Z}) + I_\ell^{n+1}(\overline{Z} + 1/2 - n) . \tag{6.38}$$

The value of $\overline{Z}$ is adjusted by a Newton's iteration until Eqs. (6.36) and (6.38) are satisfied. The derivatives are obtained from

$$\frac{\partial \overline{Z}}{\partial T} = \overline{Z}\left\{\frac{3}{2} + \frac{\overline{I}_\ell}{T}\right\} \Big/ \left\{T + \overline{Z}\,\Delta\,\overline{I}_\ell\right\} \tag{6.39}$$

and

$$\frac{\partial \overline{Z}}{\partial \rho} = -\frac{\overline{Z}T}{\rho\{T + \overline{Z}\,\Delta\,\overline{I}_\ell\}} , \tag{6.40}$$

where

$$\Delta\overline{I}_\ell = I_\ell^{n+1} - I_\ell^n . \tag{6.41}$$

This is the complete single-element calculation.

VI-2. Multiple-Element Ionization

The multielement calculation is similar to the single-element version. Here a value of $\overline{Z}$ is guessed and the values of $\overline{Z}_\ell$ calculated as described below. In general, this set of $\overline{Z}_\ell$ will not yield a value of $\overline{Z}$ by (6.7) consistent with the assumed value. Again we use a Newton's correction, where

$$\Delta\overline{Z} = \frac{\overline{Z} - \sum_\ell C_\ell \overline{Z}_\ell}{\sum_\ell C_\ell \frac{\partial \overline{Z}_\ell}{\partial \overline{Z}} - 1} \tag{6.42}$$

is the change in $\overline{Z}$ for the next iteration.

For each element the calculation is similar to the previous one, except that both $\overline{Z}$ and $\overline{Z}_\ell$ are included in each relation. The results are, for $\overline{Z}_\ell \leq 1/2$:

$$\overline{Z}_\ell = K_{\ell 1}/(K_{\ell 1} + \overline{Z}) \ , \tag{6.43}$$

$$\frac{\partial \overline{Z}_\ell}{\partial \overline{Z}} = \frac{(\overline{Z}_\ell)^2}{K_{\ell 1}} = -\frac{K_{\ell 1}}{(K_{\ell 1} + \overline{Z})^2} \ , \tag{6.44}$$

$$\frac{\partial \overline{Z}_\ell}{\partial T} = \frac{\overline{Z}(\overline{Z}_\ell)^2}{K_{\ell 1} T}\left\{\frac{3}{2} + \frac{I_\ell^1}{T}\right\} - \frac{K_{\ell 1}}{(K_{\ell 1} + \overline{Z})^2}\frac{\partial \overline{Z}}{\partial T} \ , \tag{6.45}$$

and

$$\frac{\partial \overline{Z}_\ell}{\partial \rho} = -\frac{\overline{Z}(\overline{Z}_\ell)^2}{K_{\ell 1}\rho} - \frac{(\overline{Z}_\ell)^2}{K_{\ell 1}}\frac{\partial \overline{Z}}{\partial \rho} \ , \tag{6.46}$$

with

$$K_{\ell 1} = \frac{AT^{3/2}}{\rho N_o} \exp\left(-\frac{I_\ell^1}{T}\right) \ . \tag{6.47}$$

For $\overline{Z}_\ell \geq Z_\ell - 1/2$:

$$\overline{Z}_\ell = Z_\ell - \frac{\overline{Z}}{\overline{Z} + K_{\ell 2}} \ , \tag{6.48}$$

$$\frac{\partial \overline{Z}_\ell}{\partial \overline{Z}} = - \frac{K_{\ell 2}}{(Z + K_{\ell 2})^2} , \tag{6.49}$$

$$\frac{\partial \overline{Z}_\ell}{\partial T} = \frac{\overline{Z}}{(\overline{Z} + K_{\ell 2})^2} \frac{K_{\ell 2}}{T} \left\{ \frac{3}{2} + \frac{I_\ell^{Z_\ell}}{T} \right\} - \frac{K_{\ell 2}}{(\overline{Z} + K_{\ell 2})^2} \frac{\partial \overline{Z}}{\partial T} , \tag{6.50}$$

and

$$\frac{\partial \overline{K}_\ell}{\partial \rho} = - \frac{\overline{Z} K_{\ell 2}}{\rho (\overline{Z} + K_{\ell 2})^2} - \frac{K_{\ell 2}}{(\overline{Z} + K_{\ell 2})^2} \frac{\partial \overline{Z}}{\partial \rho} , \tag{6.51}$$

with

$$K_{\ell 2} = \frac{A T^{3/2}}{\rho N_o} \exp \left(- I_\ell^{Z_\ell} / T \right) . \tag{6.52}$$

For $1/2 < \overline{Z}_\ell < Z_\ell - 1/2$:

$$\overline{Z}_\ell = \frac{I_\ell^{n+1} (n - 1/2) - I_\ell^n (n + 1/2) + T \ell n \left\{ \dfrac{A T^{3/2}}{\overline{Z} \rho N_o} \right\}}{\Delta I_\ell^n} , \tag{6.53}$$

$$\frac{\partial \overline{Z}_\ell}{\partial \overline{Z}} = - \frac{T}{\overline{Z} \Delta I_\ell^n} , \tag{6.54}$$

$$\frac{\partial \overline{Z}_\ell}{\partial T} = \left\{ \ell n \left(\frac{A T^{3/2}}{\overline{Z} \rho N_o} \right) + \frac{3}{2} - \frac{T}{\overline{Z}} \frac{\partial \overline{Z}}{\partial T} \right\} / \Delta I_\ell^n , \tag{6.55}$$

and

$$\frac{\partial \overline{Z}_\ell}{\partial \rho} = - \left\{ \frac{T}{\rho} + \frac{T}{\overline{Z}} \frac{\partial \overline{Z}}{\partial \rho} \right\} / \Delta I_\ell^n , \tag{6.56}$$

where n is an integer,

$$n - 1/2 \leq \overline{Z}_\ell < n + 1/2 \quad , \tag{6.57}$$

and

$$\Delta I_\ell^n = I_\ell^{n+1} - I_\ell^n \quad . \tag{6.58}$$

The derivatives of $\overline{Z}$ required in (6.17), (6.18), and (6.19) are calculated by noting in each of the above cases that

$$\frac{\partial \overline{Z}_\ell}{\partial T} = \alpha_\ell + \frac{\partial \overline{Z}_\ell}{\partial \overline{Z}} \frac{\partial \overline{Z}}{\partial T} \tag{6.59}$$

and

$$\frac{\partial \overline{Z}_\ell}{\partial \rho} = \beta_\ell + \frac{\partial \overline{Z}_\ell}{\partial \overline{Z}} \frac{\partial \overline{Z}}{\partial \rho} \quad , \tag{6.60}$$

where α_ℓ and β_ℓ are known. With the application of (6.7), the result is

$$\frac{\partial \overline{Z}}{\partial T} = \frac{\sum C_\ell \alpha_\ell}{1 - \sum C_\ell \dfrac{\partial \overline{Z}_\ell}{\partial \overline{Z}}} \tag{6.61}$$

and

$$\frac{\partial \overline{Z}}{\partial \rho} = \frac{\sum C_\ell \beta_\ell}{1 - \sum C_\ell \dfrac{\partial \overline{Z}_\ell}{\partial \overline{Z}}} \quad , \tag{6.62}$$

which completes the multielement calculation.

VII. RADIATION FIELD AND ENERGY TRANSPORT PROPERTIES

The thermodynamic properties of the radiation field are not included as part of the analytic equation-of-state package in the current coding. In CHART D the radiation terms are added in a separate computation as detailed in R4. At sufficiently elevated temperatures, these terms are dominant. If it is desirable to include these terms in the package, the best position would be just before the computation of the sound speed in the subroutine ANEOS (see card 4082 in Appendix G of R4).

Since this EOS package is to operate in a radiation diffusion-hydrodynamic code, a value must also be supplied for the Rosseland mean opacity. Define λ as the Rosseland mean free path and K_r as the Rosseland mean absorption coefficient. These two quantities are related by

$$\lambda = \frac{1}{\rho K_r} , \tag{7.1}$$

where ρ is the density.

It is possible to include the effects of other transport phenomena in the radiation diffusion relations. Complete details are given in R4. Two processes treated in this manner in the current coding are normal thermal conduction (phonon) and hot electron transport. The term K_r in (7.1) is replaced by K_{eff} where

$$\frac{1}{K_{eff}} = \frac{1}{K_r} + \frac{1}{K_H} + \frac{1}{K_L} . \tag{7.2}$$

Expressions for the three terms on the right hand side of (7.2) are developed below. However, it should be remembered that these are approximate relations and the results are not of the same caliber as the information in the tabular EOS.

VII-1. Rosseland Mean Opacity

An analytic formulation of the Rosseland mean which has the wide range of validity required for the present calculation was developed by the Russians in conjunction with the ionization calculation given earlier. The end result of their elegant calculation is[19]

$$K_R = \frac{10^{11} \rho \bar{Z} \overline{Z^2}}{\bar{A}^2 T^{7/2}} + \frac{0.4 Z_m}{\bar{A}} , \tag{7.3}$$

where

$$\overline{Z^2} = \sum_{\ell} C_{\ell} \overline{Z}_{\ell}^2 \quad . \tag{7.4}$$

At high temperatures, Eq. (7.3) gives answers close to the most detailed calculations available. In general, it tends to slightly overpredict K_r. At low temperatures, Eq. (7.3) is, of course, not valid; however, in this case, radiation diffusion is usually not important. The following material becomes dominant in (7.2).

VII-2. Thermal Conduction

At sufficiently low temperatures the most important term in (7.2) is the thermal or phonon conduction term. As with most properties of solids, it is hard to predict from theoretical models. A simple representation of experimental data is employed. Two input parameters are required.

The heat flux is

$$F_H = - H \nabla T \, , \tag{7.5}$$

where H is the conductivity and a characteristic function of the material. Generally, the dependence of H on density is slight, and it is possible to represent approximately the experimental data for many materials over limited ranges of temperature by the expression

$$H = H_o T^{C_{41}} \, , \tag{7.6}$$

where H_o and C_{41} are material constants and input parameters. The conduction term in (7.2) is then[4]

$$K_H = \frac{16\sigma T^3}{3\rho H} = \frac{C_{22} T^{3-C_{41}}}{\rho} \, , \tag{7.7}$$

where

$$C_{22} = \frac{16\sigma}{3H_o} \tag{7.8}$$

and σ is the Stefan-Boltzmann constant. Note that the units required of H are ergs/(cm sec eV) which should be reflected in H_o and C_{41}.

Obviously, it is not possible to describe abrupt changes in conductivity by (7.6). Such changes sometimes occur with phase transitions but data are limited. If these effects are important, either the coding must be modified or a tabular EOS should be employed.

VII-3. Hot Electron Conduction

At intermediate temperatures and high densities, the dominant energy transport mechanism is the diffusion of hot electrons. The relations to describe this phenomenon have been developed by Mestel[22] and put in good numerical form by Cox,[23]

Unfortunately, accurate evaluation requires good values of the electronic chemical potential. The calculation in Section VI assumed nondegenerate statistics, which affects the computed chemical potential. As a result, only the nondegenerate limit of the conductivity expressions can be used. However, a low-temperature modification is made to ensure a proper joining to the phonon conduction term.

The energy flux resulting from electron diffusion is written as[4]

$$F_L = - L \nabla T , \tag{7.9}$$

where L is the conductivity. In the nondegenerate limit[23]

$$L = \frac{32\, k^{7/2}\, T^{5/2}}{\pi \sqrt{2\pi m}\, e^4\, \overline{Z}\, \circledast} , \tag{7.10}$$

$$\circledast = \frac{1}{2} \ell n \left\{ \frac{2}{1 - \cos \theta} \right\} , \tag{7.11}$$

and

$$\theta = \left\{ \frac{N_o \rho}{3\pi^2} \right\}^{1/3} \frac{h}{\sqrt{3mkT}} \leq \frac{1}{2}\pi , \tag{7.12}$$

where k is Boltzmann's constant, m the electronic mass, e the electronic charge, h Planck's constant, $\overline{Z}$ is given by (6.7) and N_o by (6.10). The term $\circledast$ varies greatly only for small θ. In light of the other approximations, it seems reasonable to use

$$\circledast \sim \ell n \left(\frac{2}{\theta}\right) = \ell n \left\{ \frac{2\sqrt{3mk}\,(3\pi^2)^{1/3}\sqrt{T}}{h\,(\rho N_o)^{1/3}} \right\} = \ell n \left\{ \frac{6.18 \times 10^7 \sqrt{T}}{(\rho N_o)^{1/3}} \right\} \geq \frac{1}{2} \ell n\, 2 . \tag{7.13}$$

This approximation eliminates the necessity of computing the cosine function. The expression required for (7.2) is

$$K_L = \frac{16\sigma T^3}{3\rho L}$$

$$= \frac{\pi\sigma\sqrt{2\pi m}\, e^4 \sqrt{T}\, \bar{Z}\, \circledR}{6\, k^{7/2}\, \rho} \qquad (7.14)$$

$$= 416\, \sqrt{T}\, \bar{Z}\, \circledR/\rho\,.$$

There is a problem with this expression at low temperatures, since $\bar{Z}$ approaches zero so rapidly that (7.14) tends to overshadow the phonon conduction term. This unreasonable behavior is a result of the approximations and can be fixed by requiring

$$\bar{Z} \geq C_{42} = C_{22}/144\ , \qquad (7.15)$$

where C_{22} is given by (7.8). This strange relation results from forcing the electronic and phonon conduction terms to join smoothly together at a temperature of 1 eV. In the case that phonon conduction is not included,

$$C_{42} = 0.1 \qquad (7.16)$$

is assumed.

It must be admitted that the above relations are very crude representations of Mestel's expressions. However, unless the computation in Section VI is completely reworked, little improvement is possible. For the present purpose, it was felt that a crude approximation was better than completely ignoring the process. Much better values are available with the tabular EOS data.

VIII. HUGONIOT RELATIONS

An equation of state can be completely defined without any reference to experimental Hugoniot data. As a result, a routine is included to calculate the Hugoniot. In Section VIII-1, an input option is discussed which allows approximate inclusion of experimental data.

The Rankine-Hugoniot relations which describe the behavior at a shock front are well known. If ρ_i, T_i, P_i, and E_i are the initial conditions and ρ_s, T_s, P_s, and E_s are those of the shocked material, the conservation relations yield

$$E_s - E_i = \frac{1}{2}(P_s + P_i)\left\{\frac{\rho_s - \rho_i}{\rho_i \rho_s}\right\}. \tag{8.1}$$

At a fixed set of temperatures, the values of ρ_s which solve this expression are computed by an iterative procedure. The shock and material velocities are computed from the relations

$$U_s = \left\{\frac{P_s - P_i}{\rho_i(1 - \rho_i/\rho_s)}\right\}^{1/2} \tag{8.2}$$

and

$$U_m = U_s(1 - \rho_i/\rho_s). \tag{8.3}$$

The inputs required for this computation are ρ_i and T_i. As related in Appendix A, these variables are named RHUG and THUG. Any initial state can be defined, although the most interesting case is from the reference points ρ_o and T_o.

In some cases, approximate Hugoniots for distended materials may be determined with this computation. If the initial density is sufficiently small that it lies to the left of the shaded area in Fig. 6, the code will treat the material as a solid-vapor mixture. The initial pressure is the vapor pressure which is zero insofar as this calculation is concerned. This state is much like a porous material of zero crush strength. More exact calculations are available with the test programs in R5.

VIII-1. Relation of Experimental Hugoniot Data and Input Parameters

An option is available which permits experimental data to be defined in place of the parameters B_o and T_Γ defined in Section III. As is shown below, this computation is approximate, and results should be checked carefully.

It is often observed that experimental Hugoniot data may be expressed in the form

$$U_s = S_o + S_1 U_m \tag{8.4}$$

within experimental error, where S_o and S_1 are constants. It can easily be shown that (8.4) cannot describe any material to very high pressures. Neither is it possible to generate an EOS with the current package which will exactly satisfy (8.4). On the other hand, (8.4) is a good

approximation at low pressure for a large number of substances. Here, this is employed by using expansions of the thermodynamic functions about the points ρ_o and T_o and relating these to S_o and S_1.

If the initial state i is taken to be the reference point, (8.2) and (8.3) may be written as

$$P = P_o + \rho_o U_s U_m \tag{8.5}$$

and

$$\frac{\rho}{\rho_o} = \frac{U_s}{U_s - U_m} . \tag{8.6}$$

By combining these relations it may be shown that

$$\left(\frac{\partial P}{\partial \rho}\right)_s \Bigg|_{\rho_o T_o} = S_o^2 \tag{8.7}$$

and

$$\left(\frac{\partial^2 P}{\partial \rho^2}\right)_s \Bigg|_{\rho_o T_o} = \frac{2S_o^2}{\rho_o} (2S_1 - 1) , \tag{8.8}$$

where the well known property of second-order tangency between the Hugoniot and reference isentrope has been employed.[19] If it is assumed that the thermal component of pressure is independent of the density near $\rho = \rho_o$, the relation

$$\left(\frac{\partial P}{\partial \rho}\right)_s = \left(\frac{\partial P}{\partial \rho}\right)_T + \frac{T\left[\left(\frac{\partial P}{\partial T}\right)_\rho\right]^2}{\rho^2 C_v} \tag{8.9}$$

may be used to show that

$$\left(\frac{\partial P}{\partial \rho}\right)_s \Bigg|_{\rho_o T_o} = \left(\frac{\partial P}{\partial \rho}\right)_T \Bigg|_{\rho_o T_o} + 3\Gamma_o^2 N_o k T_o , \tag{8.10}$$

and hence

$$B_o = \rho_o \left\{ S_o^2 - 3\Gamma_o^2 N_o k T_o \right\} . \tag{8.11}$$

In the same manner the second derivative yields an expression for T_Γ. The relation is somewhat more complex than that in R2. The current form is

$$T_\Gamma = \frac{3\Phi \rho_o S_o^2}{B_o} \left\{ 2S_1 - 1 - \left(\frac{\Gamma_o - 2}{2} \right) \left(1 - \frac{B_o}{\rho_o S_o^2} \right) \right\} - 3\Gamma_o \ , \tag{8.12}$$

where

$$\Phi = \frac{\rho_{oo}^2 B_o}{\rho_o^2 B_{oo}} . \tag{8.13}$$

Unfortunately, neither ρ_{oo} or B_{oo} are known at this point in the calculation. The value Φ is near unity, but better values can be obtained by using the expressions

$$B_{oo} \approx \frac{1}{2} \left\{ C_1 (1 + 2 C_2) + B_o \right\} \left\{ 1 + \sqrt{1 - \frac{8 C_2 C_1^2}{C_1 (1 + 2 C_2) + B_o}} \right\} \tag{8.14}$$

and

$$\rho_{oo} \approx \rho_o \left\{ 1 - \frac{C_1}{B_{oo}} \right\}^{-1} , \tag{8.15}$$

where

$$C_1 = 3 \Gamma_o \rho_o N_o k T_o \tag{8.16}$$

and

$$C_2 = \frac{\Phi \rho_o S_o^2}{B_o} \left\{ 2 S_1 - 1 - \left(\frac{\Gamma_o - 2}{2} \right) \left(1 - \frac{B_o}{\rho_o S_o^2} \right) \right\} . \tag{8.17}$$

In (8.17), $\Phi = 1$ is used to allow solution without iteration.

Thus approximate values of the input parameters B_o and T_Γ may be determined from the experimental constants in (8.4). However, again it should be stressed that the results should be checked to determine their acceptability.

IX. PROPERTIES OF THE ANEOS PACKAGE

A complete listing of the ANEOS package is given in R4. In that version the dimensions are set for 20 different equations of state. The storage required on the CDC 6600 with the FUN compiler is about 37200 octal locations. The speed of evaluation varies considerably with the various options. An average is approximately 10^{-3} second per point (3.6×10^{6} points/hr), but it can easily vary by a factor of two either way. By far the slowest computation in the present package is for mixed liquid-solid states, as discussed in Section V-1. These will be improved in the future.

IX-1. Coding Structure

The entire ANEOS package is made up of 14 subroutines. The following list gives the name and purpose of each. Only those subroutines which may be called externally include the argument list.

(1)	ANEOS (T, RHO, P, E, S, CV, DPDT, DPDR, FKROS, CS, KPA, MAT)	Running entry point controls all calculations after initialization.
(2)	ANEOS1	Nuclear and cold components.
(3)	ANEOS2 (IGK, NUM, ITAPE, IZETL)	Main setup routine.
(4)	ANION1	Single-element ionization calculation.
(5)	ANION2	Multielement ionization calculation.
(6)	ANION3	A part of the multielement ionization calculation.
(7)	EPINT3	Evaluates the third exponential integral.
(8)	ANTWOPH	Evaluates thermodynamic functions for liquid-vapor and solid-vapor states.
(9)	ANPHASE	Setup for liquid-vapor and solid-vapor calculations.
(10)	ANMAXW	A part of the setup for liquid-vapor and solid-vapor calculations.
(11)	ANLS	Treats the liquid-solid (melt) transition.
(12)	ANHUG	Calculates Hugoniots.
(13)	ANPHTR	Setup for solid-solid transitions.
(14)	ANDATA	Contains all constants, such as ionization potentials, required by the other routines.

There are only three external links, detailed below (a, b, c), which couple the ANEOS package to the rest of the hydrodynamic code.

(a) Subroutine ANEOS is the running mode entry point. Three of the arguments must be defined as inputs to the computation. They are the temperature T, the density RHO, and MAT. The latter is the absolute value of the EOS number assigned to the material in question in the computation under item (b), below. All other arguments are computed by the various routines and returned as answers. P is pressure, E is the energy, S is the entropy, CV is the constant volume heat capacity, DPDT is the pressure derivative with respect to temperature, DPDR is the pressure derivative with respect to density, FKROS is the effective Rosseland mean absorption coefficient, and CS is the sound speed. The variable KPA indicates what type of phase structure is present. The code is

1 = A one-phase state for an EOS without the melt transition.

2 = A liquid-vapor or solid-vapor state.

3 = Indicates that a negative pressure has been set to zero as discussed in Section V-6. Code should not be run in this condition.

4 = A solid state for an EOS with the melt transition.

5 = A liquid-solid state for an EOS with the melt transition.

6 = A liquid state for an EOS with the melt transition. This also includes pure vapor states.

(b) Subroutine ANEOS2 is the initialization mode entry point. This computation must be completed before any calls to ANEOS are made. In CHART D this subroutine is called only once to generate all required equations of state. However, the coding is such that separate calls can be made for each material under consideration. Results can be requested from ANEOS for each material after that material has been initialized.

The argument IGK may be 1, 2, or 3. The initialization occurs for IGK = 1. NUM is the number of equations of state to be generated and IZETL is an array containing the EOS numbers. All data cards discussed in Appendix A are read during this call. When IGK = 2, a complete dump of the calculated constants sufficient to restart the computation is produced on tape unit ITAPE. For IGK = 3, this dump is read from ITAPE. The latter two calls are designed to operate in conjunction with hydrodynamic code restart options. No input cards are necessary for a restart.

(c) COMMON/BIG/ is used in subroutines ANHUG and ANDATA for initial data storage. The size of this block depends on the number of EOS stored in the library. After initialization is complete, the common block is not required and can be used elsewhere. In CHART D this space is used to store tabular EOS data read from tape following the ANEOS package initialization.

IX-2. Library Features

Library facilities have been provided as a convenience to the users so that frequently employed EOS information need not be punched for each problem. The required input data is listed in Appendix A. Basically, the information put on cards 2, 3, 4, and 5 is stored in data statements. Each user can modify the library to meet his requirements. For illustrative purposes, an example is shown at the end of subroutine ANDATA in the listing in R4. The information necessary to modify the library is obvious. The variable NUMTAB is the total number of library equations of state in the list and should be adjusted with each addition or deletion. The contents of the example library are given in Appendix C.

REFERENCES

1. Thompson, S. L., CHART D: A Computer Program for Calculating Problems of Coupled Hydrodynamic Motion and Radiation Flow in One Dimension, SC-RR-69-613, Sandia Laboratories, Albuquerque, New Mexico, November 1969.

2. Thompson, S. L., Improvements in the CHART D Radiation-Hydrodynamic Code I: Analytic Equations of State, SC-RR-70-28, Sandia Laboratories, Albuquerque, New Mexico, January 1970.

3. Thompson, S. L., User's Manual for CHART D, SC-DR-70-654, Sandia Laboratories, Albuquerque, New Mexico, December 1970.

4. Thompson, S. L., and Lauson, H. S., Improvements in the CHART D Radiation-Hydrodynamic Code II: A Revised Program, SC-RR-710713, Sandia Laboratories, Albuquerque, New Mexico, February 1972.

5. Thompson, S. L., and Lauson, H. S., Improvements in the CHART D Radiation-Hydrodynamic Code IV: User Aid Programs, SC-DR-710715, Sandia Laboratories, Albuquerque, New Mexico, February 1972.

6. Thompson, S. L. and McCloskey, D. J., THERMOS-A Thermodynamic Equation of State, Sandia Laboratories, Albuquerque, New Mexico, to be published.

7. Kirzhnits, D. A., JETP 32, 115 (1957), [Soviet Physics - JETP 5, 64 (1957)].

8. Kalitkin, N. N., JETP 38, 1534 (1960), [Soviet Physics - JETP 11, 1106 (1960)].

9. Al'tshuler, L. V., and Bakanova, A. A., USP. Fiz. Nauk 96, 193 (1968), [Soviet Physics - Uspekhi 11, 678 (1969)].

10. Kalitkin, N. N., and Govorukhina, I. A., Fizika Tverdoga Tela 7, 355 (1965), [Soviet Physics - Solid State 7, 287 (1965)].

11. Barnes, J. F., Phys. Rev. 153, 269 (1967).

12. Slater, J. C., Introduction to Chemical Physics (McGraw-Hill Book Co., New York, 1939).

13. Dugdale, J. S., and MacDonald, D. K. C., Phys. Rev. 89, 832 (1953).

14. Hirschfelder, J. O., Curtiss, C. F., and Bird, R. B., Molecular Theory of Gases and Liquids (John Wiley and Sons, New York, 1954).

15. Al'tshuler, L. V., Usp. Fiz. Nauk 85, 197 (1965), [Soviet Physics Uspekhi 8, 52 (1965)].

16. Kormer, S. B., Funtikov, A. I., Urlin, V. D., and Kolesnikova, A. N., JETP 42, 686 (1962), [Soviet Physics - JETP 15, 477 (1962)].

17. Boade, R. R., X-Ray Induced Impulse in Porous Metals (U), SC-DR-710705, Sandia Laboratories, Albuquerque, New Mexico, February 1972, SRD.

18. Grover, R., J. Chem. Phys. 55, 3435 (1971).

19. Zel'dovich, Ya. B., and Raizer, Yu. P., Physics of Shock Waves and High Temperature Hydrodynamic Phenomena, [ed. Hayes, W. D., and Probstein, R. F.] (Academic Press, New York, 1966).

20. Developed by D. J. McCloskey, Sandia Laboratories, Albuquerque, New Mexico.

21. Aller, L. H., Astrophysics - The Atomospheres of the Sun and Stars (Ronald Press, New York, 1963).

22. Mestel, L., Proceedings of the Cambridge Philosophical Society, 46, 331 (1950).

23. Cox, A. N., Stars and Stellar Systems, Vol VIII, Stellar Structures, [ed. Aller and McLaughlin] (University of Chicago, 1965).

Appendix A

INPUT CARDS

Appendix A

INPUT CARDS

The input cards described here are the same as those in Appendix I of R4. The information in brackets refers to sections or equations in this report. The equation-of-state number must be from -1 to -20. All temperatures are in units of electron volts. Other units are cgs.

Card 1. Format (I3, I5, I2, 5A10, 2E10.3)

Variable 1. (1-3)	Equation-of-state number (negative number).
Variable 2. (4-8)	Library equation-of-state number if desired; otherwise zero.†
Variable 3. (9-10)	Used only with a library equation of state. This variable determines the type of analytic calculation (see variable 2, card 2 below). If out of range 0 to 4, or library information is only for a gas, this input is ignored.
Variables 4-8. (11-60)	Fifty-column identification label: any BCD information.
Variable 9. (61-70)	RHUG = The initial density for the Hugoniot calculation. If zero, the calculation is skipped. If negative, the initial density is taken to be the reference density (variable 3, card 2 below) [VIII].
Variable 10. (71-80)	THUG = The initial temperature for the Hugoniot calculation. If zero, the calculation is skipped. If negative, the initial temperature is taken to be the reference temperature (variable 4, card 2 below) [VIII].

†See Appendix C for contents.

 67,68

The Hugoniot calculation should normally be used only to test new equation of state information.

If a library equation of state is requested, no further data cards are required.

Cards 2, 3, and 4. Format (8E10.3)

In the listing, the following variables are called ZB(I), I = 1, 24.

Variable 1. (1-10) — The number of elements in this material.

Variable 2. (11-20) — Switch for type of equation of state.

- 0. - Solid-gas without electronic terms and without detailed treatment of the liquid-vapor region.
- 1. - Solid-gas with electronic terms but without detailed treatment of the liquid-vapor region.
- 2. - Gas only with electronic terms.
- 3. - Same as 0., but with a detailed treatment of the liquid-vapor region.
- 4. - Same as 1., but with a detailed treatment of the liquid-vapor region.

Variable 3. (21-30) — ρ_o - Reference density [III-3].

Variable 4. (31-40) — T_o - Reference temperature [III-3]. If $T_o \leq 0$, code sets T_o = 0.02567785ev (298°K).

Variable 5. (41-50) — P_o - Reference pressure (normally 0) [III-3].

Variable 6. (51-60) — B_o - Reference bulk modulus (positive number) [III-3], or

$(-S_o)$ - Constant in linear Hugoniot shock-particle velocity relation (negative number) [VIII-1].

Variable 7. (61-70) — Γ_o - Reference Grüneisen coefficient [4.11].

Variable 8. (71-80) — θ_o - Reference Debye temperature. If $\theta_o \leq 0$, code sets θ_o = 0.025 [4.12].

Variable 9. (1-10)

T_Γ - Parameter [3.10].

$T_\Gamma = -1$, Slater theory,

$T_\Gamma = 0$, Dugdale and MacDonald theory,

$T_\Gamma = 1$, free-volume theory,

or

S_1 - Constant in linear Hugoniot shock-particle velocity relation [VIII-1].

Input variable is defined in relation to variable 6.

Variable 10. (11-20)

$3C_{24}$ - Three times the limiting value of the Grüneisen coefficient for large compressions, usually either 2 or 0. When a value of 2 is used, $C_{24} = 2/3$ [4.11].

Variable 11. (21-30)

E_s - Zero temperature separation energy [3.23].

Variable 12. (31-40)

T_m - Melting temperature [V-5],

or

$(-E_m)$ - Energy to the melting point at zero pressure from the reference point [V-5].

Variable 13. (41-50)

C_{53} - Parameter for low density P_c modification to move critical point (normally zero) [3.33].

Variable 14. (51-60)

C_{54} - Parameter for low density P_c modification to move critical point (normally zero) [3.33].

If $C_{54} = 0$ and $C_{53} \neq 0$, codes sets $C_{54} = 0.95$.

Variable 15. (61-70)

H_o - Thermal conductivity coefficient. If zero, thermal conduction is not included. Note that the units of $H = H_o T^{C_{41}}$ are ergs/(cm sec eV) [7.6].

Variable 16 (71-80)

C_{41} - Temperature dependence of thermal conduction coefficient (see variable 15) [7.6].

Variable 17. (1-10)

ρ_{min} - Lowest allowed solid density, usually about $0.8\ \rho_o$. If zero or negative, code sets $\rho_{min} = 0.8\ \rho_o$ [V-3].

Variable 18. (11-20) — Parameter D_1

Variable 19. (21-30) — Parameter D_2

Variable 20. (31-40) — Parameter D_3

Variable 21. (41-50) — Parameter D_4

Variable 22. (51-60) — Parameter D_5

Solid - solid phase transition parameters (normally 0) [V-7].

Variable 23. (61-70)

H_f - Heat of fusion to determine melt transition parameters [V-1].

If $H_f = 0$, no transition is included.

If $H_f < 0$, code sets $H_f = 1.117 \times 10^{12} T_m/A$ (ergs/gm), where A is the average atomic weight.

NOTE: Code will run slower if the melt transition is included. Use only when necessary and after testing.

Variable 24. (71-80)

ρ_ℓ/ρ_s - Ratio of liquid to solid density at melt point.

or

$(-\rho_\ell)$ - Density of liquid at melt point.

If $H_f \neq 0$ and $\rho_\ell/\rho_s = 0$, code sets $\rho_\ell/\rho_s = 0.95$ [V-1].

For a gaseous equation of state, variables 5 to 14 and 17 to 24 are read but not used.

Card 5. Format (5(F5.0, E10.3))

There is one set of the following variables for each element in variable 1, card 2. I = 1, number of elements [VI].

Variable Odd — Z(I) - Atomic number of element.

Variable Even. — Unnormalized atomic number fraction of element [COT(I)],

or

-Unnormalized atomic weight fraction of element. All elements should be defined in the same way.

Appendix B

SUMMARY OF CONTENTS OF THE C ARRAY

Appendix B

SUMMARY OF CONTENTS OF THE C ARRAY

Throughout this report a set of constants (C_j, j = 1, 54) has been defined to describe a material. Here a summary is given with references to the point of definition in the text.

C. Storage for:

1. η_1 of Eq. (5.60) if defined for a solid-solid phase transition; otherwise, large number.
2. η_2 of Eq. (5.61).
3. B_{oo} [Eq. (3.7)].
4. Constant in Eq. (3.20).
5. Constant in Eq. (3.20).
6. Constant in Eq. (3.20).
7. P_{ctr} (Section V-7) if defined for a phase transition.
8. $E_c(\eta_1)$ in Eq. (5.62) if defined for a phase transition.
9. Constant in Eq. (5.65) if defined for a phase transition.
10. E_S [Eq. (3.23)].
11. ρ_o reference density [Section III-3].
12. T_o reference temperature [Section III-3]
13. Constant in Eq. (4.20).
14. Constant in Eq. (4.26).
15. Γ_o [Section IV-1].
16. Constant in Eq. (4.24).
17. Constant in Eq. (4.24).
18. T_m [Section V-5].
19. ρ_{oo} [Section III].
20. P_o [Section III-3].

21. B_o [Section III-3].

22. Constant in Eq. (7.8).

23. ρ_{min} [Section V-3].

24. Constant in Eq. (4.11).

25. θ_o [Eq. (4.12)].

26. Z_m [Eq. (6.5)].

27. N_o [Eq. (6.10)].

28. Number of elements in material.

29. $\bar{A}$ [Eq. (6.2)].

30. EOS type switch, input variable 2.

31. Internal storage location.

32. Constant in Eq. (3.4).

33. Constant in Eq. (3.4).

34. Constant in Eq. (3.4).

35. Constant in Eq. (3.4).

36. Constant in Eq. (3.4).

37. Constant in Eq. (3.18).

38. Constant in Eq. (5.63).

39. Constant in Eq. (5.63).

40. Constant in Eq. (5.63).

41. Constant in Eq. (7.6).

42. Constant in Eq. (7.15).

43. Constant in Eq. (5.22).

44. Constant in Eq. (5.22).

45. Constant in Eq. (5.22).

46. ρ_{sm} [Section V-1].

47. $\rho_{\ell m}$ [Section V-1].

48. [Section V-1].

49. [Section V-1].

50. Constant in Eq. (5.41).

51. Constant in Eq. (5.42).

52. [Section V-1].

53. Constant in Eq. (3.33).

54. Constant in Eq. (3.33).

Appendix C

SAMPLE LIBRARY

The following tables list the contents of the sample library given in R4 at the end of subroutine ANDATA. These are for illustrative purposes and might not represent the best available data. Tables 1 through 5 are as given in R2. Tables 6 through 9 include both a melt transition and thermal conduction.

ANEOS LIBRARY NUMBER 1 AIR(DRY)

ZR(1)= 3.000000E+00	ZR(9)= 0.	ZR(17)= 0.
ZR(2)= 2.000000E+00	ZR(10)= 0.	ZR(18)= 0.
ZR(3)= 0.	ZR(11)= 0.	ZR(19)= 0.
ZR(4)= 0.	ZR(12)= 0.	ZR(20)= 0.
ZR(5)= 0.	ZR(13)= 0.	ZR(21)= 0.
ZR(6)= 0.	ZR(14)= 0.	ZR(22)= 0.
ZR(7)= 0.	ZR(15)= 0.	ZR(23)= 0.
ZR(8)= 0.	ZR(16)= 0.	ZR(24)= 0.

Z(1)= 7	COT(1)= 7.8455E-01
Z(2)= 8	COT(2)= 2.1075E-01
Z(3)= 18	COT(3)= 4.7000E-03

ANEOS LIBRARY NUMBER 2 GOLD

ZR(1)= 1.000000E+00	ZR(9)= 0.	ZR(17)= 0.
ZR(2)= 4.000000E+00	ZR(10)= 2.000000E+00	ZR(18)= 0.
ZR(3)= 1.930000E+01	ZR(11)= 1.450000E+10	ZR(19)= 0.
ZR(4)= 0.	ZR(12)= 1.151000E-01	ZR(20)= 0.
ZR(5)= 0.	ZR(13)= 0.	ZR(21)= 0.
ZR(6)= 1.750000E+12	ZR(14)= 0.	ZR(22)= 0.
ZR(7)= 3.054000E+00	ZR(15)= 0.	ZR(23)= 0.
ZR(8)= 1.551000E-02	ZR(16)= 0.	ZR(24)= 0.

Z(1)= 79	COT(1)= 1.0000E+00

ANEOS LIBRARY NUMBER 3 ALUMINUM

ZB(1)= 1.000000E+00 ZB(9)= -1.000000E+00 ZB(17)= 0.
ZB(2)= 4.000000E+00 ZB(10)= 2.000000E+00 ZB(18)= 0.
ZB(3)= 2.700000E+00 ZB(11)= 1.200000E+11 ZB(19)= 0.
ZB(4)= 0. ZB(12)= 8.000000E-02 ZB(20)= 0.
ZB(5)= 0. ZB(13)= 0. ZB(21)= 0.
ZB(6)= 7.630000E+11 ZB(14)= 0. ZB(22)= 0.
ZB(7)= 2.060000E+00 ZB(15)= 0. ZB(23)= 0.
ZB(8)= 3.430000E-02 ZB(16)= 0. ZB(24)= 0.

Z(1)= 13 COT(1)= 1.0000E+00

ANEOS LIBRARY NUMBER 4 BERYLLIUM

ZB(1)= 1.000000E+00 ZB(9)= 1.001000E+00 ZB(17)= 0.
ZB(2)= 4.000000E+00 ZB(10)= 2.000000E+00 ZB(18)= 0.
ZB(3)= 1.845000E+00 ZB(11)= 3.630000E+11 ZB(19)= 0.
ZB(4)= 0. ZB(12)= 1.740000E-01 ZB(20)= 0.
ZB(5)= 0. ZB(13)= 0. ZB(21)= 0.
ZB(6)= -7.970000E+05 ZB(14)= 0. ZB(22)= 0.
ZB(7)= 1.170000E+00 ZB(15)= 0. ZB(23)= 0.
ZB(8)= 9.995000E-02 ZB(16)= 0. ZB(24)= 0.

Z(1)= 4 COT(1)= 1.0000E+00

ANEOS LIBRARY NUMBER 5 IRON 130PT

ZR(1)= 1.000000E+00	ZR(9)= 0.	ZR(17)= 0.
ZR(2)= 4.000000E+00	ZR(10)= 2.000000E+00	ZR(18)= 8.360000E+00
ZR(3)= 7.850000E+00	ZR(11)= 7.300000E+10	ZR(19)= 8.750000E+00
ZR(4)= 0.	ZR(12)= 2.820000E-01	ZR(20)= 1.120000E+11
ZR(5)= 0.	ZR(13)= 0.	ZR(21)= 2.300000E+12
ZR(6)= 1.930000E+12	ZR(14)= 0.	ZR(22)= 5.000000E+12
ZR(7)= 1.750000E+00	ZR(15)= 0.	ZR(23)= 0.
ZR(8)= 0.	ZR(16)= 0.	ZR(24)= 0.

Z(1)= 26 COT(1)= 1.0000E+00

ANEOS LIBRARY NUMBER 6 ALUMINUM/M

ZR(1)= 1.000000E+00	ZR(9)= -1.000000E+00	ZR(17)= 2.305000E+00
ZR(2)= 4.000000E+00	ZR(10)= 2.000000E+00	ZR(18)= 0.
ZR(3)= 2.700000E+00	ZR(11)= 1.200000E+11	ZR(19)= 0.
ZR(4)= 0.	ZR(12)= -6.639000E+09	ZR(20)= 0.
ZR(5)= 0.	ZR(13)= 3.500000E+12	ZR(21)= 0.
ZR(6)= 7.630000E+11	ZR(14)= 8.000000E-01	ZR(22)= 0.
ZR(7)= 2.060000E+00	ZR(15)= 2.700000E+11	ZR(23)= 3.980000E+09
ZR(8)= 3.430000E-02	ZR(16)= 0.	ZR(24)= 9.240000E-01

Z(1)= 13 COT(1)= 1.0000E+00

ANEOS LIBRARY NUMBER 7 LEAD/M

ZB(1)= 1.000000E+00	ZB(9)= 1.460000E+00	ZB(17)= 9.940000E+00
ZB(2)= 4.000000E+00	ZB(10)= 2.000000E+00	ZB(18)= 0.
ZB(3)= 1.135000E+01	ZB(11)= 9.500000E+09	ZB(19)= 0.
ZB(4)= 0.	ZB(12)= -4.090000E+08	ZB(20)= 0.
ZB(5)= 0.	ZB(13)= 2.000000E+12	ZB(21)= 0.
ZB(6)= -2.051000E+05	ZB(14)= 0.	ZB(22)= 0.
ZB(7)= 2.770000E+00	ZB(15)= 4.000000E+10	ZB(23)= 2.300000E+08
ZB(8)= 7.600000E-03	ZB(16)= 0.	ZB(24)= 9.670000E-01

Z(1)= 82 COT(1)= 1.0000E+00

ANEOS LIBRARY NUMBER 8 BE/M

ZB(1)= 1.000000E+00	ZB(9)= 1.124000E+00	ZB(17)= 0.
ZB(2)= 4.000000E+00	ZB(10)= 2.000000E+00	ZB(18)= 0.
ZB(3)= 1.851000E+00	ZB(11)= 3.690000E+11	ZB(19)= 0.
ZB(4)= 0.	ZB(12)= -3.680000E+10	ZB(20)= 0.
ZB(5)= 0.	ZB(13)= 0.	ZB(21)= 0.
ZB(6)= -7.998000E+05	ZB(14)= 0.	ZB(22)= 0.
ZB(7)= 1.160000E+00	ZB(15)= 2.900000E+10	ZB(23)= 1.300000E+10
ZB(8)= 9.995000E-02	ZB(16)= -5.434700E-01	ZB(24)= 0.

Z(1)= 4 COT(1)= 1.0000E+00

ANEOS LIBRARY NUMBER 9 COPPER/M

ZB(1)= 1.000000E+00	ZB(9)= 1.489000E+00	ZB(17)= 0.
ZB(2)= 4.000000E+00	ZB(10)= 2.000000E+00	ZB(18)= 0.
ZB(3)= 8.940000E+00	ZB(11)= 5.250000E+10	ZB(19)= 0.
ZB(4)= 0.	ZB(12)= -4.637000E+09	ZB(20)= 0.
ZB(5)= 0.	ZB(13)= 6.000000E+12	ZB(21)= 0.
ZB(6)= -3.940000E+05	ZB(14)= 7.000000E-01	ZB(22)= 0.
ZB(7)= 1.990000E+00	ZB(15)= 4.400000E+11	ZB(23)= 2.055000E+09
ZB(8)= 2.710000E-02	ZB(16)= 0.	ZB(24)= -8.217000E+00

Z(1)= 29 COT(1)= 1.0000E+00

Appendix D

SAMPLE CALCULATIONS FOR ALUMINUM

The normal printed output produced during the generate mode for a material is shown on the following pages. The data are for library number 6 in Appendix C. In this listing, COT(I) = C_i of Eq. (6.1) and FNI(I) = N_i of Eq. (6.9). Plots of computed results are shown in Figs. D-1 through D-12. Figures D-8 through D-12 employ a grid equally spaced on log (ρ) and log (T). All plots were produced by the program CKEOS described in R5.

This equation of state was used for the example in Section V-6 of R4.

```
EOS DATA FOR ANALYTIC EOS NUMBER    -6     LIBRARY NUMBER    6     TYPE  4

 ALUMINUM

RHUG= -1.00000E+00          THUG= -1.00000E+00


LIBRARY EOS NUMBER     6 ( ALUMINUM/M ) IS REQUESTED

ZB( 1)= 1.0300000000E+00  ZB( 9)=-1.0000000000E+00  ZB(17)= 2.3050000000E+00
ZB( 2)= 4.0000000000E+00  ZB(10)= 2.0000000000E+00  ZB(18)= 0.
ZB( 3)= 2.7000000000E+00  ZB(11)= 1.2000000000E+11  ZB(19)= 0.
ZB( 4)= 2.5677850000E-02  ZB(12)=-5.6390000000E+09  ZB(20)= 0.
ZB( 5)= 0.                ZB(13)= 3.5000000000E+12  ZB(21)= 0.
ZB( 6)= 7.6300000000E+11  ZB(14)= 8.3000000000E-01  ZB(22)= 0.
ZB( 7)= 2.0600000000E+01  ZB(15)= 2.7000000000E+11  ZB(23)= 3.9800000000E+09
ZB( 8)= 3.4300000000E-02  ZB(16)= 0.                ZB(24)= 9.2400000000E-01

C( 1)= 1.0000000000E+00   C(19)= 2.752267764E+00    C(37)= 5.891943437E+12
C( 2)= 0.                 C(20)= 0.                 C(38)= 0.
C( 3)= 8.3182063962E+11   C(21)= 7.6300000000E+11   C(39)= 0.
C( 4)= 6.1137762402E+11   C(22)= 2.0296296302E+01   C(40)= 0.
C( 5)= 7.2208515302E+00   C(23)= 2.3050000006E+00   C(41)= 0.
C( 6)= 3.1391484702E+00   C(24)= 5.6666666672E-01   C(42)= 1.0000000000E-01
C( 7)= 0.                 C(25)= 3.4300000000E-02   C(43)=-1.3289896142E+10
C( 8)= 0.                 C(26)= 1.3000000000E+01   C(44)=-1.6324139532F+11
C( 9)= 0.                 C(27)= 2.2322855982E+22   C(45)= 1.5327377352E+11
C(10)= 1.2000000000E+11   C(28)= 1.0011600000E+00   C(46)= 2.5720879792E+00
C(11)= 2.7000000000E+00   C(29)= 2.6982000006E+01   C(47)= 2.3766092932E+00
C(12)= 2.5677850000E-02   C(30)= 4.0000000000E+00   C(48)= 6.6858529342E+00
C(13)= 7.7170720142E-05   C(31)= 1.0000000000E+00   C(49)= 1.8247269142E-02
C(14)= 9.2486599612E-04   C(32)= 1.6056496582E+13   C(50)= 3.0664200762E-01
C(15)= 2.0600000002E+00   C(33)= 3.1551668102E+00   C(51)= 3.2664854212E-01
C(16)=-4.2798353912E-01   C(34)= 9.7678182892E+11   C(52)= 7.8765905322E-01
C(17)= 1.5481481462E+00   C(35)=-3.6384232552F+12   C(53)= 3.5000000002E+12
C(18)= 8.2398782932E-02   C(36)= 3.3396961752E+12   C(54)= 8.0000000002E-01

Z( 1)=  13   COT( 1)= 1.00000E+00   ENI( 1)= 2.23229E+22

REFERENCE POINT CONDITIONS
T=  2.567785E-02        RHO=  2.700000E+00
P=  9.094238E-03        E=  2.805137E+09
S=  1.116398E+11        CV=  1.069397E+11
DPDT=  5.974865E+11     DPDR=  2.825926E+11
BO=  7.630000E+11       CS=  5.423966E+05
```

TWO-PHASE CALCULATION FOR MATERIAL 6
CRITICAL POINT
RHO= 4.7763421E-01 T= 9.0437242E-01 P= 5.1571289E+09
E= 1.1100303E+11 S= 6.2401285E+11 NTY= 9

TWO-PHASE BOUNDARIES

T	RHOLIQ / RHOVAP	PLIQ / PVAP	ELIQ / EVAP	SLIQ / SVAP	GLIQ / GVAP
8.35875E-01	6.30695E-01	5.09250E+09	1.00510E+11	6.07933E+11	-4.00164E+11
10	2.92772E-01	5.09250E+09	1.14667E+11	6.36729E+11	-4.00164E+11
7.67377E-01	7.67620E-01	4.12949E+09	9.44969E+10	5.99477E+11	-3.60148E+11
8	2.24773E-01	4.12949E+09	1.13687E+11	6.41415E+11	-3.60148E+11
6.98879E-01	8.36913E-01	3.26589E+09	8.92103E+10	5.91721E+11	-3.20429E+11
8	1.76232E-01	3.26589E+09	1.11796E+11	6.44975E+11	-3.20429E+11
6.30381E-01	9.99447E-01	2.50073E+09	8.42360E+10	5.83873E+11	-2.81046E+11
7	1.37701E-01	2.50073E+09	1.09381E+11	6.48160E+11	-2.81046E+11
5.61883E-01	9.61154E-01	1.87414E+09	7.93600E+10	5.75426E+11	-2.42054E+11
7	1.15548E-01	1.87414E+09	1.06578E+11	6.51797E+11	-2.42054E+11
4.97385E-01	1.02811E+00	1.26719E+09	7.43778E+10	5.65768E+11	-2.03531E+11
6	7.79970E-02	1.26719E+09	1.03452E+11	6.55127E+11	-2.03531E+11
4.24088E-01	1.11091E+00	8.01576E+08	6.89490E+10	5.53742E+11	-1.65607E+11
6	5.41428E-02	8.01576E+08	1.00019E+11	6.60013E+11	-1.65607E+11
3.56390E-01	1.23764E+00	4.38945E+08	6.21461E+10	5.36053E+11	-1.28543E+11
6	3.76253E-02	4.38945E+08	9.62542E+10	6.67391E+11	-1.28543E+11
2.87892E-01	1.52328E+00	1.78991E+08	5.00088E+10	4.97566E+11	-9.31191E+10
6	1.64219E-02	1.78991E+08	9.20812E+10	6.81158E+11	-9.31191E+10
2.19394E-01	1.91780E+00	3.26048E+07	3.35205E+10	4.32569E+11	-6.13657E+10
4	4.11559E-03	3.25387E+07	8.76370E+10	7.15192E+11	-6.13657E+10
1.85145E-01	2.05628E+00	6.75971E+06	2.73588E+10	4.02109E+11	-4.70864E+10
4	1.14395E-03	6.75958E+06	8.60797E+10	7.51168E+11	-4.70864E+10
1.50896E-01	2.17374E+00	3.62700E+05	2.21107E+10	3.70840E+11	-3.38474E+10
4	9.94352E-05	3.62700E+05	8.72359E+10	8.26607E+11	-3.38474E+10
1.16647E-01	2.27972E+00	2.00374E+04	1.74990E+10	3.36266E+11	-2.17255E+10
4	9.41052E-08	2.00378E+04	9.99943E+10	1.06088E+12	-2.17255E+10
8.23984E-02	2.37561E+00	-3.66211E-03	1.34213E+10	2.95030E+11	-1.08887E+10
6	2.19887E-14	5.05835E-05	1.17673E+11	1.58816E+12	-1.08887E+10
8.15744E-02	2.57408E+00	4.63867E-03	9.33963E+09	2.45488E+11	-1.06859E+10
6	1.35630E-14	3.11801E-05	1.17934E+11	1.60490E+12	-1.06859E+10
6.50347E-02	2.61324E+00	1.95713E-03	7.34197E+09	2.18149E+11	-6.85839E+09
7	1.42620E-19	3.02390E-10	1.21389E+11	2.00273E+12	-6.85839E+09
4.44951E-02	2.65955E+00	-1.13525E-12	4.93220E+09	1.73695E+11	-2.79638E+09
8	4.83728E-30	7.60518E-21	1.22196E+11	2.84446E+12	-2.79638E+09
2.78955E-02	2.70373E+00	2.62451E-03	2.60699E+09	1.03542E+11	1.30400E+08
8	6.58414E-59	5.62640E-49	1.21282E+11	5.10580E+12	1.30400E+08

LOCKP(6)= 1 LOCKPL(6)= 86

MELT CURVE

T	RS RL	PS PL	ES EL	SS SL	GS GL
1.8247E-02	2.3146E+00	-8.9489E+10	6.0649E+09	1.1212E+11	-3.4378E+10
16	1.8456E+00	-8.9489E+10	1.7704E+10	2.2690E+11	-3.4378E+10
3.9631E-02	2.3071E+00	-6.1361E+10	6.8093E+09	1.8535E+11	-2.6135E+10
8	2.1239E+00	-6.1361E+10	1.2821E+10	2.5672E+11	-2.6135E+10
6.1015E-02	2.4877E+00	-3.1524E+10	7.9374E+09	2.2254E+11	-1.8315E+10
5	2.2654E+00	-3.1524E+10	1.2631E+10	2.7312E+11	-1.8315E+10
8.2398E-02	2.5721E+00	-2.6855E-03	9.4413E+09	2.4673E+11	-1.0889E+10
0	2.3766E+00	-3.6621E-03	1.3421E+10	2.9503E+11	-1.0889E+10
1.0727E-01	2.6659E+00	3.8539E+10	1.1577E+10	2.6669E+11	-2.5744E+09
3	2.4905E+00	3.8538E+10	1.5057E+10	3.0862E+11	-2.5744E+09
1.3965E-01	2.7920E+00	9.1412E+10	1.4882E+10	2.8546E+11	7.8764E+09
3	2.6244E+00	9.1412E+10	1.7971E+10	3.2172E+11	7.8764E+09
1.8179E-01	2.9251E+00	1.6510E+11	1.9923E+10	3.0308E+11	2.1267E+10
4	2.7360E+00	1.6510E+11	2.2754E+10	3.3415E+11	2.1267E+10
2.3667E-01	3.1045E+00	2.7040E+11	2.7566E+10	3.1938E+11	3.9078E+10
4	2.9825E+00	2.7040E+11	3.0299E+10	3.4598E+11	3.9078E+10
3.0810E-01	3.3315E+00	4.2430E+11	3.9146E+10	3.3432E+11	6.3500E+10
4	3.2247E+00	4.2430E+11	4.1954E+10	3.5714E+11	6.3500E+10
4.0109E-01	3.6224E+00	6.5540E+11	5.6756E+10	3.4784E+11	9.8172E+10
4	3.5289E+00	6.5540E+11	5.9837E+10	3.6748E+11	9.8172E+10
5.2215E-01	4.0038E+00	1.0142E+12	8.3772E+10	3.5989E+11	1.4935E+11
4	3.9199E+00	1.0142E+12	8.7756E+10	3.7590E+11	1.4935E+11
6.7976E-01	4.5136E+00	1.5944E+12	1.2582E+11	3.7079E+11	2.2808E+11
4	4.4319E+00	1.5944E+12	1.3018E+11	3.8523E+11	2.2808E+11
8.8493E-01	5.1891E+00	2.5812E+12	1.9266E+11	3.7922E+11	3.5451E+11
4	5.1263E+00	2.5812E+12	1.9815E+11	3.9231E+11	3.5451E+11
1.1520E+00	6.1562E+00	4.3680E+12	3.0212E+11	3.8617E+11	5.6677E+11
4	6.1110E+00	4.3680E+12	3.0918E+11	3.9786E+11	5.6677E+11
1.4997E+00	7.5916E+00	7.3695E+12	4.8877E+11	3.9088E+11	9.4052E+11
6	7.5330E+00	7.3695E+12	4.9801E+11	4.0151E+11	9.4052E+11
1.9524E+00	9.8091E+00	1.5471E+13	8.2515E+11	3.9275E+11	1.6356E+12
9	9.7661E+00	1.5471E+13	8.3743E+11	4.0260E+11	1.6356E+12
2.5417E+00	1.3583E+01	3.4415E+13	1.4798E+12	3.9069E+11	3.0205E+12
15	1.3545E+01	3.4415E+13	1.4965E+12	4.0105E+11	3.0205E+12
3.3089E+00	2.0777E+01	9.1919E+13	2.9044E+12	3.9265E+11	6.0623E+12
26	2.0743E+01	9.1919E+13	2.9276E+12	3.9186E+11	6.0623E+12
4.3076E+00	3.7366E+01	3.3044E+14	6.6019E+12	3.6438E+11	1.3875E+13
44	3.7336E+01	3.3044E+14	6.6357E+12	3.7393E+11	1.3875E+13
5.6077E+00	9.2891E+01	2.1407E+15	2.0033E+13	3.2447E+11	4.1259E+13
79	9.2863E+01	2.1407E+15	2.0086E+13	3.3542E+11	4.1259E+13

HUGONIOT

RHO	T	P	PC	E	S	V	U	RHO/RHOO		
2.7000E+00	2.5678E-02	9.0942E-03	-1.5281E+10	2.8051E+09	1.1164E+11	5.4240E+05	0.	1.0000E+00		
2.7165E+00	2.6000E-02	4.8944E+09	-1.0578E+10	2.8106E+09	1.1164E+11	5.4692E+05	3.3145E+03	1.0061E+00	2	SOLID
2.7418E+00	2.6500E-02	1.2630E+10	-3.1419E+09	2.8188E+09	1.1166E+11	5.5392E+05	8.4450E+03	1.0155E+00	2	SOLID
2.7907E+00	2.7500E-02	2.8261E+10	1.1888E+10	2.9752E+09	1.1183E+11	5.6758E+05	1.8441E+04	1.0336E+00	3	SOLID
2.8358E+00	2.8500E-02	4.3565E+10	2.6588E+10	3.1916E+09	1.1226E+11	5.8039E+05	2.7800E+04	1.0503E+00	3	SOLID
2.8955E+00	3.0000E-02	6.5100E+10	4.7215E+10	3.6191E+09	1.1343E+11	5.9758E+05	4.0348E+04	1.0724E+00	3	SOLID
3.0395E+00	3.5000E-02	1.2366E+11	1.0273E+11	5.3631E+09	1.2017E+11	6.4033E+05	7.1525E+04	1.1257E+00	4	SOLID
3.1361E+00	4.0000E-02	1.5858E+11	1.4459E+11	7.1465E+09	1.2840E+11	6.7004E+05	9.3181E+04	1.1615E+00	4	SOLID
3.2690E+00	5.0000E-02	2.3941E+11	2.0830E+11	1.0489E+10	1.4450E+11	7.1227E+05	1.2397E+05	1.2107E+00	4	SOLID
3.3638E+00	6.0000E-02	2.9447E+11	2.5822E+11	1.3566E+10	1.5880E+11	7.4342E+05	1.4670E+05	1.2459E+00	3	SOLID
3.5019E+00	8.0000E-02	3.8627E+11	3.3762E+11	1.9184E+10	1.8245E+11	7.9036E+05	1.8099E+05	1.2970E+00	4	SOLID
3.6049E+00	1.0000E-01	4.6309E+11	4.0205E+11	2.4332E+10	2.0133E+11	8.2659E+05	2.0750E+05	1.3352E+00	3	SOLID
3.6885E+00	1.2000E-01	5.2116E+11	4.5763E+11	2.9165E+10	2.1695E+11	8.5679E+05	2.2961E+05	1.3661E+00	3	SOLID
3.7594E+00	1.4000E-01	5.9328E+11	5.0721E+11	3.3766E+10	2.3026E+11	8.8303E+05	2.4884E+05	1.3924E+00	3	SOLID
3.8215E+00	1.6000E-01	6.5105E+11	5.5238E+11	3.8188E+10	2.4183E+11	9.0644E+05	2.6602E+05	1.4154E+00	3	SOLID
3.8779E+00	1.8000E-01	7.0544E+11	5.9413E+11	4.2464E+10	2.5208E+11	9.2771E+05	2.8163E+05	1.4359E+00	3	SOLID
3.9272E+00	2.0000E-01	7.5712E+11	6.3314E+11	4.6619E+10	2.6125E+11	9.4729E+05	2.9602E+05	1.4545E+00	3	SOLID
4.0361E+00	2.5000E-01	8.7728E+11	7.2144E+11	5.6585E+10	2.8073E+11	9.9072E+05	3.2796E+05	1.4948E+00	3	SOLID
4.1279E+00	3.0000E-01	9.8791E+11	7.9999E+11	6.6088E+10	2.9667E+11	1.0285E+06	3.5576E+05	1.5288E+00	3	SOLID
4.2078E+00	3.5000E-01	1.0916E+12	8.7145E+11	7.5243E+10	3.1014E+11	1.0622E+06	3.8063E+05	1.5585E+00	3	SOLID
4.2790E+00	4.0000E-01	1.1901E+12	9.3752E+11	8.4171E+10	3.2182E+11	1.0929E+06	4.0330E+05	1.5848E+00	3	SOLID
4.3435E+00	4.5000E-01	1.2845E+12	9.9937E+11	9.2912E+10	3.3212E+11	1.1213E+06	4.2428E+05	1.6087E+00	3	SOLID
4.4029E+00	5.0000E-01	1.3757E+12	1.0579E+12	1.0134E+11	3.4134E+11	1.1478E+06	4.4392E+05	1.6307E+00	3	SOLID
4.4580E+00	5.5000E-01	1.4644E+12	1.1137E+12	1.0975E+11	3.4969E+11	1.1728E+06	4.6248E+05	1.6511E+00	3	SOLID
4.5098E+00	6.0000E-01	1.5511E+12	1.1675E+12	1.1808E+11	3.5731E+11	1.1965E+06	4.8015E+05	1.6703E+00	3	SOLID
4.5588E+00	6.5000E-01	1.6362E+12	1.2194E+12	1.2635E+11	3.6433E+11	1.2191E+06	4.9709E+05	1.6885E+00	3	SOLID
4.6056E+00	7.0000E-01	1.7201E+12	1.2700E+12	1.3460E+11	3.7084E+11	1.2409E+06	5.1341E+05	1.7058E+00	3	SOLID
4.6803E+00	7.5000E-01	1.9006E+12	1.3529E+12	1.5172E+11	3.8553E+11	1.2898E+06	5.4574E+05	1.7334E+00	3	MELT
4.7282E+00	8.0000E-01	2.0069E+12	1.4075E+12	1.6223E+11	3.9344E+11	1.3164E+06	5.6466E+05	1.7512E+00	3	LIQUID
4.7659E+00	8.5000E-01	2.0943E+12	1.4512E+12	1.7012E+11	3.9860E+11	1.3345E+06	5.7847E+05	1.7652E+00	3	LIQUID
4.8027E+00	9.0000E-01	2.1615E+12	1.4945E+12	1.7805E+11	4.0347E+11	1.3522E+06	5.9202E+05	1.7788E+00	3	LIQUID
4.8397E+00	9.5000E-01	2.2384E+12	1.5374E+12	1.8602E+11	4.0810E+11	1.3695E+06	6.0534E+05	1.7921E+00	3	LIQUID
4.8739E+00	1.0000E+00	2.3152E+12	1.5799E+12	1.9403E+11	4.1250E+11	1.3865E+06	6.1843E+05	1.8051E+00	2	LIQUID
4.9421E+00	1.1000E+00	2.4683E+12	1.6641E+12	2.1018E+11	4.2072E+11	1.4195E+06	6.4401E+05	1.8304E+00	3	LIQUID
5.0079E+00	1.2000E+00	2.6211E+12	1.7472E+12	2.2649E+11	4.2829E+11	1.4514E+06	6.6885E+05	1.8547E+00	3	LIQUID
5.0711E+00	1.3000E+00	2.7735E+12	1.8291E+12	2.4295E+11	4.3530E+11	1.4822E+06	6.9303E+05	1.8782E+00	3	LIQUID
5.1321E+00	1.4000E+00	2.9255E+12	1.9100E+12	2.5955E+11	4.4185E+11	1.5121E+06	7.1658E+05	1.9008E+00	3	LIQUID
5.1911E+00	1.5000E+00	3.0773E+12	1.9898E+12	2.7627E+11	4.4800E+11	1.5411E+06	7.3955E+05	1.9226E+00	3	LIQUID
5.3031E+00	1.7000E+00	3.3795E+12	2.1459E+12	3.1000E+11	4.5930E+11	1.5968E+06	7.8383E+05	1.9641E+00	3	LIQUID
5.4577E+00	2.0000E+00	3.8293E+12	2.3713E+12	3.6112E+11	4.7430E+11	1.6754E+06	8.4654E+05	2.0214E+00	3	LIQUID
5.6847E+00	2.5000E+00	4.5684E+12	2.7228E+12	4.4599E+11	4.9564E+11	1.7952E+06	9.4253E+05	2.1054E+00	3	LIQUID
5.8902E+00	3.0000E+00	5.2939E+12	3.0458E+12	5.3301E+11	5.1381E+11	1.9040E+06	1.0298E+06	2.1779E+00	3	LIQUID
6.2014E+00	4.0000E+00	6.7074E+12	3.6158E+12	7.0412E+11	5.4406E+11	2.0976E+06	1.1843E+06	2.2968E+00	3	LIQUID
6.4565E+00	5.0000E+00	8.0794E+12	4.1065E+12	8.7332E+11	5.6897E+11	2.2679E+06	1.3195E+06	2.3913E+00	3	LIQUID
6.6660E+00	6.0000E+00	9.4187E+12	4.5327E+12	1.0405E+12	5.9031E+11	2.4214E+06	1.4406E+06	2.4689E+00	3	LIQUID
6.8424E+00	7.0000E+00	1.0771E+13	4.9086E+12	1.2059E+12	6.0903E+11	2.5623E+06	1.5512E+06	2.5342E+00	3	LIQUID
6.9938E+00	8.0000E+00	1.2122E+13	5.2437E+12	1.3696E+12	6.2573E+11	2.6930E+06	1.6534E+06	2.5903E+00	3	LIQUID
7.1324E+00	9.0000E+00	1.3477E+13	5.5607E+12	1.5365E+12	6.4115E+11	2.8182E+06	1.7514E+06	2.6416E+00	3	LIQUID
7.2634E+00	1.0000E+01	1.4777E+13	5.9169E+12	1.7249E+12	6.5685E+11	2.9491E+06	1.8559E+06	2.6976E+00	3	LIQUID

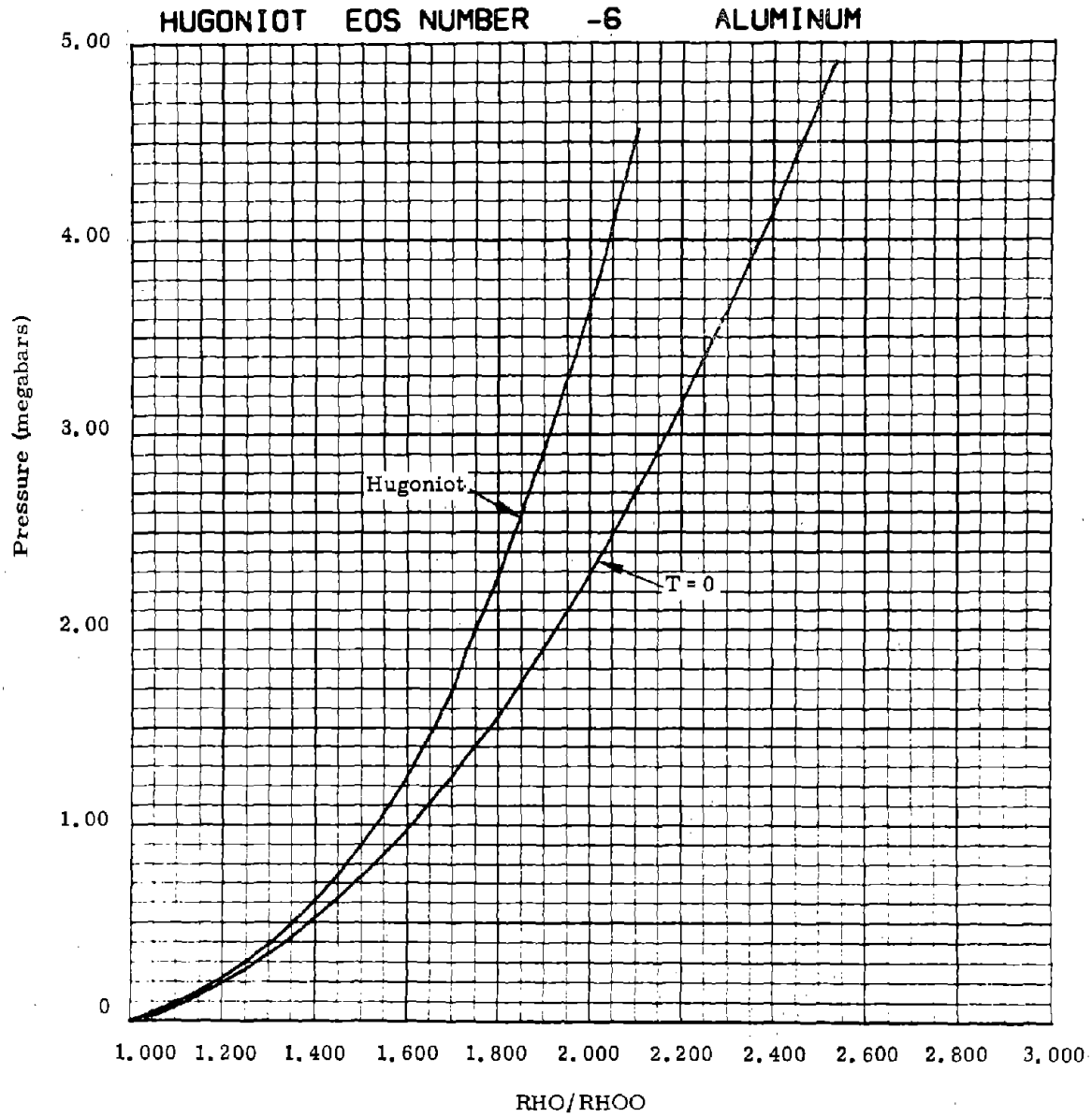
HUGONIOT EOS NUMBER -6 ALUMINUM
5.00
4.00
3.00
2.00
1.00
0
Pressure (megabars)
Hugoniot
T = 0
1.000 1.200 1.400 1.600 1.800 2.000 2.200 2.400 2.600 2.800 3.000
RHO/RHOO

Fig. D-1

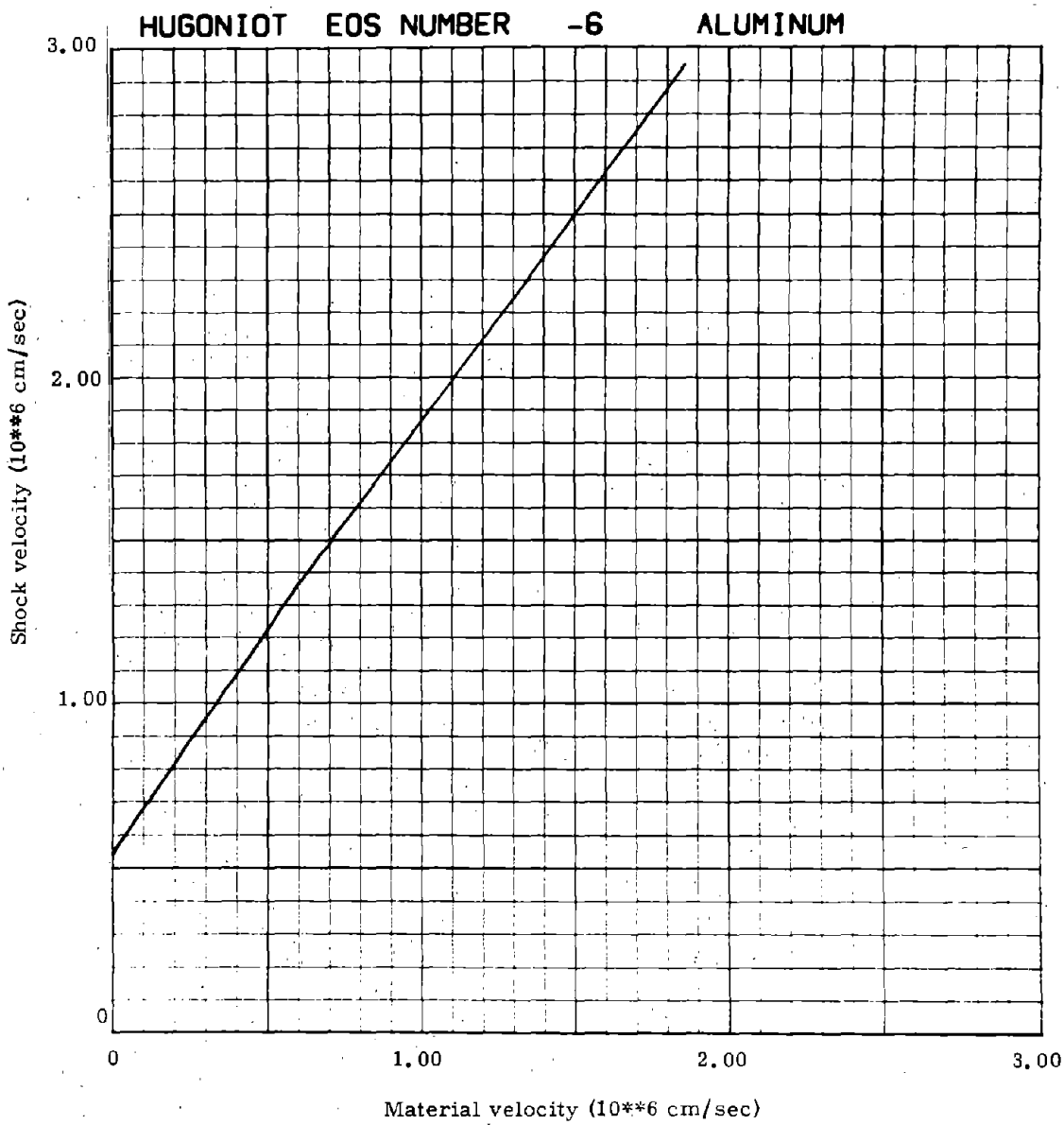
HUGONIOT EOS NUMBER -6 ALUMINUM
3.00
2.00
1.00
0
Shock velocity (10**6 cm/sec)
0
1.00
2.00
3.00
Material velocity (10**6 cm/sec)

Fig. D-2

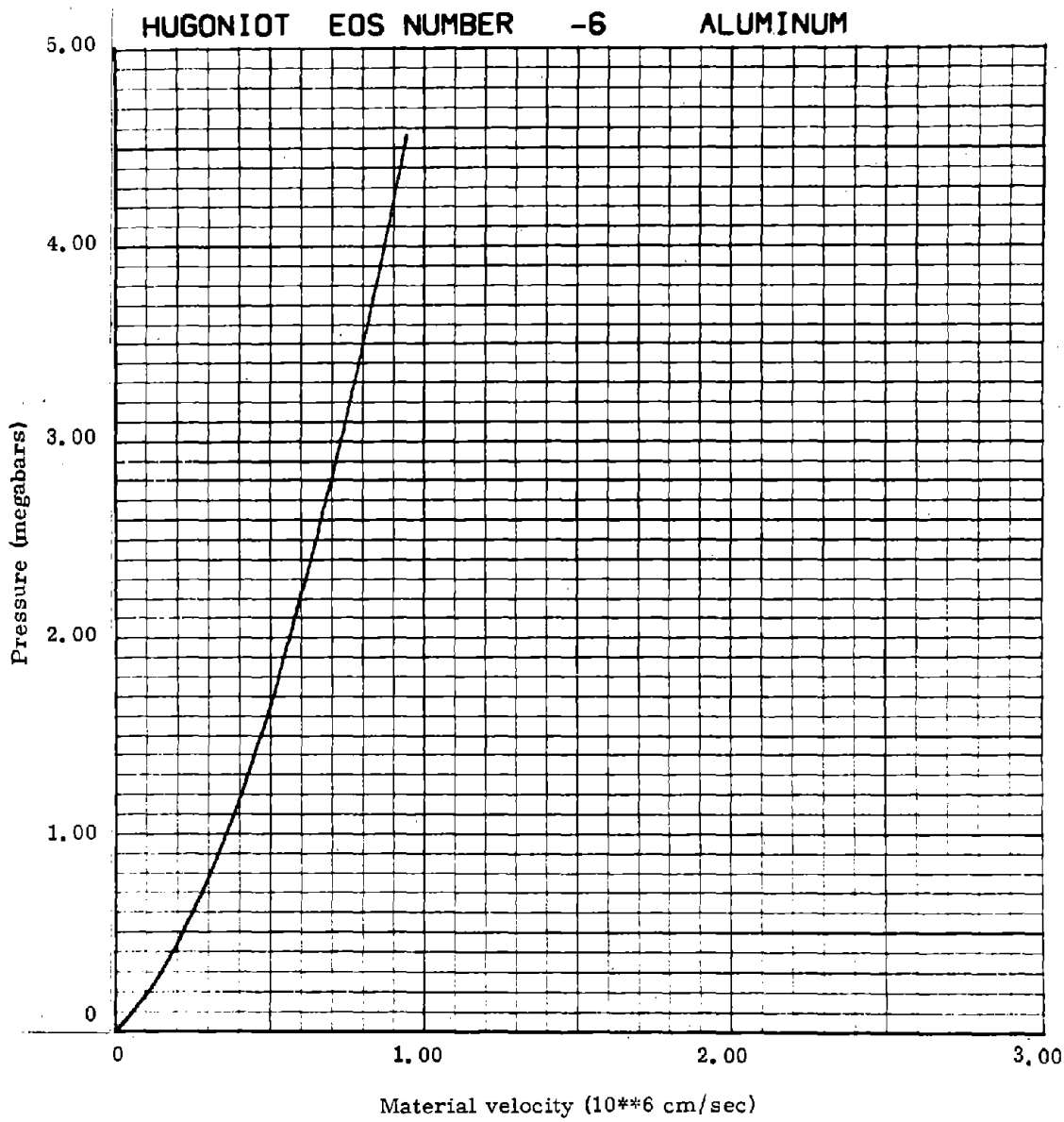
HUGONIOT EOS NUMBER -6 ALUMINUM
5.00
4.00
3.00
2.00
1.00
0
Pressure (megabars)
0
1.00
2.00
3.00
Material velocity (10**6 cm/sec)

Fig. D-3

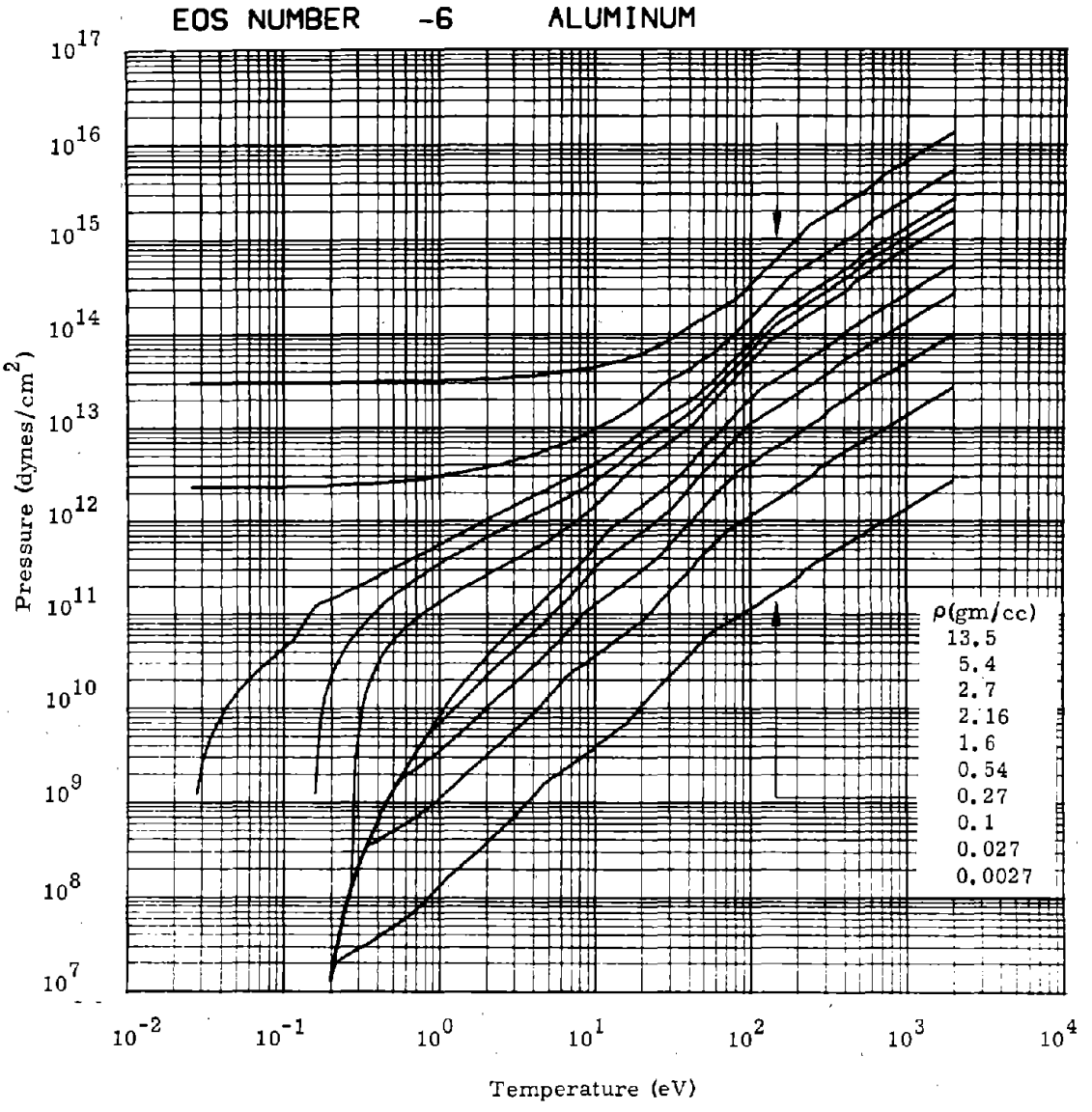
EOS NUMBER -6 ALUMINUM
Pressure (dynes/cm^2)
10^{17}
10^{16}
10^{15}
10^{14}
10^{13}
10^{12}
10^{11}
10^{10}
10^{9}
10^{8}
10^{7}
10^{-2}
10^{-1}
10^{0}
10^{1}
10^{2}
10^{3}
10^{4}
Temperature (eV)
ρ(gm/cc)
13.5
5.4
2.7
2.16
1.6
0.54
0.27
0.1
0.027
0.0027

Fig. D-4

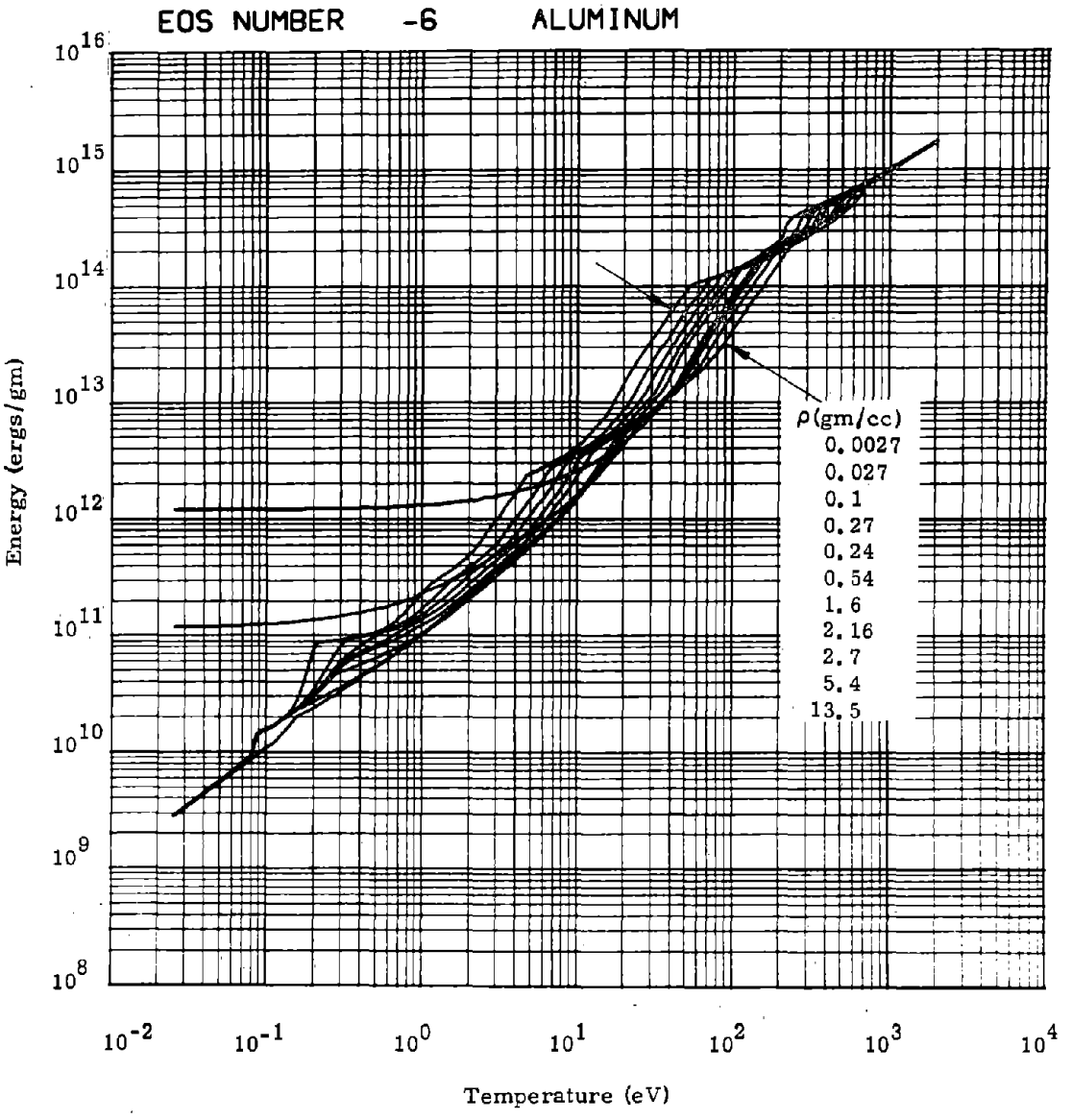
EOS NUMBER -6 ALUMINUM
Energy (ergs/gm)
10^{16}
10^{15}
10^{14}
10^{13}
10^{12}
10^{11}
10^{10}
10^{9}
10^{8}
10^{-2}
10^{-1}
10^{0}
10^{1}
10^{2}
10^{3}
10^{4}
Temperature (eV)
ρ(gm/cc)
0.0027
0.027
0.1
0.27
0.24
0.54
1.6
2.16
2.7
5.4
13.5

Fig. D-5

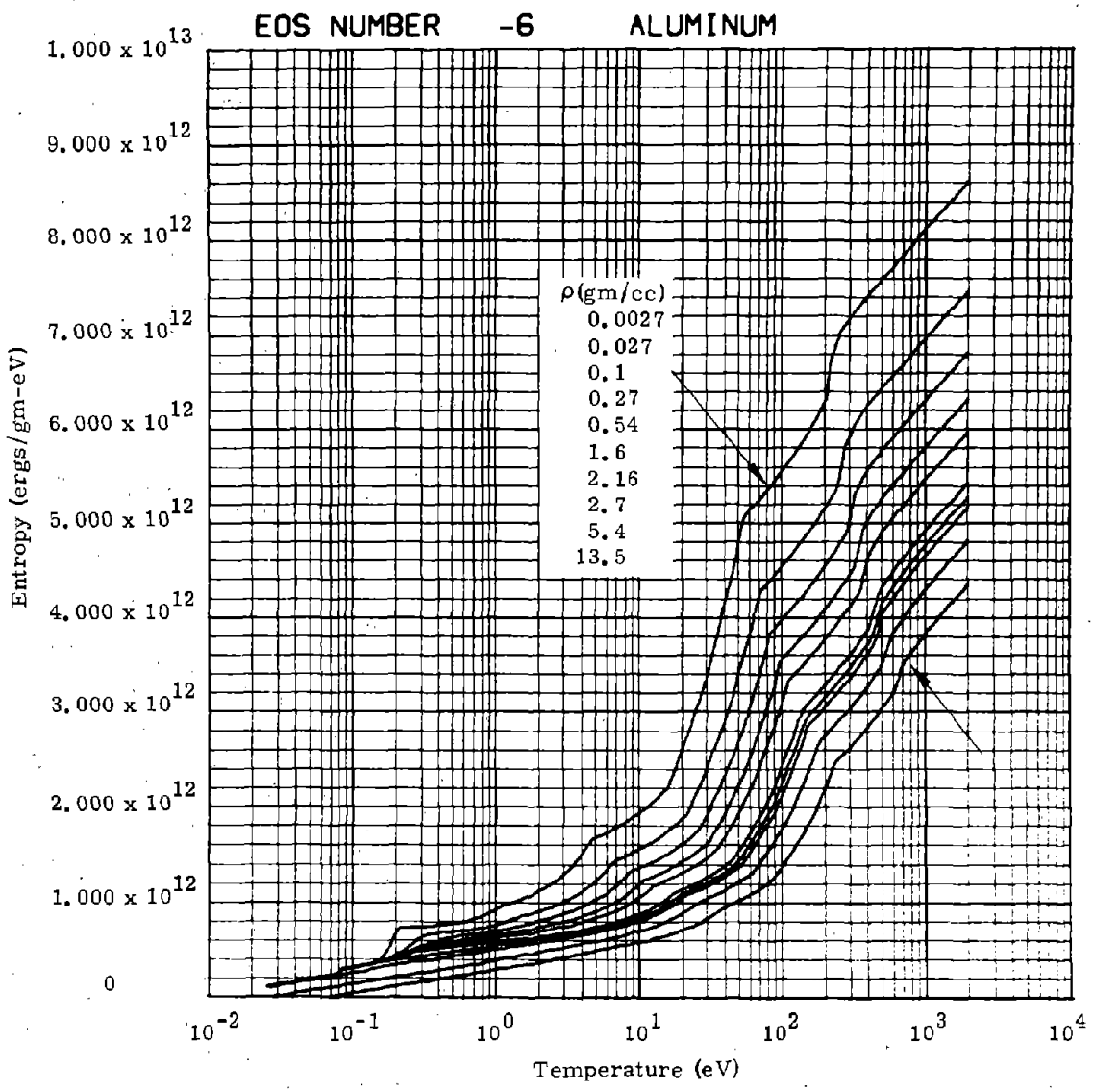
EOS NUMBER -6 ALUMINUM
Entropy (ergs/gm-eV)
1.000 x 10^13
9.000 x 10^12
8.000 x 10^12
7.000 x 10^12
6.000 x 10^12
5.000 x 10^12
4.000 x 10^12
3.000 x 10^12
2.000 x 10^12
1.000 x 10^12
0
ρ(gm/cc)
0.0027
0.027
0.1
0.27
0.54
1.6
2.16
2.7
5.4
13.5
10^-2
10^-1
10^0
10^1
10^2
10^3
10^4
Temperature (eV)

Fig. D-6

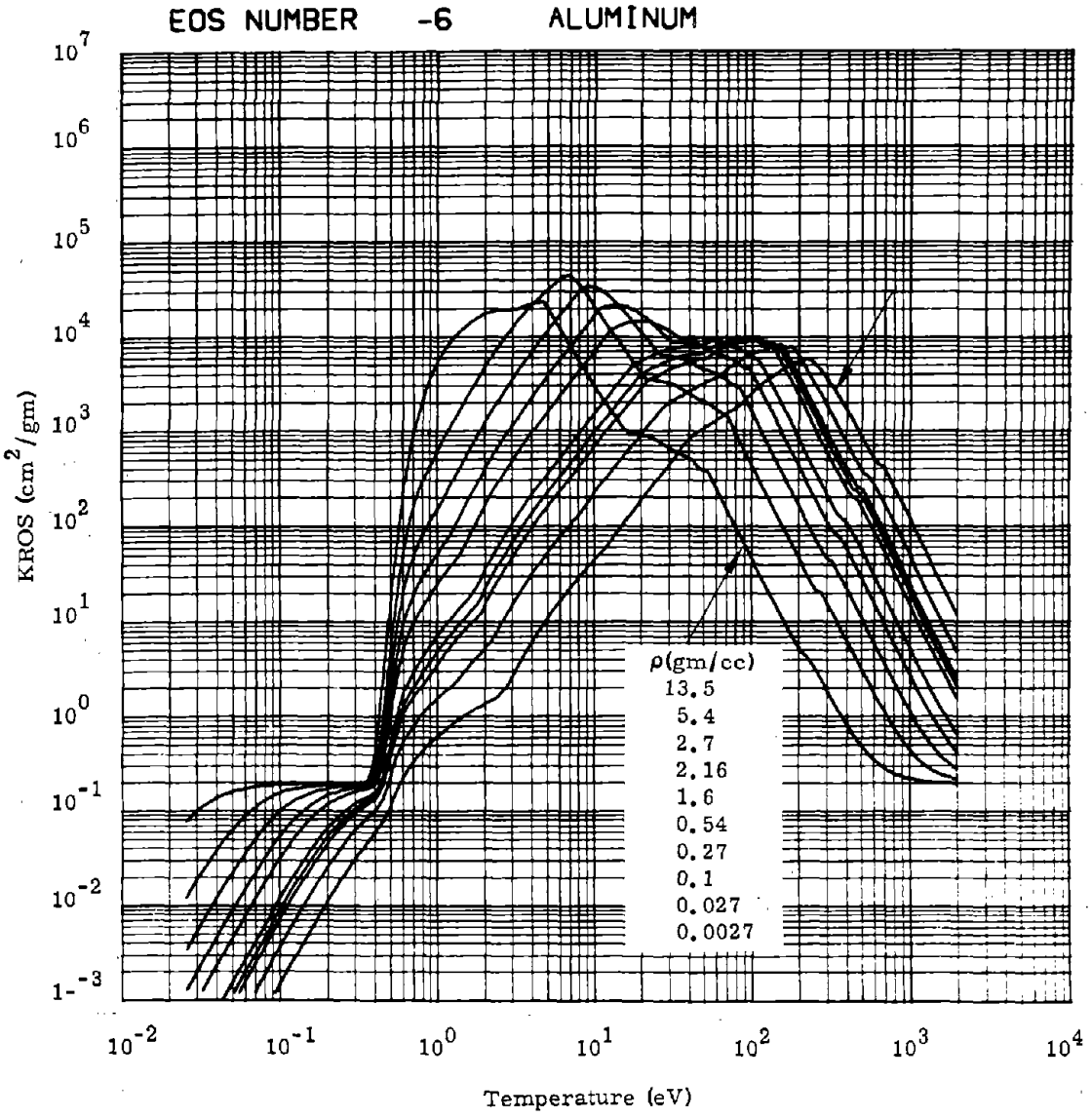
EOS NUMBER -6 ALUMINUM
KROS (cm²/gm)
Temperature (eV)
ρ(gm/cc)
13.5
5.4
2.7
2.16
1.6
0.54
0.27
0.1
0.027
0.0027

Fig. D-7

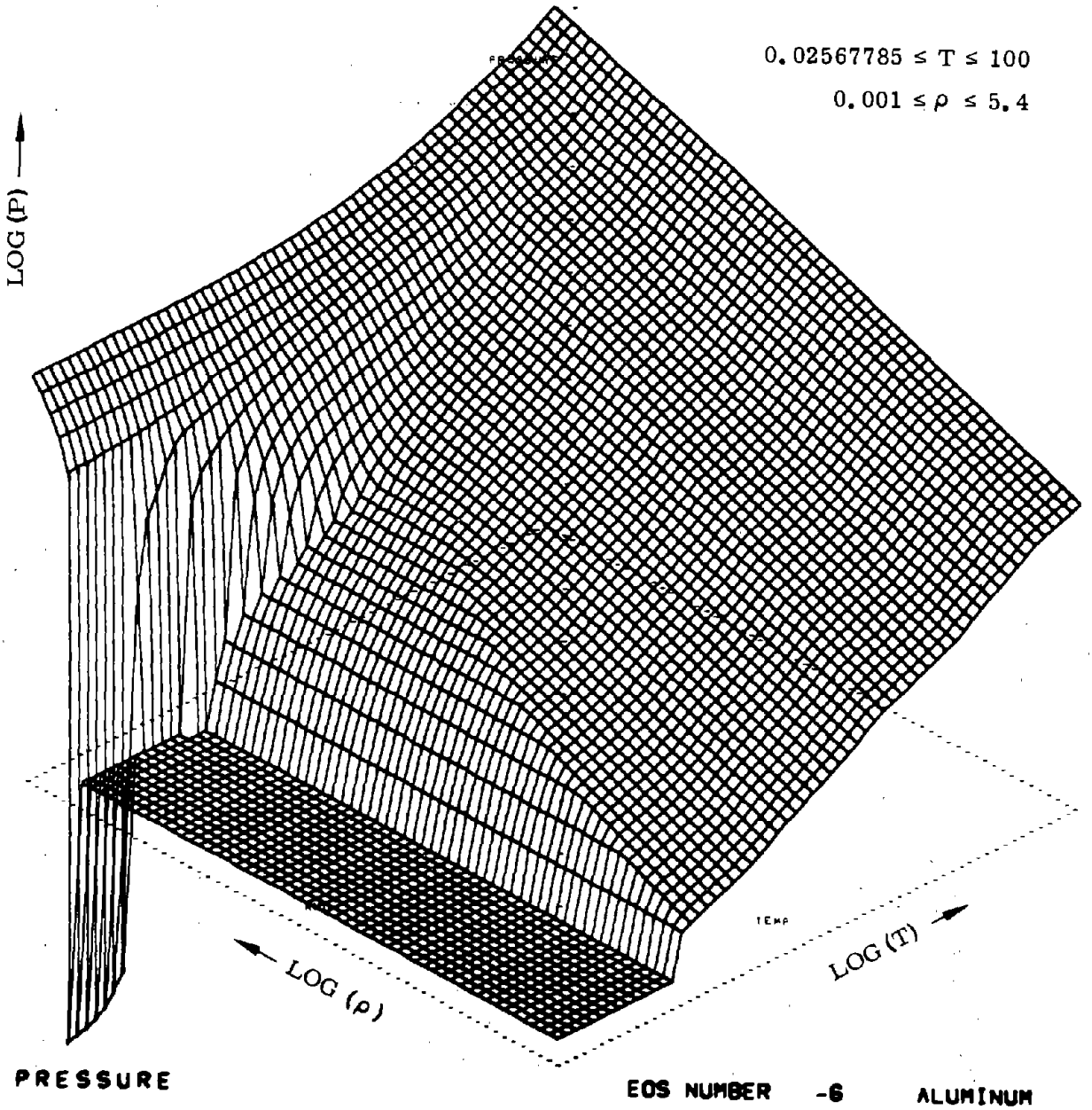
0.02567785 ≤ T ≤ 100
0.001 ≤ ρ ≤ 5.4
LOG (P)
LOG (ρ)
LOG (T)
PRESSURE
EOS NUMBER -6 ALUMINUM

Fig. D-8

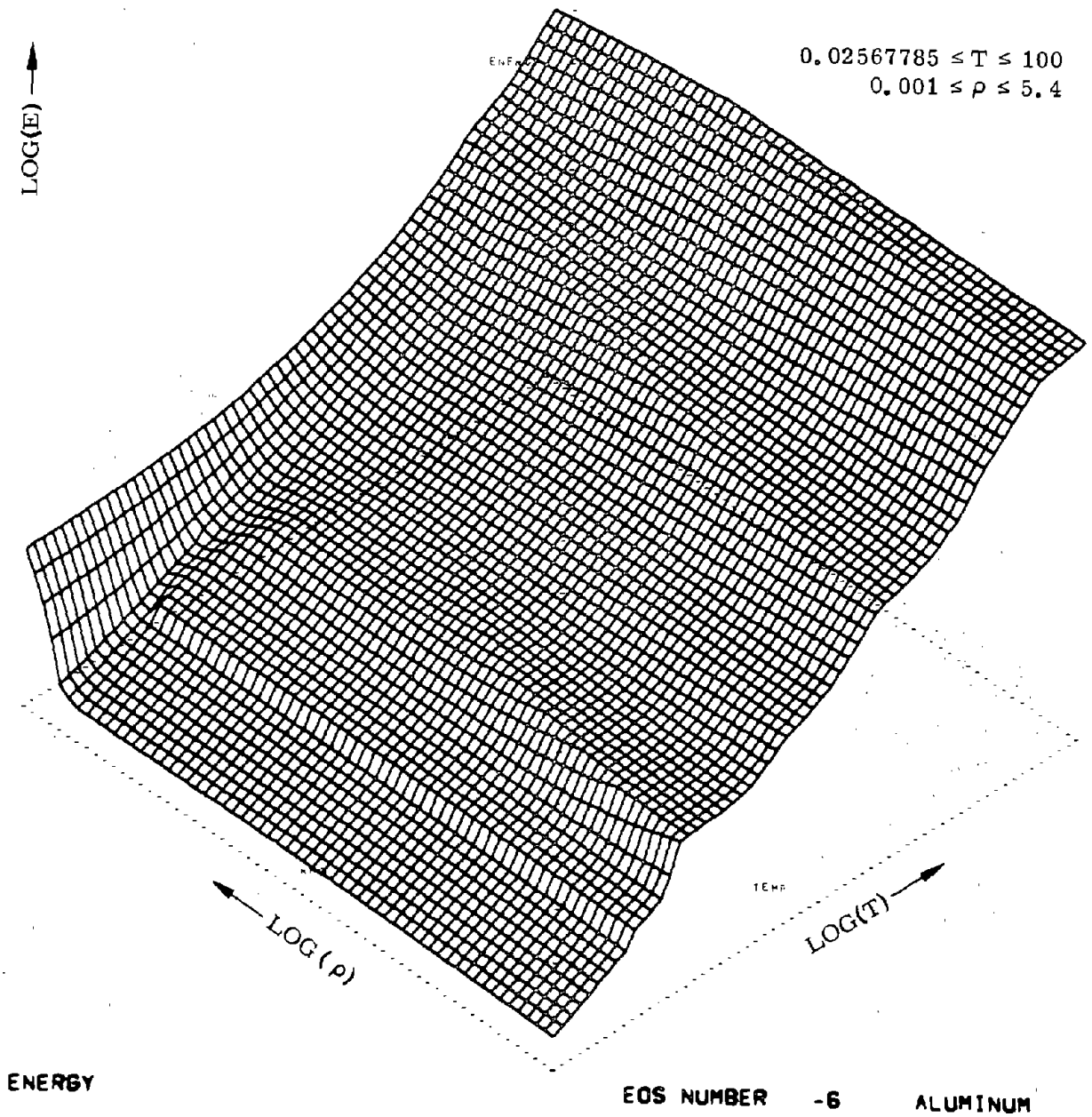
LOG(E)
0.02567785 ≤ T ≤ 100
0.001 ≤ ρ ≤ 5.4
LOG (ρ)
LOG(T)
ENERGY
EOS NUMBER -6 ALUMINUM

Fig. D-9

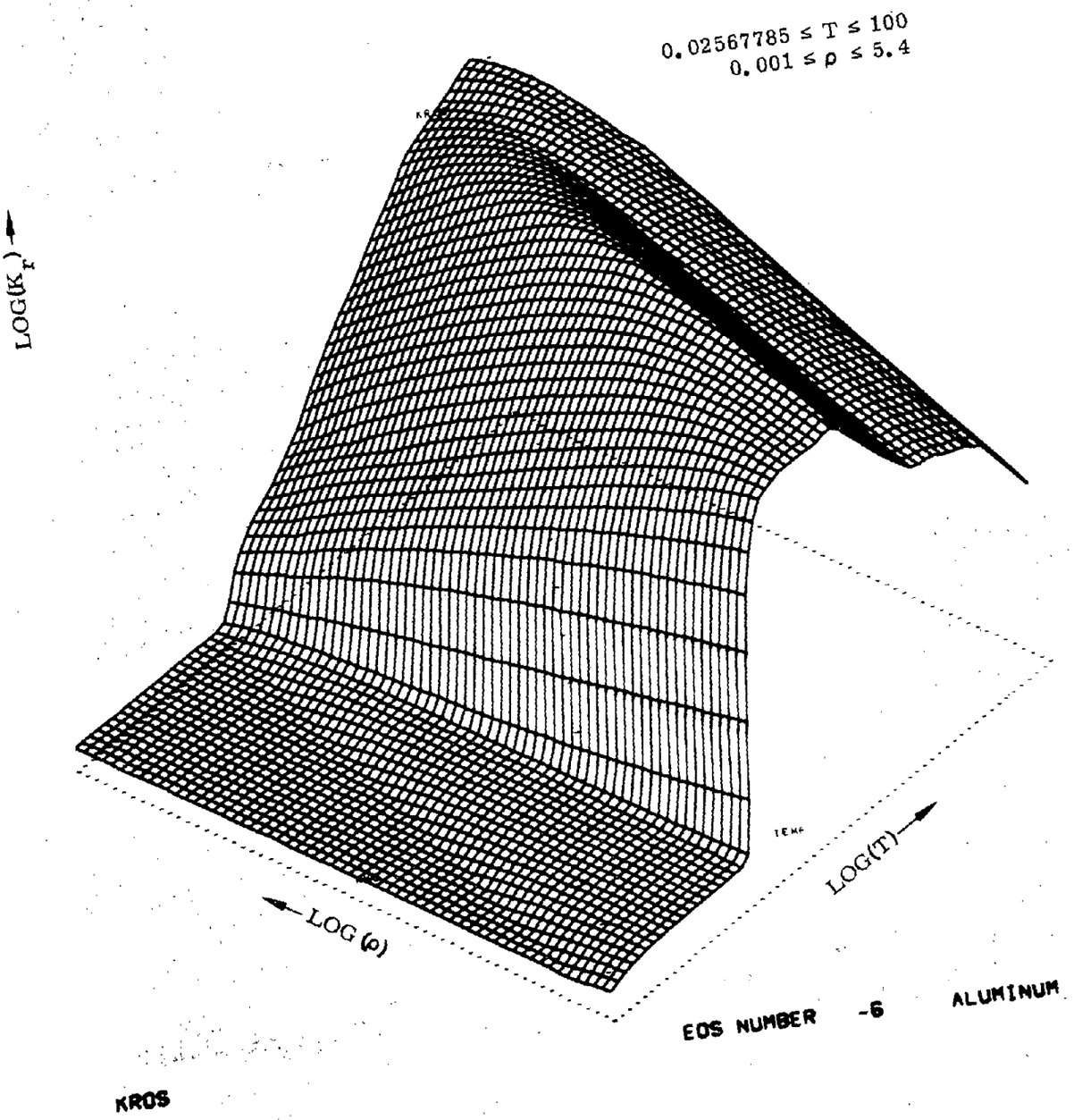
0.02567785 ≤ T ≤ 100
0.001 ≤ ρ ≤ 5.4
LOG(K_R)
LOG (ρ)
LOG(T)
EOS NUMBER -6 ALUMINUM
KROS

Fig. D-10

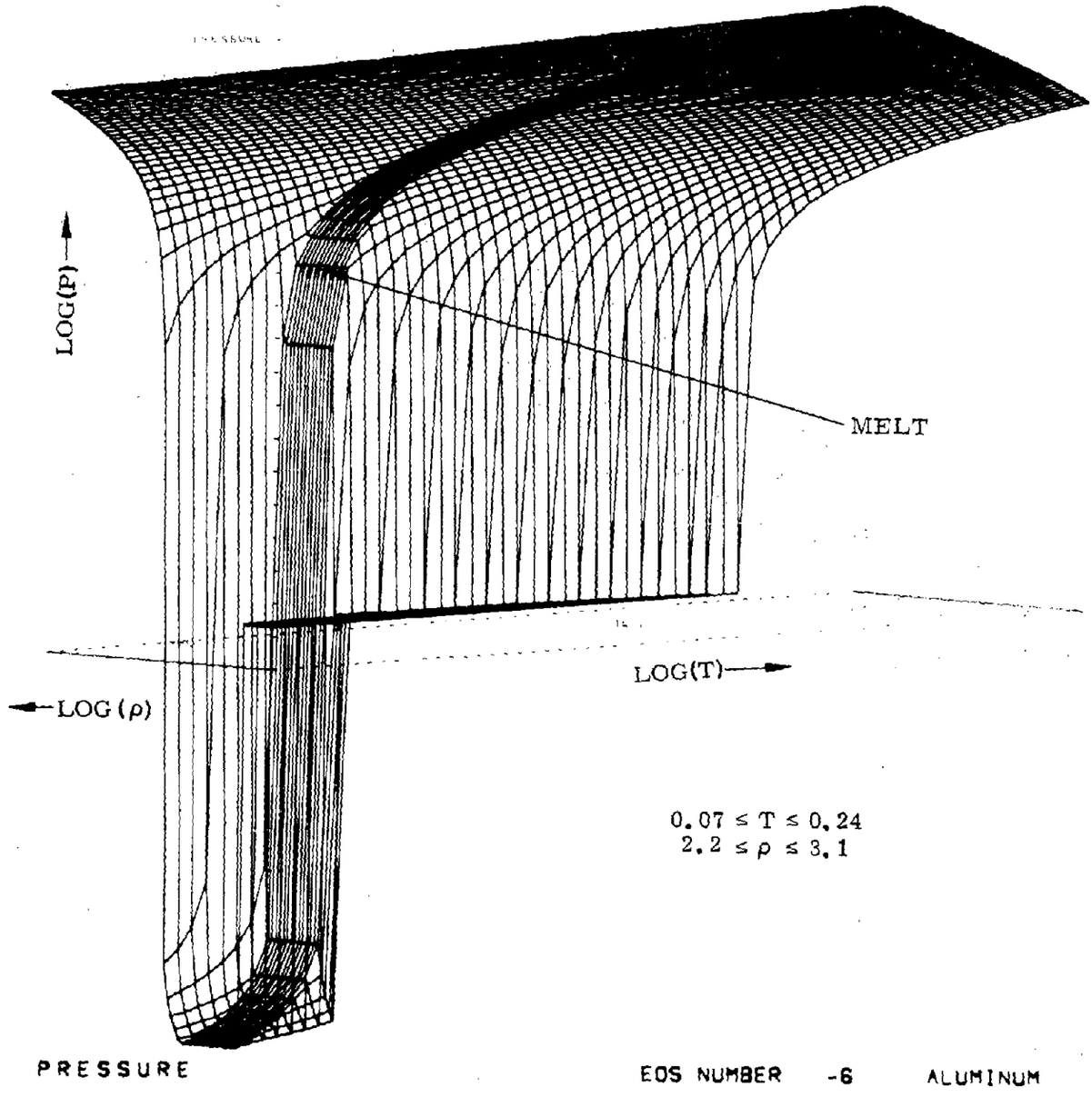
LOG(P)
MELT
LOG(T)
LOG (ρ)
0.07 ≤ T ≤ 0.24
2.2 ≤ ρ ≤ 3.1
PRESSURE
EOS NUMBER -6 ALUMINUM

Fig. D-11

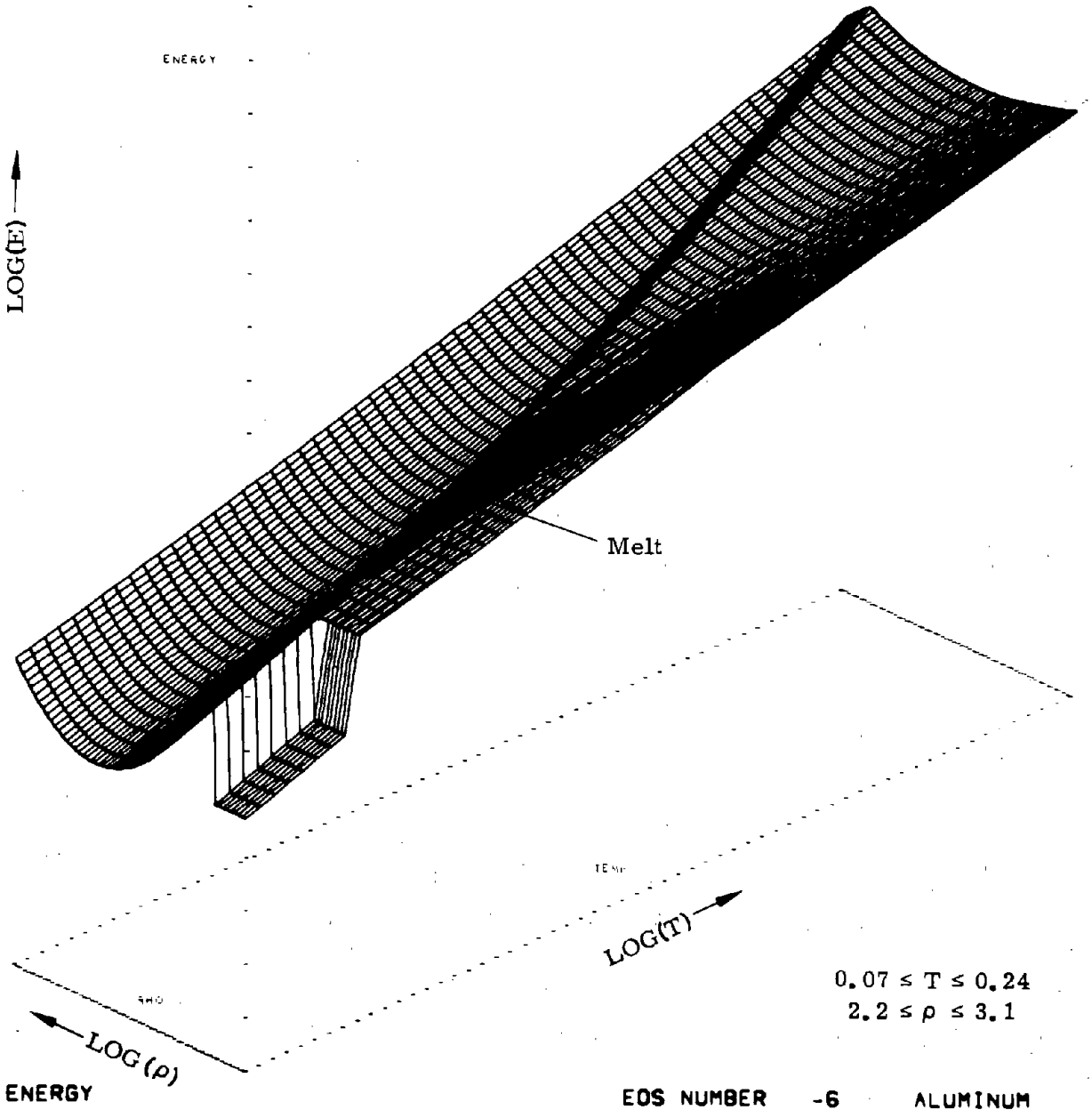
ENERGY
LOG(E)
Melt
LOG(T)
LOG (ρ)
0.07 ≤ T ≤ 0.24
2.2 ≤ ρ ≤ 3.1
ENERGY
EOS NUMBER -6 ALUMINUM

Fig. D-12

Appendix E

PROCEDURE OF ADJUSTMENT OF CRITICAL POINT

Appendix E

PROCEDURE OF ADJUSTMENT OF CRITICAL POINT

The equation of state for aluminum presented in Appendix D has had the critical point parameters adjusted by use of Eq. (3.33). The results of part of a parameter study are shown in Fig. E-1. For these curves, $C_{54} = 0.8$. Other values were tried with similar results.

On the basis of these curves, the values $C_{53} = 3.5 \times 10^{12}$ dynes/cm^2 and $C_{54} = 0.8$ were selected. While the critical point parameters of aluminum are not well known, the computed results with $C_{53} = 0$ seem to have too high a temperature and pressure to be in line with extrapolated experimental data. The values on the right-hand side of the curves are in agreement with some recent estimates.

With this equation of state it is not possible to further decrease the critical pressure by increasing C_{53} to an appreciable extent. The difficulty discussed in reference to Fig. 5 is encountered. This problem will normally control the adjustment possible by (3.33).

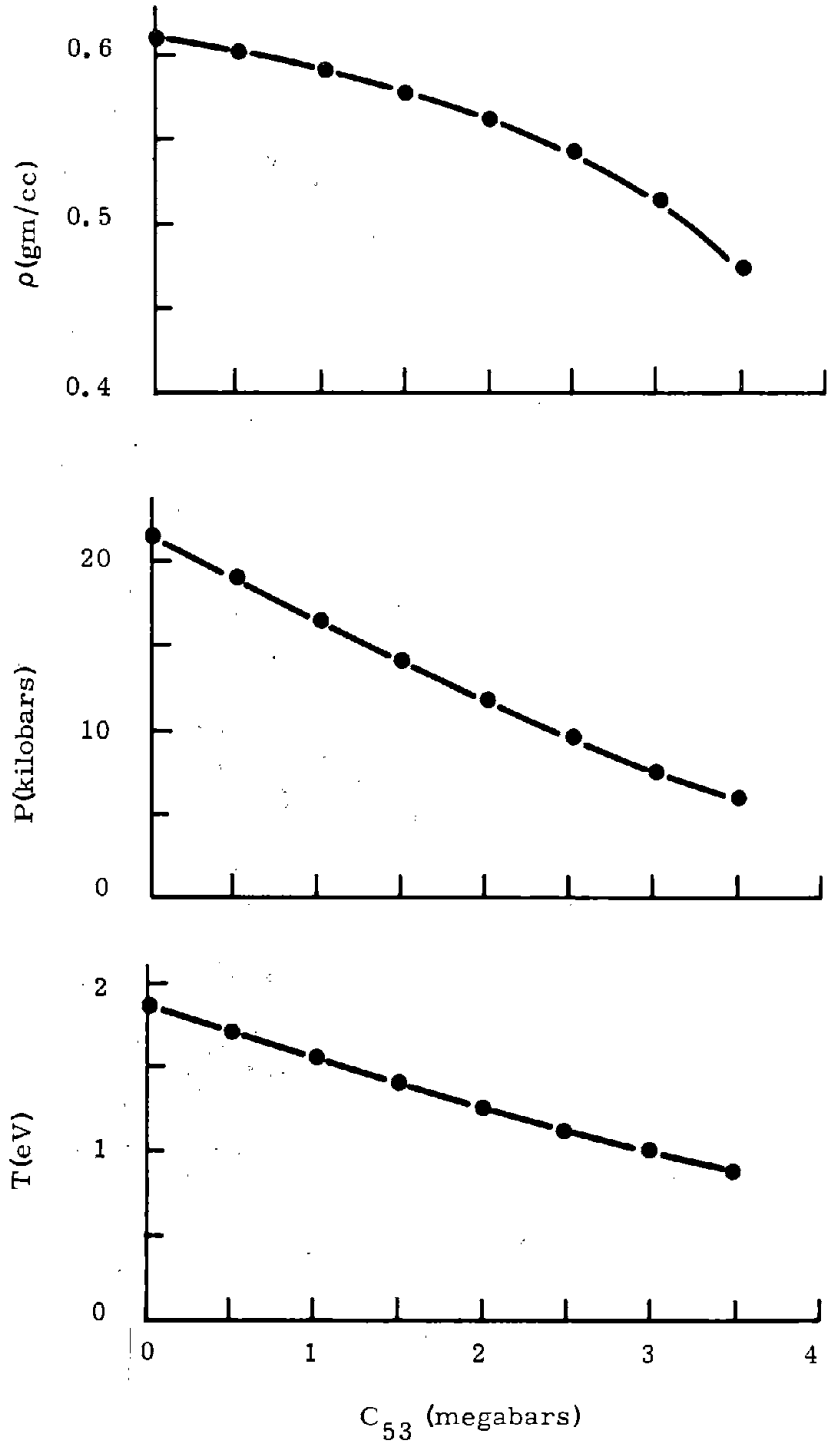

Fig. E-1 Computed critical parameters of aluminum as a function of input variable C_{53}.

UNLIMITED RELEASE

DISTRIBUTION: (March 1972)

U. S. ATOMIC ENERGY COMMISSION
DIVISION OF TECHNICAL INFORMATION
REP. SEC., HDQTRS. LIBRARY, G-017
WASHINGTON, D. C. 20545

U. S. ATOMIC ENERGY COMMISSION
ALBUQUERQUE OPERATIONS OFFICE
P. O. BOX 5400
ALBUQUERQUE, NEW MEXICO 87115
ATTN: H. C. DONNELLY

U. S. ATOMIC ENERGY COMMISSION
SANDIA AREA OFFICE
P. O. BOX 5400
ALBUQUERQUE, NEW MEXICO 87115

LAWRENCE LIVERMORE LABORATORY (29)
P. O. BOX 808
LIVERMORE, CALIFORNIA 94550
ATTN: REPORTS LIBRARY
A. G. COLE
W. J. COMFORT
G. E. COOPER
B. K. CROWLEY
W. B. CROWLEY
W. H. GRASBERGER
R. GROVER
A. C. HOLT
W. G. HOOVER
M. H. L. JESTER
R. N. KEELER
J. E. KELLER
W. A. LOKKE
E. W. MCCAULEY
W. H. MCMASTER
R. NELSON
J. J. OSBORN
J. H. PITTS
R. F. POST
E. B. ROYCE
B. F. ROZSNYAI
S. SACK
C. B. TARTER
M. VAN THIEL
R. J. WASLEY
M. L. WILKINS
J. WILSON
L. W. WOODRUFF
J. W. ZINK

LOS ALAMOS SCIENTIFIC LABORATORY (39)
P. O. BOX 1663
LOS ALAMOS, NEW MEXICO 87544
ATTN: REPORTS LIBRARY
J. F. BARNES, T-4
S. T. BENNION, J-9
P. J. BLEWETT, TD-5
R. R. BROWNLEE, J-9
D. M. BYERS, W-DO
J. M. CORTEZ, J-15
A. N. COX, J-15
A. H. DAVIS, J-9
C. G. DAVIS, J-15
N. E. DEAL, GMX-DO
D. D. EILERS, J-15
S. D. GARDNER, GMX-7
L. A. GRIEGO, GMX-3
F. H. HARLOW, T-3
L. C. HORPEDAHL, W-9
W. F. HUEBNER, T-4
M. J. KATZ, W-9
C. E. KELLER, J-9
C. F. KELLER, J-15
G. I. KERLEY, T-4
D. A. LIBERMAN, T-4
E. D. LOUGHRAN, GMX-2
C. L. MADER, T-4
N. M. MAGEE, JR., J-15
R. G. MCQUEEN, GMX-6
A. L. MERTS, T-4
R. MORALES, GMX-11
F. T. SEIBEL, W-8
R. P. SHAFER, W-10
G. R. SPILLMAN, TD-3
J. N. STEWART, J-9
J. W. TAYLOR, GMX-6
F. T. TEATUL, TD-4
D. B. THOMSON, GMX-6
R. S. THURSTON, W-10
D. VENABLE, GMX-11
J. WACKERLE, GMX-7
P. P. WHALEN, TD-1
G. N. WHITE, TD-5

UNION CARBIDE CORP. (2)
BLDG. 9732, Y-12
OAK RIDGE, TENNESSEE 37830
ATTN: S. WALLACE
C. M. DAVENPORT

R, G, FITZGERALD, 1221
M, W, EDENBURN, 1222
W, H, SCHMIDT, 1222
J, L, WENTZ, 1222
J, R, PIPER, 1223
V, J, ROH, 1223
G, E, CLARK, 1314
P, L, STANTON, 1314
P, D, WILCOX, 1316
J, P, SHOUP, 1332
R, K, TRAEGER, 1435
C, E, ALBRIGHT, 1435
O, M, STIETZER, 1440
R, H, BRAASCH, 1441
W, E, ALZHEIMER, 1517
C, H, MAUNEY, 1530
R, L, ALVIS, 1534
T, B, LANE, 1540
S, W, KEY, 1541
R, D, KRIEG, 1541
W, A, VON RIESEMANN, 1541
T, G, PRIDDY, 1542
R, C, REUTER, 1542
P, P, STIRRIS, 1542
O, M, WEBB, 1542
B, E, BADER, 1543
R, T, OTHMER, 1544
T, A, DUFFEY, 1544
O, W, LUBITZ, 1544
W, A, SERRELL, 1544
J, T, RISSE, 1553
S, O, SPRAY, 1652
C, WINTER, 1710
P, A, STOKES, 1711
O, J, MCCLOSKEY, 1715
G, V, BARTON, 1715
D, A, DAHLGREN, 1715
J, N, MIDDLETON, 1715
W, B, MURFIN, 1715
R, J, THOMPSON, 1722
L, T, RITCHIE, 1724
W, C, HINES, 1733
J, W, KANE, 1752
T, D, HERTHER, 1752
D, H, ANDERSON, 1910
D, E, BENNETT, 1923
B, L, GREGORY, 1933
G, G, SUMMERS, 1933
J, L, DUNCAN, 1934
G, J, SCRIVNER, 1935
A, M, CLOGSTON, 5000
A, NARATH, 50
O, E, JONES, 5100
F, L, VOOK, 5110
G, A, SAMARA, 5130
R, A, GRAHAM, 5132
P, C, LYSNE, 5132
L, W, DAVISON, 5131
J, E, KENNEDY, 5131

W, B, BENEDICK, 5131
J, K, NOVIATO, 5131
J, R, ASAY, 5132
B, M, BUTCHER, 5133
J, N, JOHNSON, 5133
A, L, STEVENS, 5133
L, M, LEE, 5136
J, E, SCHIMBER, 5150
A, C, SWITENDICK, 5151
B, MORRISON, 5152
W, HERRMANN, 5160
L, D, BERTHOLF, 5162
D, HICKS, 5162
H, S, LAWSON, 5162 (10)
S, L, THOMPSON, 5162 (20)
B, J, THORNE, 5162
R, T, WALSH, 5162
D, E, MONSON, 5163
L, M, BARKER, 5163
D, S, DRUMHELLER, 5163
C, D, LUNDERGAN, 5163
R, P, MAY, 5163
K, K, SCHULER, 5163
H, J, SUTHERLAND, 5163
C, H, BARNES, 5165
J, A, BRAMMER, 5165
D, J, CHAVEZ, 5165
J, LIPKIN, 5165
A, J, CHABAI, 5166
P, D, ANDERSON, 5166
R, K, BYERS, 5166
L, D, BUXTON, 5166
L, K, KENNEDY, 5166
R, J, LAWRENCE, 5166
D, S, MASON, 5166
E, G, YOUNG, 5166
L, C, HEBEL, 5200
N, C, ANDERHOLM, 5214
J, V, WALKER, 5224
R, L, COATS, 5222
L, L, BONZON, 5222
J, A, REUSCHER, 5222
L, D, POSEY, 5226
C, R, MEHL, 5230
J, H, REIKEN, 5231
F, BIGGS, 5231
R, K, COLE, 5231
C, N, VITTITOE, 5231
T, P, WRIGHT, 5231
J, M, HOFFMAN, 5233
E, H, BECKNER, 5240
J, E, MCDONALD, 5300
H, M, STOLLER, 5314
A, R, CHAMPION, 5314
T, R, GUESS, 5314
K, E, MEAD, 5322
T, V, TORMEY, 5322
R, W, LYNCH, 5323
R, R, BOADE, 5323
L, DEHGHANMANESH, 5323

A, GOODMAN, 5323
C, M, PERCIVAL, 5323
K, D, SMITH, 5323
D, G, SWANSON, 5323
G, E, JELINEK, 5324
D, L, BURCHETT, 5325
R, M, ELRICK, 5325
W, B, GAUSTER, 5325
F, C, PERRY, 5325
C, W, JENNINGS, 5332
R, R, SOWELL, 5332
J, R, HOLLAND, 5335
W, C, SCRIVNER, 5400
J, L, TISCHHAUSER, 5420
A, R, IACOLETTI, 5421
D, A, YOUNG, 5422
C, R, BAILEY, 5422
R, J, DETRY, 5422
H, C, OGDEN, 5422
B, T, FOX, 5427
A, R, ARENHOLZ, 5428
N, A, SMITH, 5428
P, VAN DELINDER, 5428
L, M, BERRY, 5500
D, R, ANDERSON, 5513
M, F, FURNEY, 5513
W, M, O'NEILL, 5520
R, W, ROHDE, 5531
D, J, MOTTERN, 5535
A, Y, POPE, 5600
R, C, MAYDEW, 5620
K, J, TOURYAN, 5640
F, G, BLOTTNER, 5643
P, J, ROACHE, 5643
J, K, COLE, 5644
G, CARLI, 7624
J, H, GRAHAM, 7624
A, F, SCHKRADE, 7624
W, D, ZINKL, 8122
P, D, GILDEA, 8124
R, D, COZINE, 8131
H, F, NORRIS, JR., 8131
D, E, GREGSON, 8150
G, L, CLARK, 8155
W, L, GUYTON, 8172
R, H, MEINKEN, 8310
J, M, BRIERLY, 8311
L, R, HILL, 8314
J, W, HEINE, 8320
J, N, ROGERS, 8321
V, K, GABRIELSON, 8321
R, E, HUDDLESTON, 8321
J, F, LATHROP, 8321
J, MANSFIELD, 8321
R, A, MCHUGH, 8321
C, H, TURNBULL, 8321
T, S, GOLD, 8324
G, W, ANDERSON, 8330
J, L, WIRTH, 8340
J, A, MOGFORD, 8341
H, R, SHEPPARD, 8342

A, N, BLACKWELL, 8357
C, W, ROBINSON, JR., 8352
M, R, BIRNBAUM, 8352
S, S, CHIU, 8352
L, M, MURPHY, 8352
R, NG, 8352
C, S, HOYLE, 8353
C, D, BROYLES, 9117
W, D, WEART, 9111
R, C, BASS, 9111
G, E, LARSEN, 9111
L, D, TYLER, 9111
J, D, PLIMPTON, 9112
M, BERMAN, 9112
J, HARRIS, 9112
J, W, KENNEDY, 9114
G, W, HARR, 9114
F, F, DEAN, 9114
A, R, SATTLER, 9114
C, W, COOK, 9116
D, K, OVERMIER, 9116
R, P, REED, 9116
J, R, HANISTER, 9150
M, L, MERRITT, 9150
E, L, HARLEY, 9225
F, H, MATHEWS, 9321
B, W, DUGGIN, 9321
M, J, FORRESTAL, 9324
L, W, RICKLE, 9324
T, L, PACE, 9420
E, K, MONTOYA, 9424
R, H, YOSHIMURA, 9461
O, J, BURCHETT, 9462
R, S, GILLESPIE, 3151 (3)
G. R. Miller, 3152
L. S. Ostrander, 8232
Central Files, 3142-1 (25)